EVALUATION AND MODELING OF PAVEMENT MARKING CHARACTERISTICS BASED ON LABORATORY AND FIELD DATA

A Dissertation
Presented in Partial Fulfillment of the Requirements for the
Degree of Doctorate of Philosophy
with a
Major in Civil Engineering
in the
College of Graduate Studies
University of Idaho
by

Maged M. Mohamed

Major Professor: Kevin Chang, Ph.D.
Committee Members: Ahmed Abdel-Rahim, Ph.D.; Emad Kassem, Ph.D.;
Christopher Williams, Ph.D.
Department Administrator: Patricia J. S. Colberg, Ph.D.

May 2019

AUTHORIZATION TO SUBMIT DISSERTATION

This dissertation of Maged M. Mohamed, submitted for the degree of Doctorate of Philosophy with a major in Civil Engineering and titled "EVALUATION AND MODELING OF PAVEMENT MARKING CHARACTERISTICS BASED ON LABORATORY AND FIELD DATA," has been reviewed in final form. Permission, as indicated by the signatures and dates below, is now granted to submit final copies to the college of Graduate Studies for approval.

Major Professor: Date:

_____ _____

Kevin Chang, Ph.D.

Committee Members: Date:

_____ _____

Ahmed Abdel-Rahim, Ph.D.

Date:

_____ _____

Emad Kassem, Ph.D.

Date:

_____ _____

Christopher Williams, Ph.D.

Department Administrator: Date:

_____ _____

Patricia J. S. Colberg, Ph.D.

ABSTRACT

Drivers rely on the visibility of pavement markings to maintain a safe road path especially during nighttime and challenging weather conditions. With the growing demand for pavement marking materials, durability and long-term weatherability of these products is critical. Current performance evaluation methodology using field test-deck protocols requires significant time and resources, and under these protocols the performance of a pavement marking can be monitored for a period of up to three years. In addition, safety-related issues such as exposing technical staff to road hazards while applying the marking materials and collecting measurements, along with road closure consequences, are of concern. The primary goals of this research were to develop an accelerated laboratory-based procedure that could evaluate the performance of pavement markings, overcome the shortcomings of current evaluation practice, and investigate the safety performance of pavement markings based on existing crash data and results from a driver simulation study.

For the laboratory-based procedure, a three-wheel polisher device (TWPD) and xenon arc chamber (XAC) were employed to replicate varying traffic, snowplowing, and weather conditions. The deterioration of the physical measurements (i.e., dry and wet retroreflectivity, color change, and durability) of waterborne and thermoplastic markings was modeled. All of the performance measures logarithmically deteriorated under different TWPD loadings, except for the durability of the thermoplastic markings which followed a linear degradation function. A significant reduction in percent retroreflectivity was observed in the initial part of the TWPD testing but leveled out as the number of cycles increased. This deterioration pattern is similar to what occurs in the field, as retroreflectivity dramatically decreases after the first few months of installation and then stabilizes before the end of its service life. On the other hand, a linear increase in retroreflectivity and color change occurred during the artificial weathering exposure time (i.e. 2,000 hours) due to the change in surface physical properties. The color analysis revealed an important relationship between pavement marking retroreflectivity and color change. After traffic loading, all colors darkened due to the exposure of the black asphaltic color or the abrasion of the upper layer of marking, and in turn

retroreflected less light while different color change patterns were experienced under the artificial weathering.

The color analysis results showed that when a color closely resembles white, the sample retroreflected more light. The TWPD and weatherometer effectively simulated and accelerated the operational and environmental effects (e.g., traffic, snowplowing, sunlight, moisture, and temperature) so that assessment of pavement marking performance could be completed in an abbreviated time frame. The results yielded a significant relationship between all performance measures assessed in both the laboratory and field. Evaluating the performance of pavement marking products using an accelerated laboratory-based procedure provides a department of transportation (DOT) with a flexible tool to cope with the rapidly evolving industry through the establishment of guidelines that might be used for the selection and maintenance of the pavement markings. This procedure can be used to compare different marking materials and assess marking materials whether they bear severe traffic operating conditions or harsh climates before implementation in short period of time.

To assess the safety performance of pavement markings, specifically on two-way, two-lane rural roads which are common in the state of Idaho, two separate approaches were adopted. First, a crash analysis study over eight years (2010-2017) on rural roads in Idaho was conducted to understand the relationship between retroreflectivity deterioration of edgelines and crash occurrence. Field retroreflectivity data for waterborne edgeline markings from thirty-eight sites were collected and modeled over twelve months across six districts with different environmental conditions. The results yielded a logarithmic relationship between retroreflectivity and age, and pavement markings in districts subjected to higher ground snow loads deteriorated faster than those with lower ground snow loads. This faster deterioration trend in northern districts was attributed to winter maintenance activities and harsh weather. Even though, a clear statistical pattern was determined for District 1, which was subjected to the higher ground snow loads among all districts, the methodology used in this study could not definitively conclude that crash rate increased with lower edgeline retroreflectivity.

Second, a study using the University of Idaho's driving simulator was implemented to evaluate the safety effects of different edgeline pavement marking widths (e.g., 4-inch and 6-inch) and deteriorations (e.g., 0%, 25%, 50%, and 75% deterioration) on driver behavior. The

results indicated that statistically significant differences were observed during nighttime conditions when comparing the driver's lane deviation (vehicle's lateral position) between the wider 6-inch longitudinal edgeline pavement markings and standard 4-inch edgeline marking. Drivers consistently maintained a lane position that slightly favored the edgeline side when exposed to a 4-inch marking and increasingly shifted away from the centerline as edgeline deterioration worsened. The results of the statistical analysis implied that 4-inch markings and severely deteriorated pavement markings cause higher variation values in driver lateral position which in turn could affect overall driver safety.

This research benefits transportation agencies, particularly those sited in cold-weather regions, by enabling them to predict the deterioration of marking materials and assist in the scheduling of maintenance marking projects to maximize the operational and safety benefits of the existing material. This research also make recommendations with regard to a minimum retroreflectivity threshold that should be maintained for pavement markings of two-way, two-lane rural roads and the use of wide pavement markings.

ACKNOWLEDGEMENTS

I would like to extend thanks to the people who generously contributed to the work presented in this dissertation.

I am deeply grateful to my enthusiastic supervisor, Dr. Kevin Chang, for his continuous support throughout the process of my Ph.D study and research, for his patience, and motivation. I gratefully acknowledge the members of my Ph.D. committee for their time and valuable feedback. Special mention goes to Dr. Ahmed Abdel-Rahim who has guided me with his immense knowledge and encouraged me to carry on through this time and has contributed to my educational journey with a major impact. I want to express my deep gratitude to Dr. Emad Kassem who has navigated me through transportation materials science and to Dr. Christopher Williams who has guided me through the statistical science to enrich my work. Their guidance helped me with the research and writing of this dissertation and I feel extremely privileged to have been their student.

I would like to thank the theory faculty at the University of Idaho, especially Dr. Armando McDonald and Dr. Brian Dyre, for the substantial influence that their help has had on my research.

I am also very thankful to Don Parks, Andrew Skinner, and Mohamed Mohamed for their help in the laboratory and with any data collection.

Finally, I would like to acknowledge family and friends who supported me during my time at the University of Idaho. My last word goes out to my family members who have lighted my life and who have given me the strength and motivation to get this work done.

.

DEDICATION

This dissertation is dedicated to the people who have become the greatest influences on my life.

To my mother, Fowzia Boshalla, who has always loved me unconditionally and granted me the spiritual support through her ceaseless prayers.

To the memory of my father, Miloud Alhassia, Ph.D., whose good example has taught me to work hard for the things that I aspire to achieve. Although he was my inspiration to pursue my doctoral degree, he was unable to see this moment, but I am sure he is proud of me.

A special feeling of gratitude to my loving brothers Jalal, Atif, and Anees for their encouragement and push for tenacity.

A distinctive dedication goes to my brilliant and beloved wife Hawa, who has been a constant source of love and encouragement during the challenges of graduate school and life. To my fisherman son Abdul Rahman, and my exuberant, sweet, and kind-hearted daughters Fouzia and Jamila.

I am truly thankful for having you in my life. Without your endless love, I would never have been able to reach this step.

Allah bless you all.

TABLE OF CONTENTS

LIST OF FIGURES

LIST OF TABLES

LIST OF EQUATIONS

CHAPTER 1: INTRODUCTION

The visibility of pavement markings plays a major role in providing a safe travel environment and enabling the driver to discern the road path especially at nighttime. The existence and continuity of longitudinal pavement markings deliver continuous information to drivers related to roadway alignment, vehicle positioning, and other significant driving-related duties such as controlling the steering wheel and braking. One approach to potentially reduce crashes is to provide better continuous information to the driver in the form of wider or higher-quality (e.g., more retroreflective or brighter) longitudinal pavement markings. Thus, it is important to study the relationship between pavement marking characteristics and single-vehicle roadway departure crashes and investigate safety improvements associated with installing brighter or wider pavement markings.

Maintaining adequate visibility of pavement markings can reduce crashes during the daytime and nighttime; however, the retroreflectivity of pavement markings is critical at night. Therefore, a safe threshold of pavement marking retroreflectivity should be maintained. The performance of some pavement markings can be degraded significantly after a short time of service. New pavement markings may have unknown performance until they are used on roads. For these reasons, there is value in developing a method to evaluate pavement marking materials in the laboratory to save time and money for a state department of transportation when selecting pavement marking materials and developing restriping schedules.

The primary goals of this research were to investigate the safety performance of existing pavement marking applications and to develop solutions to enhance roadway safety. To achieve these goals, several tasks were completed:

a) Pavement marking test sections were selected across six districts in Idaho with different environmental conditions (e.g., snowfall).
b) Retroreflectivity data of the pavement markings were collected over time to measure aging effects for the selected segments.
c) Performance deterioration models for pavement markings in each district were developed using the retroreflectivity field data along with other information such as the date of marking application and ground snow loads.

d) The correlation between the pavement marking quality (retroreflectivity) and crash frequency and severity on two-way, two-lane rural roads in Idaho was investigated by applying a crash analysis study using the WebCARS crash data.
e) The effect of different pavement marking deterioration levels and widths on driving behavior was investigated using a driving simulator study.
f) Due to the importance of developing a laboratory-based procedure to evaluate pavement marking materials, a full evaluation procedure was proposed and applied as part of this study using a TWPD and a weatherometer to model the performance of waterborne (nondurable) and thermoplastic (durable) marking materials, which are commonly used in the state of Idaho.
    1. Asphalt substrates were prepared, striped with different marking materials and colors, and tested using a three-wheel polisher in a laboratory under different simulated loading conditions (e.g., pneumatic tires, steel wheels, and scraper blade simulating snowplowing).
    2. Aluminum substrates were prepared, striped with different marking materials and colors, and tested using a weatherometer (e.g., xenon-arc chamber).
    3. Performance measures were conducted, modeled, and evaluated under various traffic loads, duration intervals, and controlled climatic conditions.
    4. Various types of pavement markings were evaluated in the laboratory to determine their performance and recommended for use in cold regions.
g) The relationship between field and laboratory performance of various pavement markings was established.
h) A comprehensive methodology and standard procedure that could be adapted by a state department of transportation to evaluate different marking materials in a laboratory-controlled environment was identified.
i) Specifications for pavement markings that can be used in cold regions was developed.
j) Recommendations were developed for future research based on the results of this study.

1.1.Dissertation Organization

The reminder of this dissertation is organized into six chapters. Chapter 2 describes the background of this research, including the existing specifications, application technologies that underlie it, and the previous research in this area. Chapter 3 describes the methodology

used for developing an accelerated laboratory-based procedure for pavement marking performance evaluation. Chapter 4 presents the laboratory procedure results and analysis. Chapter 5 presents the methodology of modeling pavement marking deterioration in the field and how winter maintenance activities impact the deterioration of pavement markings in Idaho. Chapter 6 presents the crash analysis study results, which investigated the correlation between the retroreflectivity of edgeline pavement markings and delineation-related crashes on rural highways. Chapter 7 presents the methodology, analysis, and results of implementing wider longitudinal pavement markings based on driving simulator study. Finally, Chapter 8 describes the significance of the research, summarizes the conclusions, and provides recommendations for future research.

CHAPTER 2: BACKGROUND AND LITERATURE REVIEW

Pavement markings provide key information to drivers about roadway alignment, vehicle positioning, and other driving-related tasks (Carlson et al. 2009). Maintaining pavement markings for adequate visibility and retroreflectivity is essential for the safety of motorists. Departments of Transportation (DOTs) in different states use various pavement marking materials based on local conditions and performance. The service life of the pavement marking represents the time that the pavement marking can be expected to be "serviceable" while fulfilling its duty towards road users. However, the service life of different materials varies greatly; each pavement marking material has its own unique characteristics which differ when used in different conditions (e.g., pavement surface, climate, and operating conditions). Previous studies have defined the pavement marking service life as the time required for its retroreflectivity to drop below a preselected threshold value or in terms of material percent lost (durability) as control performance measures (Lee et al. 1999; Jiang 2008a; Mull and Sitzabee 2012; Migletz et al. 2002; Parker and Meja 2003).

2.1. Types of Lane Markings (Geometrical classification)

Pavement markings can be longitudinal, transverse, or temporary. The color (white or yellow) and pattern (double or single/broken or solid) of longitudinal pavement markings are important characteristics that need to be specified based on location and purpose.

2.1.1. Longitudinal Pavement Markings

Longitudinal markings are continuous lines which are used on roads to assist drivers to discern the road usage. In other words, longitudinal markings define the boundary between the travel lane and the opposing direction, road edge, other lanes, or turning movements (WSDOT, Design Manual 2017). Longitudinal pavement markings can be an edge line, lane line, or a center line/skip line (passing line or no-passing barriers) (Craig et al. 2007). Figure 2.1 shows an example of a common lane marking system for divided rural two-lane roads.

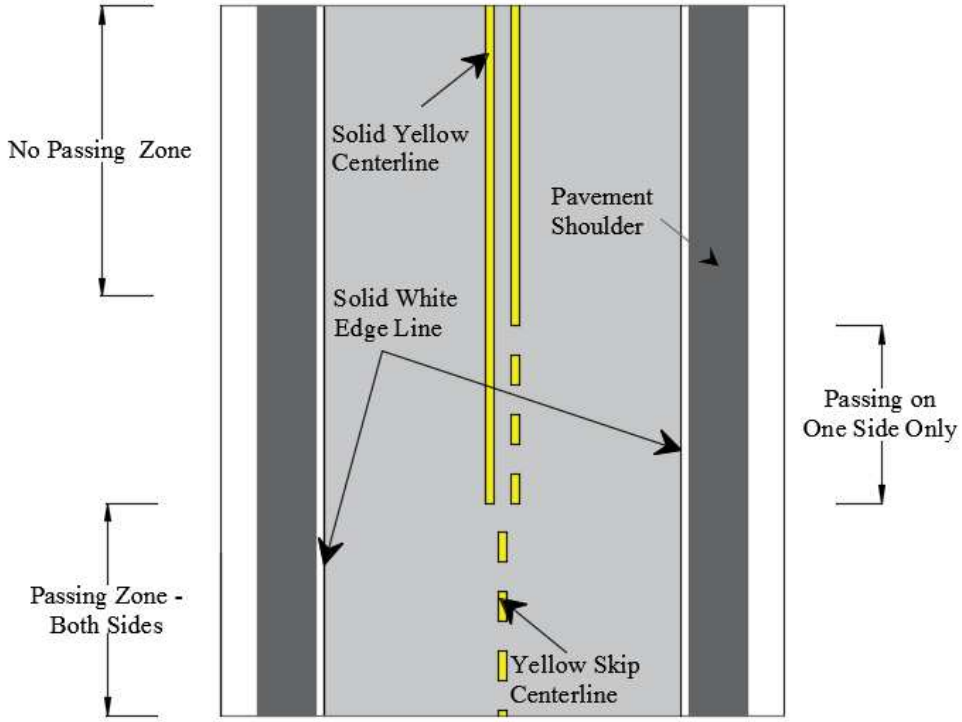

Figure 2.1: Lane marking system for divided rural two-lane roads

2.1.2. Transverse Pavement Markings

All pavement markings installed crosswise on top of the pavement, from side-to-side, or perpendicular to the road center line are called transverse pavement markings. Based on the Manual on Uniform Traffic Control Devices (MUTCD), the term transverse marking covers all word and symbol markings, shoulder markings, stop line markings, crosswalk markings, speed measurement markings, parking markings, and transverse median markings. The colors used for common transverse pavement markings are white and yellow, while blue and red colors are permitted under certain conditions (Moser et al. 2015). Unique configurations and designs of transverse pavement markings make them instantly recognized and understood by roadway users (Wang 2010).

2.1.3. Temporary Pavement Markings

Temporary pavement markings are used for a short time as a substitute for permanent traffic markings. Temporary pavement markings are installed and maintained during construction phases in work zones for maintenance or utility projects (Pendleton 1988).

2.2. Color Specifications

Color is one of the important physical properties that can efficiently characterize pavement markings, and the use of different roadway pavement marking colors delivers different messages to road users. In the United States, the Department of Transportation (DOT) is the authority responsible for selecting and enforcing pavement marking color standards. All DOTs and transportation agencies refer to the MUTCD in their policies for decisions related to pavement marking locations, patterns, and colors. Based on the MUTCD, there are four standard colors that can be used on public roads: yellow, white, red, and blue. In general, yellow lines are used as a center line that separates traffic in opposite directions. White longitudinal markings are used to separate traffic flows in the same direction and are also used as a right-side edgeline. Red markings are used for roads that should not be entered or used. Blue markings are used for handicapped parking spots (*MUTCD* 2009).

Pavement marking color is evaluated through subjective or objective approaches. The subjective approach is based on experienced practitioners who judge the sample color using a pre-designed rating list of colors or "reference colors" painted on chips or charts for matching. The objective approach uses colorimeters or spectrophotometers to describe any sample using color coordinates.

The FHWA uses the Commission Internationale de l'Eclairage (CIE) color space which was developed in 1931 to describe colors to specify the color ranges of pavement markings and other retroreflective roadway materials (e.g., signs). The CIE methodology is capable of standardizing color attributes and replicating any color by defining an x and y coordinate for that color (Thomas-Meyers and Nagy 2010; Migletz and Graham 2002; Ford and Roberts 1998). Figure 2.2 depicts the acceptable color regions for the white and yellow daylight chromaticity coordinates based on the FHWA standards within the CIE 1931 x, y chromaticity diagram (Wang 2010), and four corners of each color area are shown in the table of Figure 2.2. Also, international specifications such as ASTM D 6628, ASTM D 1729, and ASTM D 2244 provide important color standards and practices related to the color measurement and evaluation of pavement markings.

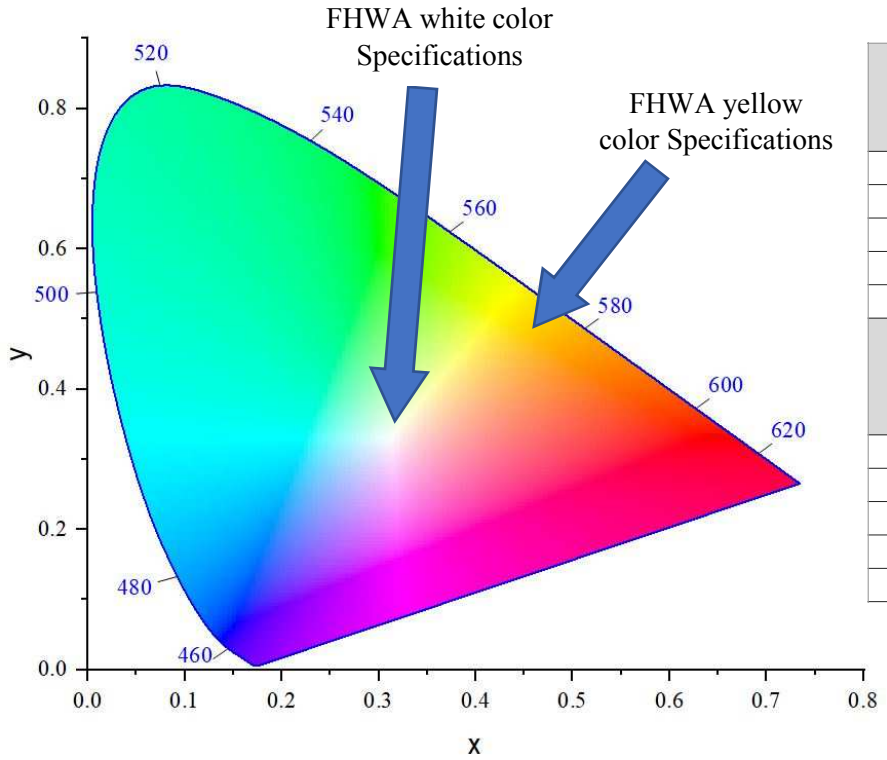

Yellow Daytime Chromaticity Coordinates (Corner Points)	
x	y
0.560	0.440
0.490	0.510
0.424	0.440
0.460	0.400
White Daytime Chromaticity Coordinates (Corner Points)	
x	y
0.355	0.355
0.305	0.305
0.285	0.325
0.335	0.385

Figure 2.2: FHWA color requirements for white and yellow markings

1.3.2. CIE Lab color scale

The CIELab color scale was developed based on CIE XYZ (1931) and suggested by CIE in 1976 with the intention of providing a uniform color scale that could easily be used to compare colors. To identify the color difference using the CIELab 1976 coordinates, total change in color (ΔE_{ab}) and difference in lightness (ΔL) were calculated using Euclidean distance Equations 1 and 2, respectively:

Equation 1: The overall color difference between the three coordinates

$$\Delta E_{ab} = \sqrt{\Delta L^2 + \Delta a^2 + \Delta b^2} \quad (1)$$

$$\Delta E_{ab} = \sqrt{(L_2 - L_1)^2 + (a_2 - a_1)^2 + (b_2 - b_1)^2}$$

Equation 2: The difference in lightness

$$\Delta L = \sqrt{\Delta L_{Reference}{}^{2} + \Delta L_{Sample}{}^{2}} \quad (2)$$

The change in color between the initial (sample 1) and final (sample 2) values is represented by three parameters: ΔL, Δa, and Δb. As L becomes more positive, the sample is lighter than the standard or initial value, indicating that the sample is illuminating (+ = lighter, - = darker). A positive Δa means that the sample is redder than standard, while a negative Δa means that the sample is greener. Along the vertical axis, a positive Δb means that the sample is yellower than the standard and a negative Δb means the sample is bluer. Figure 2.3 depicts the CIELab 1976 coordinates and shows an example of how the ΔE_{ab} was calculated using the previously mentioned equations (Molino et al. 2013).

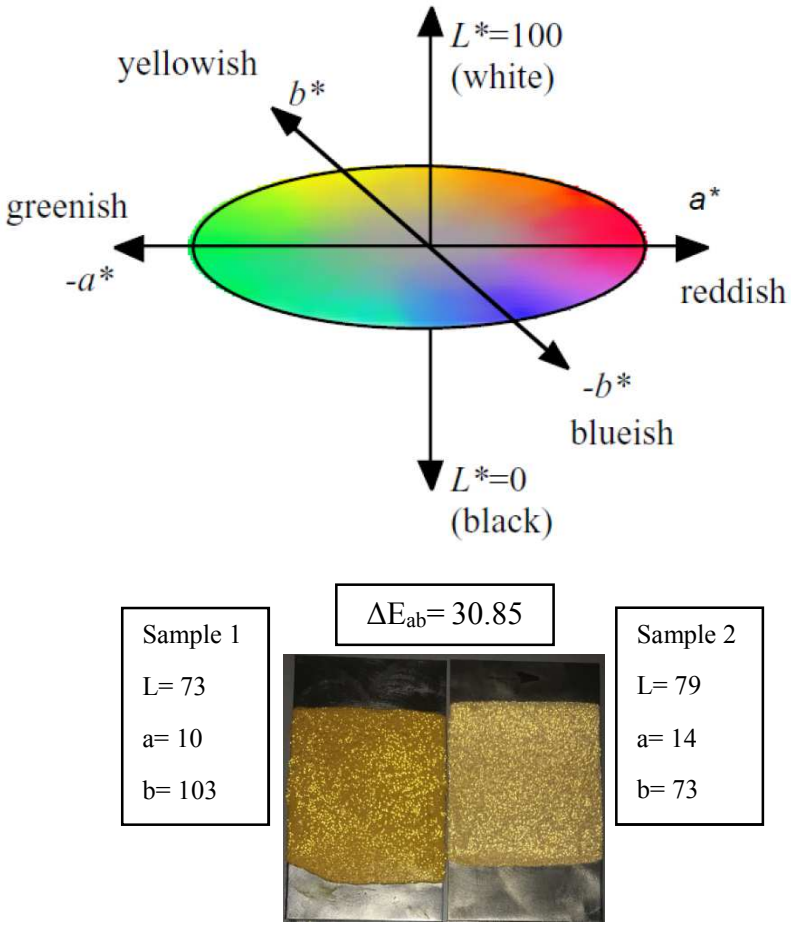

Figure 2.3: Illustration of the CIELab color space

2.3. Pavement Marking Materials

Most pavement marking materials consist of three major components: binder, pigment, and retroreflective material. The binder refers to the adhesive element that sticks to the pavement surface and provides pavement markings with the ability to resist abrasion caused by traffic and road maintenance activities (e.g., snow plowing). The pigment refers to the color used, and the retroreflective material (such as glass beads) enhances the visibility of the pavement markings (Wang 2010).

Several types of pavement marking materials are currently used in the highway industry of the United States. Pavement marking materials can be classified as either nondurable or durable. Nondurable markings often have an expected service life of less than

one year and include conventional solvent-based and water-based paints (waterborne); nondurable markings are identified by the solvent used, method of application, and drying time. On the other hand, durable markings include many chemical compounds such as epoxy, thermoplastics, methyl methacrylate, polyurea, polyurethane, and tape (Craig et al. 2007; Schalkwyk 2010; Migletz et al. 2001). The term "removable" is occasionally used in lieu of durable (e.g., tape), especially when pavement markings are classified based on service purposes. In 2002, Migletz and Graham studied 16 types of pavement marking materials available on the market; most of these materials were durable pavement markings (Sitzabee et al. 2009; Wang 2010). Figure 2.4 shows a comprehensive pavement marking material classification (Schalkwyk 2010).

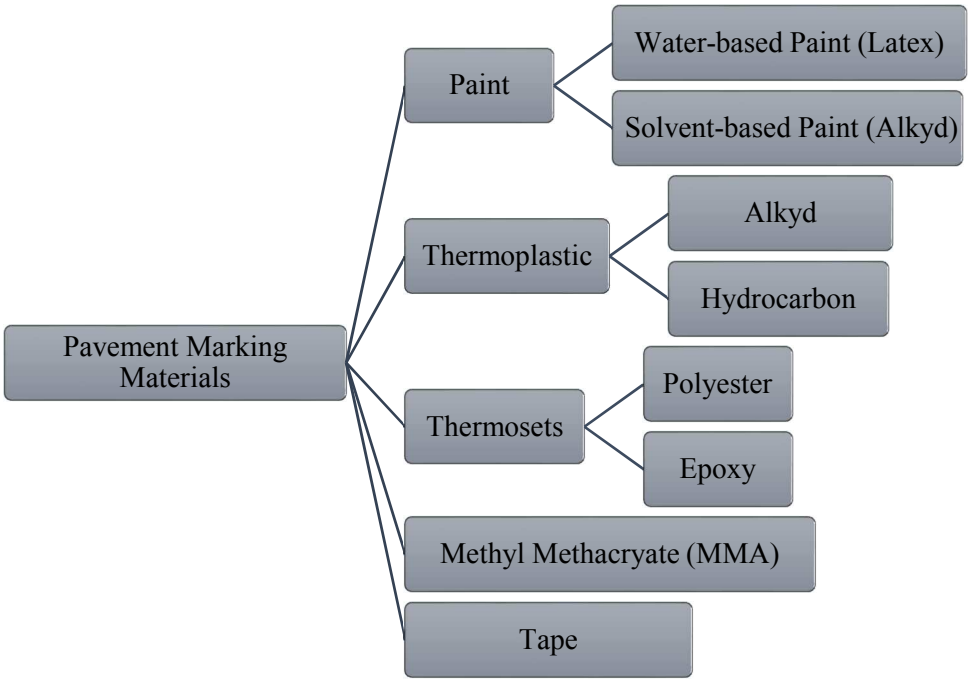

Figure 2.4: Comprehensive pavement marking material categorization

2.3.1. Non-Durable Markings

2.3.1.1.Waterborne paint (Latex)

Waterborne markings (which can also be called traffic paint or Latex) often have less than one year of expected service life. Although paint has a shorter expected service life than other markings, this material is widely used on rural roads due to its inexpensive cost and eco-friendly attributes. Waterborne paints, in particular, are friendly to the environment and safer

than solvent-based paints because they contain less volatile organic compounds (VOCs) and are characteristically less than 0.15 kilogram per liter (1.25 pounds per gallon) of VOC. The drying set-to-touch time for most waterborne paints is longer than solvent-based paint times, especially when applied during high humidity weather. In practice, after exposure to traffic, weather, and snow plowing, waterborne markings wear off and lose their retroreflectivity faster than other pavement marking materials. For this reason, many studies have recommended that waterborne markings are more suitable for low-volume roads or used as an interim pavement marking material. The waterborne paint visibility can be enhanced by adding glass beads to the binder. These glass beads can be pre-mixed with binder or sprayed on top of the binder during application while the markings are wet (Schalkwyk 2010; Jiang 2008b; Gates et al. 2003).

2.3.2. Durable Markings

Durable markings include various chemical compounds such as epoxy, thermoplastics, methyl methacrylate (MMA), poly urea, poly urethane, and tapes. Each pavement marking material has its own unique properties which differ when used on different surfaces and in different climates (Schalkwyk 2010).

2.3.2.1. Solvent-based paint (conventional paint or alkyd)

Solvent-based paints are considered durable paints and commonly consist of three ingredients: binder resin, pigments and fillers, and additives (solvents). Some popular solvents are: alkyd, acrylic, and chlorinated polyolefins. Glass beads can either be pre-mixed with binder before application or sprayed on top of the binder during application while the marking is wet. Solvent paints can be identified by the solvent used, method of application, and drying time.

The pavement marking industry is rapidly evolving because of restrictions that were imposed from updated governmental decisions related to environment protection or regarding safety issues. As a result of the Clean Air Act, which intended to control air pollution, FHWA published a memorandum that defined the impact of a new Environmental Protection Agency (EPA) rule on the usage of pavement marking material. The reduction of VOC material in pavement markings directly affected the usage of solvent-based markings in the market. Consequently, water-based paints which have low VOC content and other environmentally-

friendly pavement marking materials increased in demand at the expense of solvent-based paints. This change happened gradually during the past two decades (Jiang 2008b; Sadid et al. 2010).

2.3.2.2.Thermoplastic

Thermoplastic markings are the second most widely used material in the United States following waterborne markings. Thermoplastic pavement markings are made of several components including binder, glass beads, titanium dioxide (TiO_2), and filler such as carbon carbonate. These markings can be alkyd (a naturally occurring resin) or hydrocarbon (a petroleum-derived resin). Alkyd resists oil but it is sensitive to heat. Hydrocarbon thermoplastic is relatively more heat-stable compared to alkyd thermoplastic. Thermoplastic materials are initially in a granular or block form. The solid-state changes to liquid when the material temperature is increased to more than 204 ^{o}C (400 ^{o}F). The material is then sprayed, extruded on top of the pavement surface, or melted-in-place as preformed thermoplastic which is usually supplied in large pieces and can be used as a longitudinal rumble strip, transverse marking, or marking symbol. Both forms are heated on site to provide adhesion with the pavement surface (Carlson et al. 2013 and Wang 2010). In general, thermoplastic pavement markings adhere well with the asphalt pavement texture but can prematurely lose their adhesion with a concrete pavement texture. Thus, sealers are required prior to the installation of thermoplastic markings on concrete pavements in order to ensure an appropriate bond to the concrete surface (Schalkwyk 2010). The thickness of the thermoplastic markings varies between 2.54 to 3.81 millimeters (0.1 to 0.15 inches). The application of thermoplastic in cold regions is limited due to the poor bond between the material and pavement surfaces at low temperatures. Thermoplastic material formulation, appropriate surface cleaning, moisture removal, and priming before installation (if needed) are factors that should be considered for successful thermoplastic application and performance on concrete pavement (Jiang 2008a).

2.3.2.3.Tape

Flat preformed tape and profiled preformed tape are two commonly used tapes available in the industry. Tape generally has a high initial price and is mostly used for small areas. Newly installed tape has a higher initial retroreflectivity value than waterborne paint.

Tape is a durable pavement marking which can last up to eight years if applied properly, but it loses its retroreflectivity rapidly, so the recommended service life is three years. Tapes are free from VOCs but the adhesive that is used as a primer or for surface preparation may have VOC content (Jiang 2008b).

2.3.2.4.Epoxy

Epoxy is produced onsite by mixing two material parts. Part A (base) includes resin, pigment, extenders, and fillers while part B (hardener) is a catalyst used to speed up the setting time. Glass beads are also intermixed with the first material before application or applied on the stripe while it is still wet. Epoxy paints are highly durable and can be successfully used on both asphalt and concrete pavements because they provide exceptional adhesion to both pavement surfaces. Epoxy pavement markings have modest cost compared to other types of pavement markings and can last up to four years but they have less attractive color over time when exposed to intense ultraviolet light. The long drying time of epoxy during installation limits its use under high traffic volumes. Despite this disadvantage, some survey studies have shown that many transportation agencies are using epoxy on concrete pavement with high traffic volumes (Jiang 2008b). Modified epoxy or urethanes have comparable performance properties to epoxies; they are considered to be more durable than epoxies, have faster curing time, and have more color stability when exposed to ultraviolet rays (Carlson et al. 2013 and Wang 2010).

2.3.2.5.Methyl Methacrylate (MMA)

Methyl Methacrylate pavement marking is considered to be a nonhazardous material because it contains negligible VOCs. MMA markings often have an expected service life of more than three years. MMA pavement markings can be applied in cold climates and are resistant to oil, anti-freeze, and other chemicals usually found on pavements. MMA material adheres well on both asphalt and concrete surface textures (Gates et al. 2003 and Jiang 2008b).

2.3.2.6.Polyester

Polyester pavement markings are like epoxy markings; they are typically formed onsite by mixing two groups of materials before installation. Glass beads are then sprayed on top of the stripe surface while it is still wet. Despite the low VOC content of polyester

pavement markings, the chemicals used for producing the material are classified as hazardous. Polyester pavement markings are preferably used on asphalt pavements (Bahar et al. 2006 and Jiang 2008b).

2.3.2.7.Polyurea

Polyurea is a relatively new pavement marking material compared with those previously listed. Polyurea is produced onsite as a two-component material similar to epoxy, polyurea, and MMA but its part B is a cross linker (which is used to link one polymer chain to another). Glass beads are sprayed on the stripe while it is still wet to enhance retroreflectivity. Some manufacturers add a reflective element layer such as ceramic beads to boost retroreflectivity. Polyurea has a relatively good color stabilization when exposed to ultraviolet light. Under all temperatures, polyurea pavement markings have a low setting time and take 3 to 8 minutes to dry. It works efficiently on both asphalt and concrete pavements but the application of polyurea pavement marking material requires special equipment and higher cost (Jiang 2008).

2.3.3. Retroreflective Materials

2.3.3.1.Glass Beads

Since only a small portion of light is retro-reflected to the driver's eyes from the pavement marking, installing glass beads is a widely-used practice to increase the amount of reflected light which in turn increases driver visibility in dark and challenging conditions. Glass beads are small globular glass balls which are used to improve the retroreflectivity of any pavement marking material. Coating the glass bead surface (treated glass beads) allows them to sink into the paint to have continuous retroreflectivity while the paint is wearing. Glass beads can be intermixed with binding material before or during the application of the pavement marking by dropping them on top of the painted marking material while the marking is wet (Jiang 2008).

There are some glass bead-related factors that distinctly influence pavement marking retroreflectivity values such as the refractive index (RI), diameter, roundness, glass bead embedment depth in the paint, and glass bead density in the paint. The RI for glass beads used in pavement markings commonly ranges from 1.5 to 2.4. The Standard Specification for Glass Beads Used in Pavement Markings (AASHTO M 247-13) requires a refractive index between

1.50 and 1.55. Generally, the chemical and physical characteristics of glass material govern the glass bead refractive index. Also, other glass bead physical properties such as gradation (diameter) and roundness dictate the interaction between the glass beads and the marking binder which in turn influences the glass bead distribution and embedment scenarios on the marking surface. Regarding glass bead embedment, it has been found that the best retroreflection provided by glass beads occurs when 40% of the bead body appears above the marking surface and 60% of the bead body is secured under the marking surface. The density of the installed glass beads also has a significant effect on the retroreflectivity; lower glass bead density leads to lower pavement marking retroreflectivity and yellow pavement markings will have significantly lower retroreflectivity values than white pavement markings despite the same glass bead density because yellow markings absorb more light than white markings (Smadi 2013).

Five types of glass beads (I, II, III, IV, and V) are classified by the American Association of State Highway and Transportation Officials (AASHTO) under the Standard Specification for Glass Beads Used in Pavement Markings (AASHTO M 247). Type I is known as the standard bead or standard gradation, while types II, III, IV, and V have respectively larger bead gradation and are known as modified gradations.

Digital cameras and retroreflectometers were used to collect field or laboratory data related to glass bead studies. Bead density is calculated directly from photos. Today, computer software is used to ease the task of counting glass beads in high resolution pictures (Migletz and Graham 2002 and Zhang et al. 2009). For example, NCHRP Report 743 used high-resolution cameras and retroreflectometers to develop a laboratory procedure that can predict initial pavement marking retroreflectivity in the field from glass bead quality. A drawdown test procedure was developed as part of this research in the laboratory for measuring samples of pavement markings with different characteristics. Pavement markings with different thicknesses were painted on flat objects and glass beads were dropped on top of the wet markings in a consistent manner and evaluated (Smadi 2013).

2.4. Performance Evaluation Criteria

Two criteria are commonly used to evaluate marking performance over time: visibility and durability. The visibility of pavement markings refers to its brightness while durability

measures resistance to damage due to traffic, snowplowing, and environmental effects (Jiang 2008). During daytime conditions, drivers recognize pavement markings mostly by the color contrast, but during nighttime conditions drivers will discern pavement markings by the luminous contrast between the pavement markings and the dark road surface, which is determined by pavement marking retroreflectivity.

2.4.1. Retroreflectivity

The term retroreflectivity describes how the light that originated from vehicle headlights illuminates the visible pavement marking surface and then returns to the driver's eye. These retroreflected light rays assist roadway users in dark conditions with significant information such as: roadway alignment, vehicle lateral position, and other driving-related factors (Parker and Meja 2003). Retroreflectivity is measured in units of millicandelas per square meter per lux ($mcd/m^2/lux$) which is expressed as the coefficient of retroreflected luminance (R_L). In past research, pavement marking retroreflectivity has been extensively used as an important indicator in analyzing pavement marking material performance and cost-effectiveness (Zhang and Wu 2010).

Retroreflectivity performance is evaluated either by an objective approach (quantitative) using retroreflectometers or by a subjective approach (qualitative) by implementing visual inspections (Sitzabee 2008). The objective measures of pavement marking performance are more popular than subjective assessments and have been in service for many years because of their higher accuracy and ability to collect a large amount of data in shorter time. Based on the driver's viewing geometry, different standards have been used to measure pavement marking retroreflectivity using retroreflectometers, such as 12-meter (39.4 ft) geometry or 30-meter (98.4 ft) geometry. The American Society for Testing and Materials (ASTM) has standardized the "30-meter geometry" to be used in measuring pavement marking retroreflectivity based on the opinion that 30 meters is the farthest distance drivers can clearly observe pavement markings on the road at night. Currently, most retroreflectometers are using the 30-meter geometry for measuring pavement marking retroreflectivity (Kopf 2004 and Lopez 2004). Figure 2.5 graphically illustrates the principle of the 30-meter geometry using a handheld measuring device which simulates how the vehicle's headlight is reflected by the glass beads to the driver's eyes, assuming the vehicle

headlight shooting angle to be equal to 88.76 degrees (entrance angle) and the driver's observation angle to be equal to 1.05 degrees (Parker and Meja 2003 and Craig et al. 2007). The ASTM E 1710 describes retroreflectometer geometry in more detail.

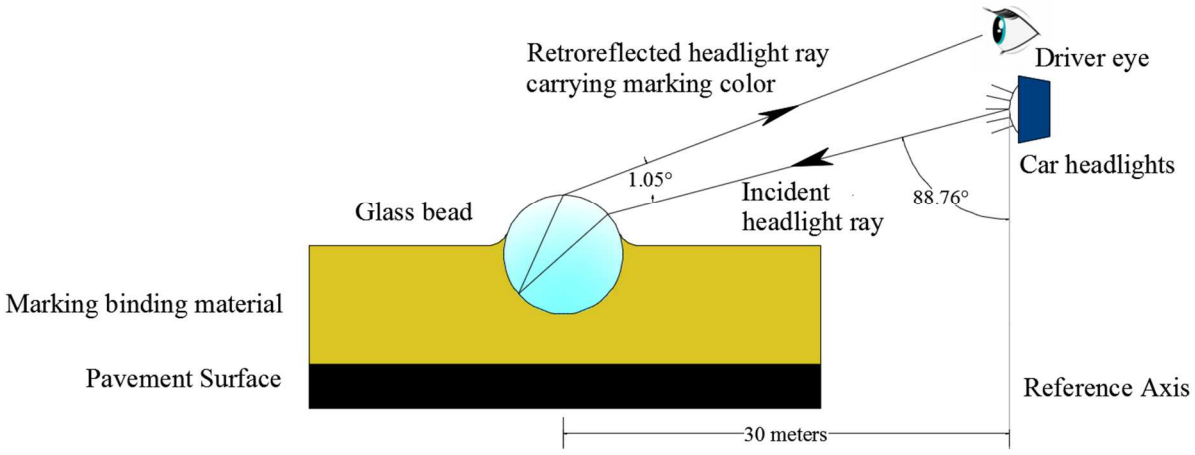

Figure 2.5: Basic Principles of Pavement-Marking Retroreflectivity

2.4.1.1.Contrast ratio

The difference between two colors can be defined as the color contrast. As colors contrast in hue and saturation, they can also contrast in retroreflectivity. The daytime contrast is measured by color difference between the roadway surface and marking colors, but the nighttime contrast is calculated as a ratio using the retroreflectivity of the pavement marking and the surrounding road surface (Benz et al. 2009). This nighttime contrast ratio (CR) is represented by Equation 3.

Equation 3: Nighttime contrast ratio

$$\mathrm{CR} = \frac{\left(R_L(\mathrm{Marking}) - R_L(\mathrm{Pavement\ surface})\right)}{R_L(\mathrm{Pavement\ surface})} \quad (3)$$

2.4.1.2.Handheld vs. mobile retroreflectometers

Portable retroreflectometers are used to measure the marking retroreflectivity in the field or the laboratory. There are two basic types of portable retroreflectometers: handheld and mobile (vehicle-mounted). The handheld retroreflectometer can be easily used in the laboratory due to its small size and light weight and does not require extensive training, but it is inconvenient when used to take a large number of measurements or on high-traffic volume

highways. On the other hand, mobile retroreflectometers are capable of taking a large number of measurements in a short period of time at highway speeds without operator exposure to traffic. However, a mobile retroreflectometer is expensive compared to a handheld retroreflectometer and requires both a highly trained operator to take measurements and more periodic maintenance than handheld units (Lopez 2004).

2.4.1.3.Retroreflectivity Thresholds

In order to control the quality of pavement marking retroreflectivity, a minimum value should be determined and set as standard. This minimum retroreflectivity value represents the lowest acceptable level of pavement marking retroreflectivity that can be allowed on roads as a measure of providing safety to drivers. Several studies have been sponsored by FHWA after the United States Congress required that a minimum requirement for highway pavement markings retroreflectivity be established in the Manual on Uniform Traffic Control Devices (MUTCD). At this time, no final standards have been published in the MUTCD (Zhang and Wu 2010; Ozelim and Turochy 2014; Bektas et al. 2016). Table 2.1 shows the proposed MUTCD minimum retroreflectivity values for longitudinal pavement markings.

Table 2.1: Proposed minimum retroreflectivity values in mcd (MUTCD2010)

Roadway Type	Posted Speed (mph)		
	≤30	35–50	≥55
Two-lane roads with center line markings only	N/A	100	250
All other roads	N/A	50	100

The task of establishing a reasonable and manageable minimum retroreflectivity threshold standard is complicated due to the wide range of factors influencing the final decision. These factors relate to the uncertainty of the exact relationship between driver safety and pavement marking retroreflectivity, human visibility awareness, and the unpredictability of service life of different pavement markings materials under different weather conditions.

2.4.2. Durability

The durability of pavement marking material is defined as its ability to withstand the reasons behind deterioration over time. The two approaches used to measure pavement marking durability performance are either by estimating the proportion of remaining material

by the naked eye from a targeted area on the pavement surface or by testing the cohesiveness between the marking material and the pavement surface. In the first approach, the amount of material remaining on the pavement surface is measured on a scale of 0 to 10 (with 0 indicating that the material has been totally removed and 10 indicating that 100% of the material is still remaining). Figure 2.6 shows the concept of the durability-rating graphical procedure used by the FHWA (Jiang 2008a and Migletz et al. 2002).

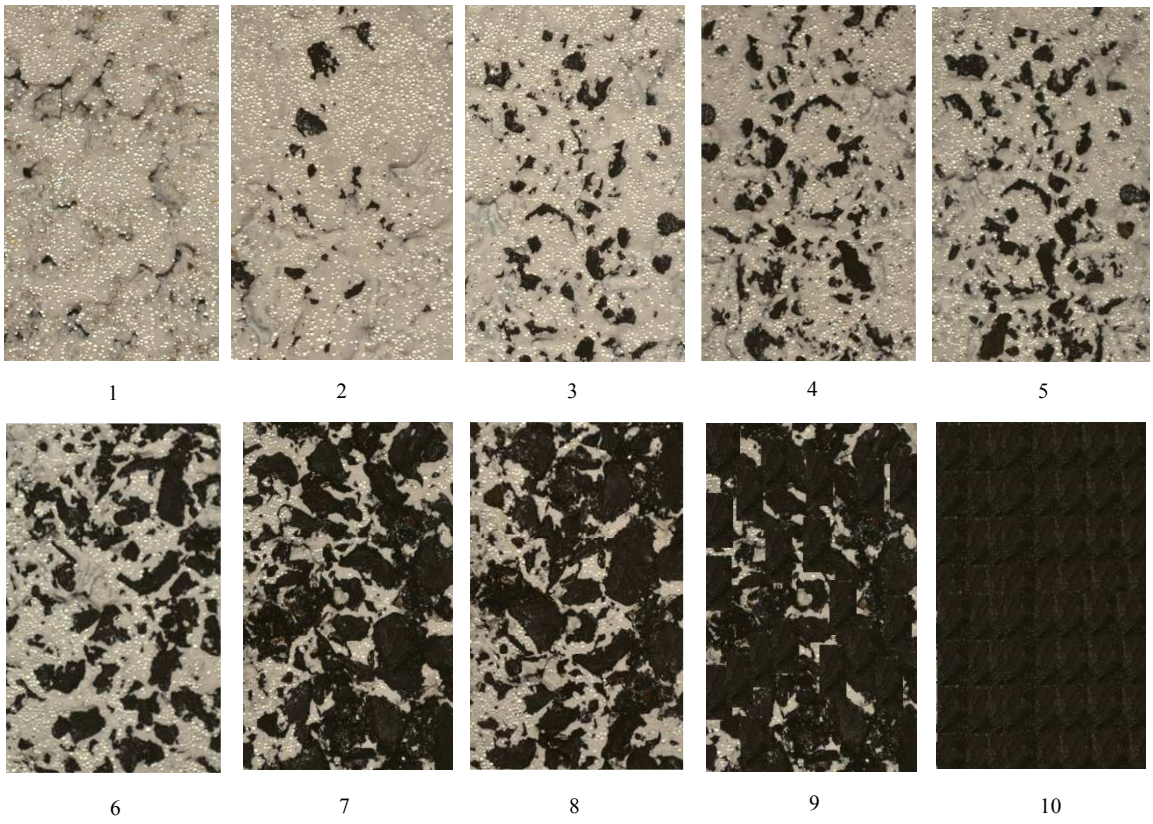

Figure 2.6: Subjective durability rating procedure

2.5. European standards

The European standard for pavement markings (IS EN 1436) identifies the performance of both white and yellow pavement markings based on luminance (color), daytime visibility, nighttime visibility and skid resistance combined with durability. There are six classes of dry retroreflection performance under car headlamp illumination (in ascending order from R_0 to R_5) and five classes of pavement markings for wet conditions. In addition, reflection in daylight or under street lighting (Q_d) has three classes. In terms of color, there are

six classes of luminance performance (β value). Color coordinates must fall within defined squares on the chromaticity diagram for the white and yellow colors. The skid resistance (SRT value) which was carried out using the standard British pendulum apparatus should range from S1 (≥ 45) to S5 (≥ 65) (EN 2018).

2.6. Pavement Marking Specifications and Material Selection Criteria

In the US, transportation agencies follow the Manual on Uniform Traffic Control Devices for Streets and Highways (MUTCD) in their policies related to pavement marking locations, patterns, and colors. Standard specifications for pavement marking material are published by the Federal Highway Administration (FHWA), American Society for Testing and Materials (ASTM), and other transportation agencies. Each state agency develops its own criteria for selecting suitable pavement marking materials to fulfill project needs. There are three types of specifications that are often used in pavement marking projects and research and these specifications include: 1) prescriptive/material specifications, 2) performance-based specifications, and 3) warranty provision specifications. State agencies rely on several factors including line type (e.g., longitudinal, transversal, or auxiliary line), pavement surface and condition, traffic volume and speed, material service life, weather (e.g., snowfall), and lane geometry to choose an appropriate pavement marking material. According to NCHRP Synthesis 306, most states in the United States use the line type criteria followed by pavement surface type to select the pavement marking material that fulfills the purpose and location. Three types of pavement surfaces were classified: Asphalt Concrete (AC), Portland Cement Concrete (PCC), and PCC bridge decks. Traffic volume was classified into four categories based on average daily traffic (ADT), and each material was used with a specific level of ADT. Highway type was ranked as the fourth factor with three different classifications for selecting the marking material (Migletz and Graham 2002).

The states of Kansas, Washington, and Wisconsin use marking service life as a factor when selecting the appropriate type of marking. For example, the Kansas Department of Transportation (KDOT) uses a material service life factor ranging from less than one year to 7 years in its policies. The NCHRP Synthesis 306 summarized all factors used in selecting pavement-marking materials in more detail (Migletz and Graham 2002).

In performance-based specifications, the pavement marking material is required to maintain a specified level of retroreflectivity, durability, and color. Some state agencies depend on the outcomes of the National Transportation Product Evaluation Program (NTPEP) test-deck evaluation which should be constructed in accordance with ASTM D713 when assessing these requirements (Chrysler et al. 2006; Migletz and Graham 2002; AASHTO-NTPEP 2019).

2.7. Pavement Marking Cost

State DOTs consider pavement markings to be one of the most effective low-cost devices for improving highway safety (Miles et al. 2010). Each pavement marking material has its own unique method of installation, different lane closure durations, and service life. Consequently, each material has a different cost. Reducing cost by selecting a suitable pavement marking material that meets specifications is of great interest to state DOTs. Thus, a cost-benefit analysis should be implemented to determine how well, or how poorly, each option performs. Several factors are considered when selecting the pavement marking material such as climate, service life (durability), and cost. When calculating cost, it is crucial to consider not only the material cost but also the cost associated with staff time and the use of installation equipment. In addition, the life-cycle cost of the pavement marking material is directly affected by its durability and its ability to resist surrounding effects. In other words, marking materials that have a short lifespan need to be restriped more frequently (Gibbons et al. 2013). Also, retroreflectivity has been broadly identified in previous studies as a significant factor in analyzing the cost-effectiveness of the marking material.

In the literature, life-cycle cost analysis (LCCA) studies were carried out to assist in selecting the best alternative of pavement marking material. These studies analyzed several potential factors such as material cost, appreciation cost, delay cost, and societal crash costs during the implementation of the LCCA for road marking projects. For example, Zhang and Wu conducted a 30 year LCCA between thermoplastic and paint and found that thermoplastic costs 3.1 times as much as the paint under low traffic volume roads (2,000 vph) and 2.0 times as much along high traffic volume roads (4,000 vph) (Zhang and Wu 2010).

2.8. Installation and Removal

2.8.1. Construction Practices Specifications

All pavement marking widths, patterns, or locations must be applied according to the MUTCD and design plan documents. When final marking patterns and locations are identified, a specific procedure must be carefully followed according to the Standard Specifications for Construction of Roads and Bridges on Federal Highway Projects (FP-14), published by FHWA for pavement marking construction. A summary of the procedure is listed below:

- Obtain approval from competent authorities before removing or applying markings.
- Removal of temporary markings, or any other materials, may impede the installation process.
- Apply markings on the surface according to manufacturer recommendations.
- Glass beads must be applied instantly after marking installation.
- Clean tracking marks and defective markings.
- Protect markings from traffic until completely dried.

Important specification factors that should be considered before applying pavement markings include pavement temperature, application thickness, bead types, and application rates (Migletz and Graham 2002).

2.8.2. Pavement Markings Removal

Pavement surface preparation commonly starts before the striping procedure and involves activities such as old marking removal by grinding, scraping, or burning of surfaces followed by installation of bonding materials or primers. Old pavement markings are ideally removed from the pavement surface without leaving reflective marks which could confuse drivers. Grinding old markings off of the pavement surface is a common approach but leaves a trace on the pavement surface and is more expensive than other approaches. Old markings can be burned off using a propane torch at a high temperature but this approach could severely damage the pavement surface. Even though each method can be effective under different circumstances and marking types, sandblasting is the most effective method compared to the other options. Darkening the treated area is a second option, and chemical

compounds made of kerosene, and linseed oil, and road oil, or lubricating oil are used for darkening pavements (Migletz and Graham 2002).

2.9. Pavement Marking Evaluation

The pavement marking service life can be quantified as the time or the number of traffic passes that degrades a specific performance measure (e.g., initial retroreflectivity or durability) until it reaches a defined minimum threshold value. However, the service life of particular materials varies greatly.

Current standards for evaluation of pavement marking performance is based heavily on the National Transportation Product Evaluation Program (NTPEP) test-deck method. The current practice is to construct a "testing deck" by applying different pavement marking materials across a roadway and then monitoring the degradation (or wear) over time and under continuous traffic loading. Like other traffic control devices, maintaining pavement markings that are highly visible and long lasting presents a major challenge to DOTs. In the United States, the NTPEP test deck is the commonly used pre-qualification test (wear testing) that checks the endurance and determines the service life of pavement marking products. The performance of the pavement material is monitored and reported for a period of up to three years depending on the type of pavement marking material (Pike and Songchitruksa 2015). In the test deck, various types of pavement markings are evaluated on both Hot Mix Asphalt (HMA) and Portland Cement Concrete (PCC) pavements in different climates using the standard recommended practice as outlined by AASHTO. Field test data (performance measures) are conducted in a timely manner under the NTPEP test deck. These tests include: daytime luminance (luminance coefficient in diffused illumination) and nighttime retroreflectance (using a retroreflectometer, color using CIE coordinates, and durability (Donnell et al. 2009 and Wang 2010).

Pavement marking materials are tested for durability, performance, and economic feasibility (e.g., cost-benefit analysis) before they can be used on roads. Although the NTPEP test deck provides an evaluation that utilizes live traffic under ideal weather conditions found within the region of the test deck, this method requires significant time and resources in addition to safety-related issues such as exposing technical staff to road hazards while applying the marking materials and during data collection of measurements and any road

closure consequences. This practice also has several limitations given the dynamic nature of the pavement marking industry and changes to the chemical composition of pavement marking materials complying with Environmental Protection Agency (EPA) requirements. For this reason, there is value to developing an accelerated laboratory test procedure that can provide a shorter field-representative assessment of pavement marking material performance while maintaining system reliability. An accelerated laboratory test should simulate environmental and operating conditions, including those in the Pacific Northwest where snowplowing is common.

2.9.1. Test Decks Retroreflectivity vs. Longitudinal Retroreflectivity

Another NTPEP test deck drawback is that vehicle tires are typically travelling adjacent to the longitudinal pavement marking and not directly over it. Transverse test decks may be beneficial for comparing products, but their outcomes cannot be fully representative of longitudinal pavement marking performance because of the difference in orientation. For this reason, the exact relationship between pavement markings subjected to accelerated wear testing or test decks and longitudinal pavement markings is still relatively unknown. Pike and Songchitruksa (2015) developed an exponential decay model for different marking materials to predict the retroreflectivity value of longitudinal pavement markings from transverse pavement marking test deck data in the state of Texas; the limitation of using this model was that retroreflectivity data from a transverse test was needed to apply the model (Pike and Songchitruksa 2015).

2.9.2. Evaluation of Pavement Markings and Accelerated Laboratory Testing

Accelerated pavement marking wear testing simulators have been proposed and previously used as a research tool. Accelerated wear testing simulators provide pre-qualifying pavement marking tests in controlled environments over a short time period (Vollor and Hanson 2006; Donnell et al. 2009; Hawkins et al. 2015). These simulators can be categorized as full-scale simulators or small-scale simulators. The German Federal Highway Research Institute (BASt) wear simulator, and the Asociacion para el Estudio de las Technologicas de Equipamiento de Carreteras (AETEC) wear simulator are considered full-scale while the Model Mobile Load Simulator (MMLS) and the Three Wheel Polisher Device (TWPD) are

considered small-scale accelerated pavement tests (and small enough to be operated in both a laboratory or on-site).

The BASt accelerated wear testing simulator uses full-size tires to polish pavement marking surfaces. It can test up to 72 samples by applying more than one wheel on a rotating steel turntable (with a 21 foot diameter). One week of simulation using the BASt simulator is approximately equal to one year of real traffic loadings. Based on the German specifications, after the sample meets baseline material property requirements, prototype tests are performed to evaluate each product. These tests are: daytime visibility (luminance coefficient in diffuse illumination), nighttime visibility (coefficient of retroreflected luminance), durability, drying time, and skid resistance. By comparison, four Spanish marking companies have developed the AETEC wear simulator. Similar to the BASt accelerated wear simulator, the AETEC simulator uses the same units for the endurance test and can evaluate up to 72 test samples and apply approximately 1 million cycles per week (Donnell et al. 2009).

The MMLS and TWPD were developed in the United States to study and accelerate pavement testing using a more affordable approach. The MMLS utilizes wheel contact stresses for evaluating pavement construction material performance. Unlike the European accelerated pavement testing machines, the MMLS has smaller size and can be used in both an actual and controlled environment. The MMLS was designed to apply up to 7,200 cycles per hour. The feasibility of using the MMLS to evaluate pavement markings and Raised Pavement Markers (RPM) performances was conducted, and it was found that the MMLS was a feasible method (Choubane et al. 2006 and Donnell et al. 2009). The TWPD was originally designed to evaluate skid resistance of asphalt pavements; however, it recently evaluated pavement markings in a research study funded by the Illinois Department of Transportation and preliminary results demonstrated this method produces gradual deterioration of pavement markings. Historically, the BASt, AETEC, and MMLS accelerated wear testing simulators were used to provide pre-qualifying pavement marking tests in controlled environments over a short time period. Thus, laboratory accelerated wear testing can be achieved in a much shorter time, is less expensive, and is safer because road closure is not necessary.

The TWPD is laboratory equipment designed to simulate and accelerate the friction forces that stochastically result from the interaction between car tires and the roadway

surface. The device was originally designed to minimize the cost of testing the aggregate's proclivity to be polished and to establish a laboratory-based procedure. The TWPD has also been used to simulate the abrasion of the pavement surface due to traffic loading to study skid resistance of pavements (Kassem et al. 2013). Other equipment such as the Circular Texture Meter (CT Meter) and the Dynamic Friction Tester (DF Tester) have been used to evaluate the physical properties of the pavement texture and friction forces applied on concrete or asphalt slabs (Vollor and Hanson 2006). Using the TWPD, painted asphalt slabs were fixed under three rotating wheels for a varying number of cycles to simulate traffic passing-over behavior. This method was recently developed in research for evaluating all-weather pavement markings in Illinois. The preliminary results of this study showed that this method produced gradual deterioration of pavement markings, but there is room for improvement (Hawkins et al. 2015; Heitzman et al. 2015; Heitzman and Erukulla 2011).

2.10. Factors Impacting Marking Performance

Longitudinal pavement markings are used to assist drivers in detecting the right road path and keep them in safe lateral positions. Visibility factors that are related to driver vision capabilities (to fulfill the purpose of markings), and durability factors which are related to the material's ability to withstand damage due to weather and abrasion (to take advantage of the material to the maximum extent possible) influence pavement marking performance. Both categories are described in detail in Table 2.2 (Benz et al. 2009b). Such factors should be considered when evaluating the performance of pavement markings in the laboratory to replicate traffic operations, roadway maintenance activities, and weathering effects responsible for pavement marking deterioration over time.

Table 2.2: Factors impacting pavement marking performance

Visibility Factors	Durability Factors
Color contrast between pavement marking and the surrounding environment	Pavement marking material type
Marking color (white or yellow)	Pavement marking thickness and width
Pavement color	Pavement type (PCC or ACC)
Retroreflectivity of pavement marking material	Pavement texture (e.g., surface roughness, and surface porosity)
Pavement texture	Traffic volume (AADT)
Presence of pavement markings	Weathering process
Pavement marking material type	Maintenance activities (e.g., repainting and snow removal)
Pavement marking width (width, 4, 6, or 8 inches)	Marking location (edge line, centerline, lane line)
Vehicle headlamp type	Roadway geometry (horizontal curves, weaving areas, etc.)
Viewing geometry	
Ambient lighting conditions	

In studying the factors that influence pavement marking performance, the Texas Department of Transportation (TxDOT) developed another classification system which divided the factors influencing pavement marking performance into two major groups: external factors and internal factors. The external factors are categorized by pavement surface characteristics, traffic characteristics, and environmental conditions. These three categories play an important role during the material selection procedure. The internal factors are related to the properties of the material itself (Lopez 2004).

In addition, seal coat and pavement microsurfacing treatments negatively affect the bond between the marking material and the pavement surface because these types of surfaces have a certain degree of rock loss which contributes to a loss of pavement marking material. Also, the coarse surface condition of the seal coat influences the ability to place the marking material at a sufficient thickness which in turn influences the marking material performance and glass bead placement (Hawkins and Smadi 2011).

2.10.1. Traffic Impact on Pavement Marking Performance:

Pavement marking retroreflectivity deterioration can be modeled as a function of time, environmental condition, and cumulative traffic passage (CTP) after its application (Migletz et al. 2001 and Onyango et al. 2014). The marking service life is defined as the time duration or the CTP required for the retroreflectivity of the marking to degrade from its initial value to the minimum acceptable value. It is clear that traffic has a significant effect on transverse markings because tires are passing directly on top of it. For longitudinal pavement markings, early studies could not determine a statistical correlation between traffic volume and pavement marking retroreflectivity degradation (Taek et al. 1999), but a 2009 study on Tennessee highways using retroreflectivity data collected on asphalt highways indicated that the annual average daily traffic (AADT) does have significant impact on waterborne pavement marking retroreflectivity degradation (Sasidharan et al. 2009). A 2011 North Carolina study concluded that AADT has a small but significant effect on the deterioration of waterborne markings (Mull 2011).

2.10.2. Winter Maintenance Impact on Pavement Marking Performance:

The overall purpose of snow and ice control is to provide the safest, most efficient, eco-friendly, and inexpensive outcome during the winter. Plowing is typically the most effective technique in snow-removal operation compared to others (e.g., sand application, de-icing, and anti-icing). Several techniques are traditionally used to enhance the operational efficiency of snow and ice control operational efficiency. These techniques can be used before, during, or after the plowing operation. Anti-icing chemicals and abrasives are commonly used before the plowing operation, while deicing chemicals are used after plowing operation to break the bonds that have already been created between the snow and roadway surface. To make the chemicals and abrasives more effective, a pre-wetting technique can be used with both anti-icing and deicing chemicals to make the solid chemicals further adhere to the road surface, while a warm-wetted sand method helps to solve the problem of removing abrasives due to continuous traffic flow.

Abrasive material is commonly added on the road surface to increase traction between vehicle tires and compacted snow. Abrasives do not last very long on roads because of continuous traffic flow which push the solids out of the road path. Therefore, an

implementation strategy must be periodically used to ensure that abrasives remain on the road for a longer time.

To make snow plowing more effective, anti-icing chemicals are used as a pre-treatment technique. When an anti-icing chemical is used in snow and ice control operations, the amount of energy to plow through snow can be reduced by one-fifth. Anti-icing chemicals are typically applied when pavement surface temperatures are above 20°F and before the arrival of a snowstorm. Anti-icing chemical compounds include: calcium chloride ($CaCl_2$), sodium chloride (NaCl), magnesium chloride ($MgCl_2$), potassium acetate (KAc), and calcium magnesium acetate (CMA) (Elhouar et al. 2015 and Drschel 2014). Previous studies have investigated the performance of deicing and anti-icing though most were field studies.

2.10.3. Environmental Influence

Pavement marking material is directly influenced by the environment. The impact of the surrounding environment on the pavement marking performance can be classified into two time-specific groups: weather conditions during installation and year-round climate. Temperature, humidity, rain, and wind speed are the most important outdoor factors that influence pavement marking performance. Air and pavement temperatures are significant factors, especially during installation, because most marking materials demand a minimum temperature for suitable drying time. During application, high pavement surface moisture can have a serious impact on the bond between the marking material and the pavement surface. Curing time varies from material to material, and it is directly influenced by humidity and wind speed. Also, high-speed winds can cause irregular glass bead distribution on the binder material. After application, the service lifespan of pavement markings is directly influenced by climatic conditions. For instance, waterborne markings experience severe surface texture change (e.g., cracking and color fading) when exposed to intense ultraviolet rays and high temperature in sunny regions (Lopez 2004).

2.10.4. Factors Impact Pavement Marking Retroreflectivity

Pavement marking retroreflectivity is a complicated phenomenon that is impacted by many factors. One of the elements responsible for producing most of the retroreflective light is the glass bead. Thus, they have a direct impact on the retroreflectivity of pavement markings. In general, factors influencing pavement marking retroreflectivity can be classified

as either factors affecting initial retroreflectivity or affecting long-term performance. Among the factors that can influence the initial pavement marking retroreflectivity are: retroreflective material type, glass bead properties (e.g., amount and dispersion, embedment depth, refractive index, size, clarity, and roundness) and application method, binder material type, and construction characteristics (color and thickness). On the other hand, the factors that might influence the long-term retroreflectivity performance are: road surface type, application process, pavement surface roughness, dirt film or "blinding" material, retroreflectometer type, weathering process (region), traffic volume (AADT), percentage of heavy vehicles, winter maintenance activities, and initial installation quality (Ozelim and Turochy 2014 and Lopez 2004).

2.11. Modeling Pavement Marking Deterioration

2.11.1. Previous Studies

Mathematical models have been developed and proposed to describe the degradation performance of pavement markings. These models include relationships of different forms including simple linear, power, exponential, natural logarithmic, quadratic, and multiple linear regression models. In some of these models, retroreflectivity was used as a dependent variable while variables such as age, traffic volume, weather conditions, and roadway geometry were used as independent variables. Other variables such as color retention and durability (material percent lost over time) have been used as performance measures to evaluate marking degradation (Ozelim and Turochy 2014 and Wang et al. 2016). In 2003, the South Carolina Department of Transportation (SCDOT) funded a research project evaluating the effective life cycle of pavement marking retroreflectivity over time. The SCDOT's motivation for funding this study was to develop a pavement marking predictive model to estimate the rate of pavement marking degradation. This study came up with three predictive patterns that explained how South Carolina interstate highway pavement marking materials deteriorate over time, where R_L is the retroreflectivity measurement within a specific time (see Figure 2.7). The first model represented a newly installed marking material; retroreflectivity slightly increased directly after installation and then linearly decreased over time to reach the end of its service life. The second model represented an existing pavement marking material and retroreflectivity linearly dropped at first and then equilibrated before the end of its service life. The third model illustrated the shift (increase in retroreflectivity) due to restriping a new

marking material and the reduction in retroreflectivity due to the application of winter maintenance activities (e.g., snowplowing) (Craig et al. 2007).

A study conducted in 2009 reviewed and compared five independent pavement marking degradation models to create a reliable pavement marking retroreflectivity degradation model for North Carolina. The five models were developed by Andrady (1997), Lee et al. (1999), Migletz et al. (2001), Abboud and Bowman (2002), and Sarasua et al. (2003). Three of the five models developed a linear degradation model while the other two models were exponential or logarithmic decay models. The study found that both thermoplastic and paint pavement markings on asphalt pavements could be modeled as linear degradation (Sitzabee et al. 2009). Zhang and Wu (2010) proposed a nonlinear regression analysis by using a smoothing spline and Autoregressive Integrated Moving Average Model (ARIMA) time series that used time-based data to model pavement marking retroreflectivity changes over time (Zhang and Wu 2010). Sathyanarayanan et al. (2008) used the Weibull analysis to model pavement marking retroreflectivity deterioration. Other studies used graphical analysis of marking retroreflectivity degradations (Sathyanarayanan et al. 2008).

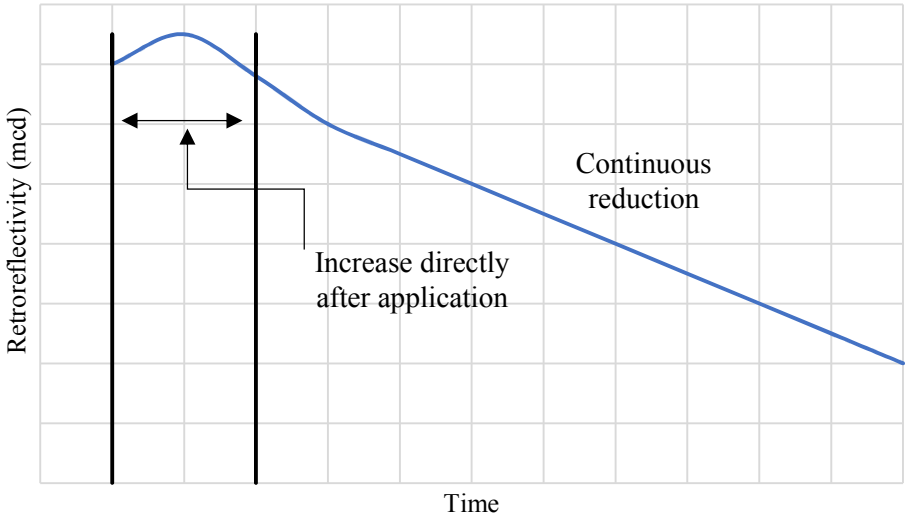

Predictive model for newly placed waterborne marking

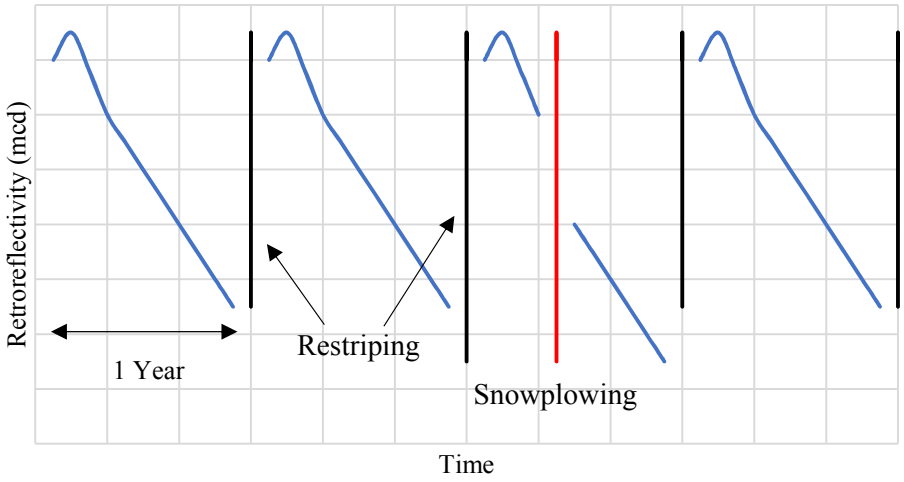

Predictive models for restriping and snowplowing

Figure 2.7: Retroreflectivity deterioration models

In 2014, a study examined ten pavement marking retroreflectivity deterioration models with the purpose of observing how existing models fit data from Alabama and developing trustworthy statistical models. This study was limited to modeling the retroreflectivity of thermoplastic pavement markings over time. The best-fitting models were a nonlinear model developed by Thamizharasan et al. (2003) and a general linear model developed by Sitzabee et al. (2009) (Ozelim and Turochy 2014). Another research effort verified four degradation models using pavement marking retroreflectivity data collected from East Tennessee. Abboud and Bowman developed a best fit model, and its R^2 was the highest (Onyango et al. 2014).

Other creative ideas have been implemented to predict the degradation of pavement marking retroreflectivity such as using transverse pavement marking test deck data to predict the life expectancy of longitudinal pavement makings (Pike and Songchitruksa 2015) or suggestions that pavement marking retroreflectivity data are similar to pavement surface condition data because both sets consist of repeated measurements. Thus, a Linear Mixed-Effects Model (LMEM) has been used in modeling pavement marking retroreflectivity (Hummer et al. 2011). A study implemented in the State of Louisiana to assist the managers of pavement marking projects used a model that estimated the economic efficiency of alternative pavement marking materials (Fu and Wilmot 2012).

It should be noted that climate and operating conditions significantly influence the degradation of pavement markings. Thus, comparing degradation models might not be practical but it can provide guidance as to the best model that should be used in modeling other field data. It is important to develop a well-validated degradation model while paying attention to regional (e.g., temperature, rain, snow, etc.) and operating conditions (e.g., studded tires, snowplowing practice, etc.). In order to establish a credible degradation model, all variables that impact pavement marking service life should be evaluated and taken into account.

In summary, in the last three decades, many different mathematical models have been developed to describe the degradation tendency of pavement marking retroreflectivity. Previous studies intended to create reliable degradation models for their regions based on the available field dataset which were collected either from longitudinal pavement markings directly or from test decks previously prepared for evaluation purposes (Abbas et al. 2009).

Few studies have employed accelerated wear equipment in the laboratory to understand and model pavement marking degradation. Table 2.3 summarizes previous pavement marking deterioration models, variables used in the studies, material evaluated in the study, R^2, and study area (Wang et al. 2016). Pavement marking retroreflectivity was used broadly as a dependent variable and other variables such as initial retroreflectivity, age, traffic volume, weather conditions, and roadway geometry were used as independent variables (Wang et al. 2016). Other variables such as color retention, and durability (material percent lost over time) were used as performance measures to evaluate degradation of pavement markings in the field.

Table 2.3: Previous pavement marking degradation models (Wang et al. 2016)

Year	Author	Model	Variable	Material	R-squared	Location
1997	Andrady	Logarithmic	Time, initial R_L	Multiple	0.85+	Across the US
1999	Lee et al.	Simple linear regression	Time	Polyester, thermos., waterborne, tape	0.14 to 0.18 M	Michigan
2001	Migletz et al.	Simple linear regression, quadratic, and exponential	CTP	Multiple	NA	19 states in the US
2002	Abboud and Bowman	Logarithmic	Time, ADT	Paint and thermos.	0.32 and 0.58	Alabama
2003	Thamizharasan et al.	Multiple linear regression	Time, CTP	Thermo. and epoxy	0.21 to 0.78	South Carolina
2006	Bahar et al.	Inverse polynomial	Time	Multiple	NA	8 states in the US
2006	Zhang and Wu	Smoothing spline and time series Arima	Time	Multiple	NA	Mississippi
2007	Fitch	Logarithmic	Time	Thermo., epoxy, and polyurea	0.53 to 0.87	Vermont
2009	Sasidharan et al.	Multiple linear regression	Time, ADT, line type, pavement type	Epoxy and waterborne paint	NA	Pennsylvania
2009	Sitzabee et al.	Multiple linear regression	Time, initial R_L, AADT, line location, line color	Thermo. and paint	0.60 and 0.75	North Carolina
2011	Hummer et al.	Linear mixed-effects model	Time	Paint	NA	North Carolina
2012	Sitzabee et al.	Multiple linear regression	Time, AADT, bead type, initial R_L, line location	Polyurea	0.64	North Carolina
2012	Mull and Sitzabee	Multiple linear regression	Time, initial R_L, AADT, and plow events	Paint	0.76	North Carolina
2012	Robertson et al.	Multiple linear regression	Time, AADT, CTP, lane width, and shoulder width	Waterborne paint and high-build paint	0.24 to 0.34	South Carolina
2012	Fu and Wilmot	Multiple linear regression	Time, AADT, CTP	Thermo., tape, and inverted profile thermos.	0.18 to 0.89	Louisiana
2014	Ozelim and Turochy	Multiple linear regression	Time, AADT, initial R_L	Thermoplastic	0.45 to 0.49	Alabama
2016	Wang et al.	Piecewise multiple linear regression	NTPEP data, transverse test deck	Tape and MMA	0.64 to 0.94	Pennsylvania, Florida, and Minnesota

2.11.2. Need

Due to the dynamic nature of the pavement marking industry and changes to the chemical composition of pavement marking materials complying with Environmental Protection Agency (EPA) requirements and the appearance of new technologies, each material has to be evaluated and modeled before application in order to be used properly. Studying the deterioration of pavement marking materials assists decision makers in the highway industry with a useful tool that can help them to predict service. Predicting the service life of pavement marking materials enables the DOTs and project managers to schedule maintenance projects at the right time so that existing material is refreshed just as its level of service (LOS) falls below a desirable level. In other words, modelling pavement marking deterioration will benefit transportation agencies by enabling them to predict the deterioration of pavement markings and assist in the scheduling of marking maintenance projects to maximize the operational and safety benefits of the existing material and minimize related costs.

Several studies have been conducted to determine the performance characteristics of various pavement marking materials in different regions in the United States and most of these studies focus on creating degradation models that simulate an actual dataset collected from the field. Thus, based on the literature review there is value in developing a rapid, cost-effective, and practical laboratory-based procedure to understand and evaluate the performance of pavement markings.

2.12. Pavement Markings in Idaho

Approximately 98 percent of pavement markings used in the state of Idaho are waterborne with methyl methacrylate (MMA) and tape representing the remaining two percent, while thermoplastic material is increasingly used as transverse markings like crosswalks, arrows, and symbols (DOT). The ITD decision for the comprehensive usage of waterborne pavement markings was chosen based on cost-effectiveness (Sadid et al. 2010). The state of Idaho chooses to restripe its rural two-way highways with waterborne pavement markings on a fixed repeated schedule (during non-winter times) instead of restriping when the retroreflectivity falls below an identified threshold. Pavement marking striping activities in Idaho usually start at the end of March and continue through early August. Other factors

such as installation cost, manufacturer warranties over a specified time, life-cycle cost, retroreflectivity degradation of the pavement marking material, and durability are taken into account at the decision-making level of pavement marking contracts. Since waterborne paint and thermoplastic are the most commonly used materials in Idaho, the laboratory-based procedure developed for ITD as part of this research utilized these two particular materials. However, all of the marking types described earlier could be evaluated using the procedure to be described.

CHAPTER 3: ACCELERATED LABORATORY-BASED PROCEDURE FOR PAVEMENT MARKING PERFORMANCE EVALUATION

"Deterioration Characteristics of Waterborne Pavement Markings Subjected to Different Operating Conditions." *American Society of Civil Engineers, Journal of Transportation Engineering, Part B: Pavements, Vol. 145, no. 2 (2019): 04019003.*

The natural exposure of pavement markings to environmental conditions (e.g., sunlight, temperature, relative humidity, rain), maintenance activities (e.g., snowplowing), and traffic level contribute to its deterioration. Two laboratory procedures were established and evaluated to assess their ability to simulate degradation of pavement markings in the field. First, to replicate traffic, a three-wheel polisher device (TWPD) was used to accelerate the "wearing out action" of different pavement marking materials. Second, to replicate the weathering process, a xenon arc chamber (XAC) (model Q-SUN Xe-1) was employed to accelerate the deterioration due to sun, temperature, and humidity. In short, the deterioration of pavement markings in terms of specific performance measures was determined by exposing two types of pavement markings (waterborne and thermoplastic) with two colors (white and yellow) to different dynamic loadings using a TWPD and to weathering using an XAC.

The performance measures developed to evaluate pavement marking performance after traffic loading or accelerated weathering exposure in a timely manner capture physical changes such as retroreflectivity, retention of color, and durability (presence). The deterioration of each performance measure was determined in terms of the number of cycles under the TWPD and in terms of hours in the XAC. The TWPD and the XAC were used to evaluate the performance of the pavement marking material in a controlled laboratory environment. To place the marking samples in the two devices, two different substrates were prepared (asphalt slabs and aluminum plates) and were striped with white and yellow colors from each material.

3.1.Sample Preparation

Twenty-inch square asphalt slabs with a two-inch thickness were prepared and subsequently striped with pavement markings. The asphalt mixture in this study was a typical dense-graded mix commonly used in Idaho. The mixture was prepared with basalt aggregates and PG 64-34 asphalt binder (5.5% by weight). Figure 3.1 shows the aggregate gradation of the mix.

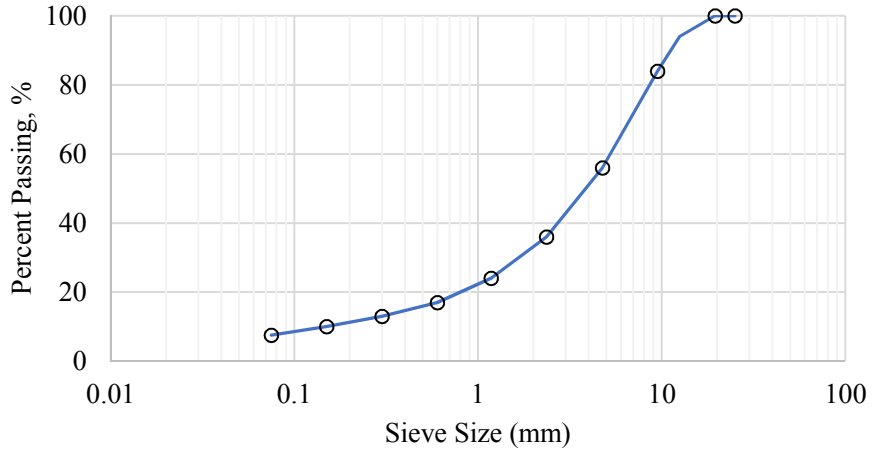

Figure 3.1: Aggregate gradation of asphalt mixtures

The asphalt slabs were prepared using a steel mold and plate compactor. A construction zone plate compactor was used for vibrating and compacting the hot asphalt mixture in a steel mold to provide a flat surface and prevent deformation. During mechanical compaction, two paper sheets were placed on the top and bottom of the hot mixed asphalt to prevent the mold surface and the mixture from sticking together. Figure 3.2 shows the casting mold and compaction process.

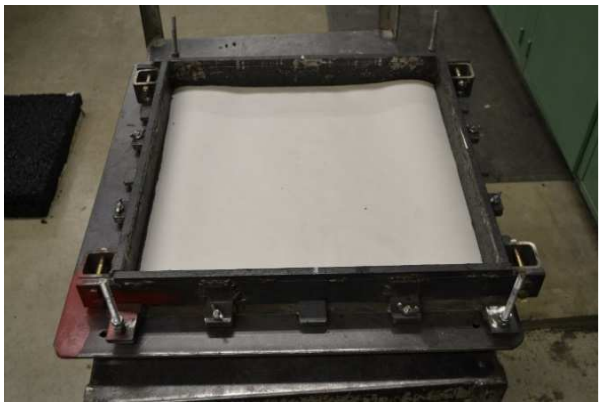

Casting mold (20”x20”x2”)

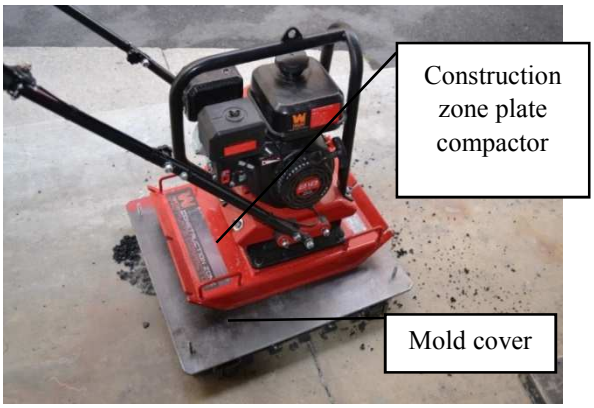

Construction zone plate compactor

Paper sheet removal

Asphalt slab after compaction

Figure 3.2: Asphalt slab preparation

Aluminum plates (7”x4”x0.2”) were also striped with both waterborne paint and a preformed thermoplastic marking. These small samples were tested using an XAC while the asphalt substrates were tested using the TWPD.

The asphalt slabs and aluminum plates were transported to the Idaho Transportation Department (ITD) office in Lewiston, ID and striped (4-inch wide) using the same pavement marking material and machine used for actual roadway applications. Twelve asphalt slabs and twelve aluminum plates were striped with yellow and white waterborne and thermoplastic markings, three per each color of pavement marking material. The six slabs were partially buried with the upper surface of the slab level with the ground surface to simulate the waterborne painting process in the field while the other six slabs were striped with thermoplastic.

The waterborne paint used in this procedure was one of the ITD preapproved products as identified on the most current Qualified Products List (color of category 707, sub-category No. 14 waterborne), and the striping truck was calibrated per ASTM D713-12. The pavement markings were applied to the slabs at a striping truck speed of approximately 5 miles per hour and bead dropping rate (glass bead dosage) of 8 pounds per gallon to minimize loss of beads. The resulting wet paint thickness was 17 milli-inches, standard for rural Idaho roadways. Figure 3.3 illustrates the waterborne pavement marking application.

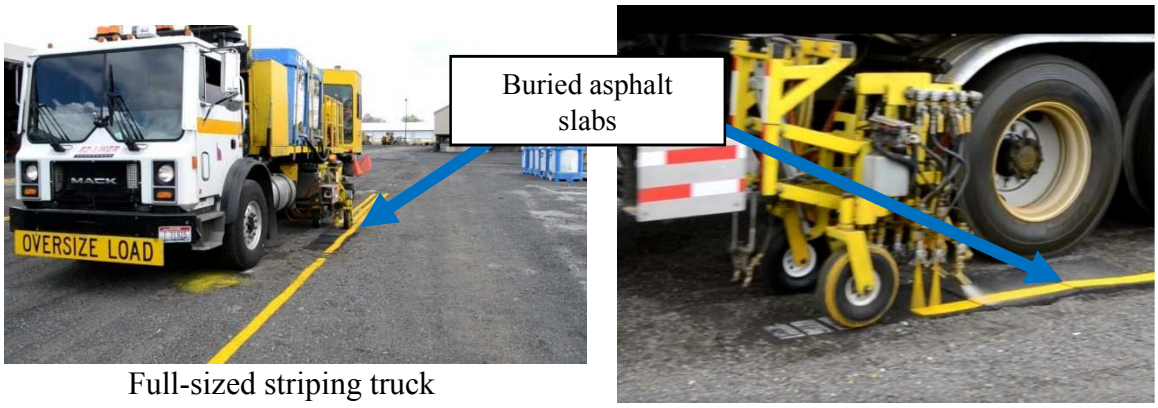

Full-sized striping truck

Guns used to spray waterborne paint and glass beads

Figure 3.3: Waterborne pavement marking application

One application of AASHTO M-247 Type I beads was added to the wet waterborne pavement markings during operation. Table 3.1 provides the chemical and the physical properties for the AASHTO M-247 Type I glass beads.

Table 3.1: AASHTO M-247 Type I glass bead properties

Chemical Composition (by weight)	**Physical Properties**
Silica (SiO_2) 62-75%	Specific Gravity 2.48-2.52 g/cm^3
Aluminum Oxide (Al_2O_3) 0-5%	Softening Temperature 650˚C
Calcium Oxide (CaO) 6-17%	Coefficient of Thermal Expansion 90 x 10-7/˚C (30-300˚C)
Magnesium Oxide (MgO) 1-5%	Strength 60,000 to 65,000 psi
Sodium Oxide (Na_2O) 10-20%	Vicker Hardness 756,250 psi
Iron Oxide (Fe_2O_3) < 0.8%	Refractive Index 1.50 to 1.55

The second stage of preparing the marking samples consisted of applying Melt-In-Place preformed thermoplastic (alkyd formulation) on the remaining six slabs. This study chose to evaluate the performance of preformed thermoplastic markings because of their frequent use by ITD in short-line marking applications, legends, and symbols. The preformed thermoplastic pavement marking material that was used in this procedure was one of the ITD preapproved products as identified on the most current Qualified Products List (section 630-Pavement Markings, Chapter 3 of the ITD Traffic Manual). This type of thermoplastic pavement marking was supplied to the site as solid segments which were placed on the pavement and then fused to the surface with heat. In general, the materials used in preformed thermoplastic pavement markings are similar to regular thermoplastic but have been previously combined into preformed solid strips which do not require application equipment. The asphalt slab surface was preheated prior to application, and then a preformed thermoplastic strip (hot type) was placed on top of the slab surface while the surface was still hot. The solid material was melted into the surface using a propane torch as a heat source. The preformed thermoplastic pavement markings were already premixed with glass beads, so no additional glass beads were added. Figure 3.4 documents the Melt-In-Place Preformed Thermoplastic application on both the asphalt slabs and aluminum plates.

Preheating prior to application

Placing the thermoplastic hot tape

Heating up the thermoplastic tape

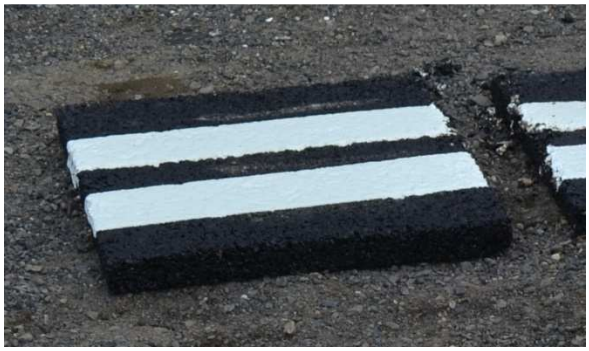

Final production

Applying thermoplastic markings on aluminum plates

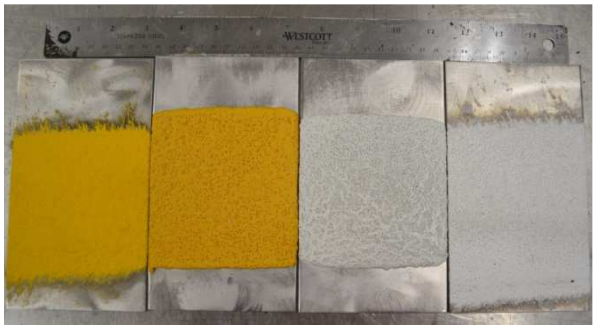

Aluminum plates striped with pavement markings

Figure 3.4: Thermoplastic application on asphalt slabs and the aluminum plates

3.2. Developing an Accelerated Laboratory Procedure to Simulate Pavement Marking Degradation Due to Traffic and Snowplowing

3.2.1. Three Wheel Polishing Device (TWPD) components

A TWPD was designed to polish a circular path on top of the square asphalt slab to evaluate the friction characteristics. To provide this rotational motion, three caster wheels (8" X 3") were attached to a turntable by three ball bearings, one for each wheel; the wheels tracked in a 11" diameter circle. Figure 3.5 shows a detailed description for all of the TWPD components. The wheels can be pneumatic-tires, studded-tires, neoprene tires, or steel wheels, and tire weight can be controlled by placing circular iron plates on top of the turntable (10 pounds each). The abrasion wheel assembly shown in Figure 3.6 was attached to a motor by a shaft which could be adjusted to move the assembly vertically (up and down) to provide space for adding or subtracting loads. A half horsepower motor fixed on top of the device drove the gearbox which in turn controlled the rotational wheel speed. A motor speed controller was added to set up the desired number of revolutions. The TWPD can be operated at different speeds from 10 to 100 revolutions per minute. An omega digital counter was used to automatically count the cycles of the turntable and automatically turn off when polishing was complete. The three-wheel assembly was put inside a steel mesh chamber to insure safety. Only one pavement slab could be tested at one time; this slab was placed under the three wheels from a top-hinged steel mesh door installed on the front face of the chamber.

The polisher was supported by a water spray system to: simulate rainy conditions, wash away abraided particles, and reduce the wear of the rubber wheels during the polishing operation. The water spray system consisted of a small pump circulating water from the basin to a U shaped punctured pipe (PVC-¼") fixed to the frame on three sides. The punctured pipe sprayed water to the top of the pavement slab during operation. The amount of water was controlled using an electric cutoff valve. This valve was connected to a digital counter to stop the flow when the desired number of cycles was obtained.

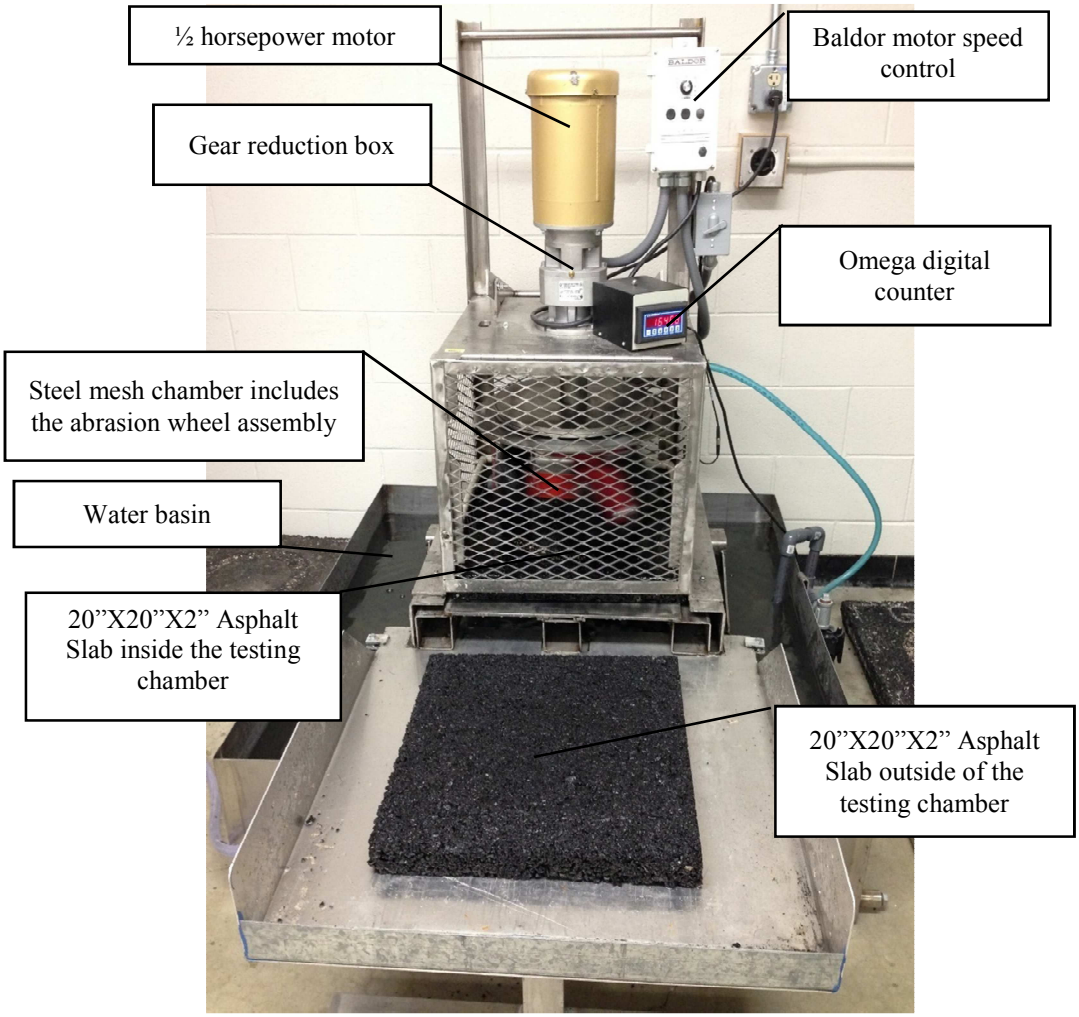

Figure 3.5: Three Wheel Polishing Device (TWPD) at University of Idaho

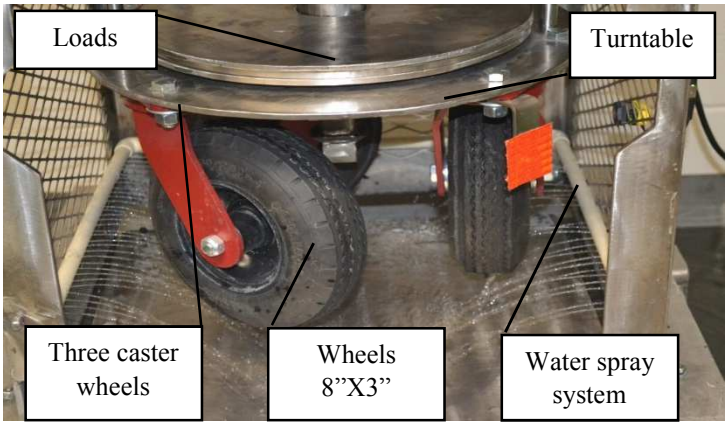

Figure 3.6: Abrasion wheel assembly

3.2.2. Snow Plow Simulator

A snowplow is usually mounted on winter service vehicles to remove snow and ice from road surfaces during or after snow storms in cold regions. Snow scraping blades can be either classic or serrated blades, and can be installed on a front-mounted plow or underbody blades; serrated blades are commonly used in Idaho. The serrated blades have higher performance compared to classic blades and increase scraping effectiveness by 25% to 67%. The key factors for a snow plowing mechanism are the attack angle and cutting angle. The attack angle is the rotation of the plow from the vertical axis, and the cutting angle is the rotation of the blade from the horizontal axis of the road surface (Elhouar et al. 2015). Figure 3.7 provides a photo for a front-mounted plow on a tandem dump truck used in Idaho for snow removal.

Figure 3.7: Front-mounted plow on tandem dump truck used in Idaho

Figure 3.8 shows the attack and cutting angles and the setup of the dowel-type steel blade with carbide inserts. To simulate snow removal in the laboratory, a scraper blade was installed onto a pneumatic wheelset on the TWPD's turntable. The cutting angle was reversed to prevent the machine from stopping due to the interaction between the blade and an irregular asphalt texture.

Figure 3.8: Description of the attack and cutting angles

Figure 3.9 shows how the scraper blade was fixed under the turning table with the pneumatic wheel to simulate snowplow action in the laboratory.

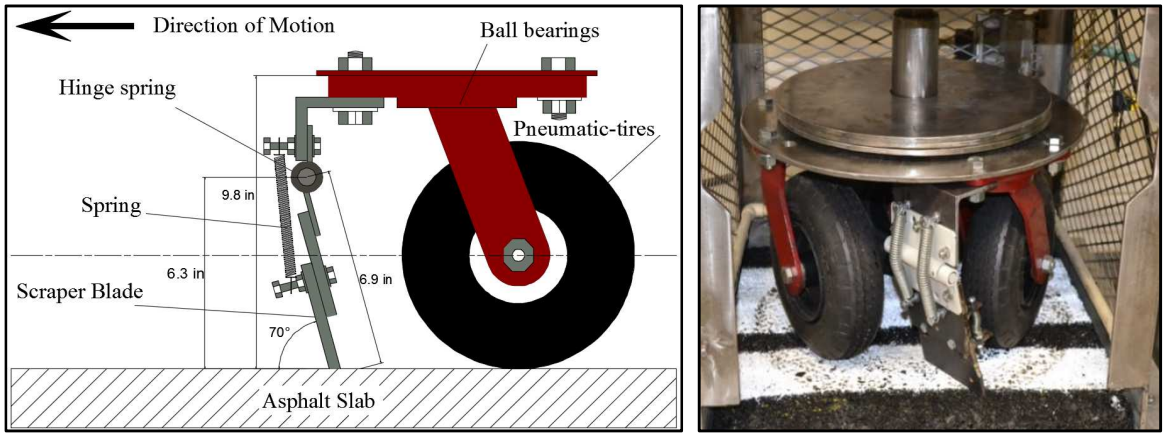

Figure 3.9: Snowplow simulator

3.2.3. Friction between TWPD wheelset and pavement surface

The friction between the pneumatic tires of the TWPD and pavement surface could be influenced by several factors. These factors, grouped into four categories, included: pavement surface characteristics (e.g., micro-texture, macro-texture, and material properties), vehicle operation parameters (e.g., slip speed, and driving maneuver), tire properties (e.g., foot print, tire tread shape and condition, rubber compound, and hardness, tire pressure, and weight), and environmental factors (e.g., climate and contaminants). The friction forces under the tire can be analyzed in either the longitudinal or lateral direction.

3.2.3.1.Longitudinal Frictional Forces:

The resistance force initiated between the vehicle's tire and a pavement surface when a vehicle is moving is identified as pavement friction force. This non-dimensional friction coefficient (μ) can be described using Equation 4:

Equation 4: The non-dimensional friction coefficient (μ)

$$\mu = F/F_w \quad (4)$$

where: F = tangential friction force between the rubber tire tread and the horizontal traveled surface, and F_W = weight of vehicle.

In a free rolling mode, there is no braking action; thus, the relative speed between the tire circumference and the pavement surface is zero. In this case, the longitudinal frictional force that occurs between the rolling pneumatic tire in the longitudinal direction and the road surface is just the free-rolling resistance. Figure 3.10 shows the rolling resistance force of the free-rolling pneumatic tire of the TWPD and the blade at a constant speed on a bare, dry paved surface. From Figure 3.10, the rolling resistance force (F_r) is the force required to resist the moment resulting from ground force eccentricity (a) which directly depends on tire speed. Therefore, F_r increases with speed. During braking action, the coefficient of friction value increases with increasing braking until this value reaches a peak value (critical slip status) and then decreases before the tire fully locks and begins sliding. The coefficient of friction is principally influenced by tire characteristics which are in turn affected by its size, tire pressure, rubber compound, tread configuration, and carcass construction (Hall et al. 2009 and Al-Qadi et al. 2002).

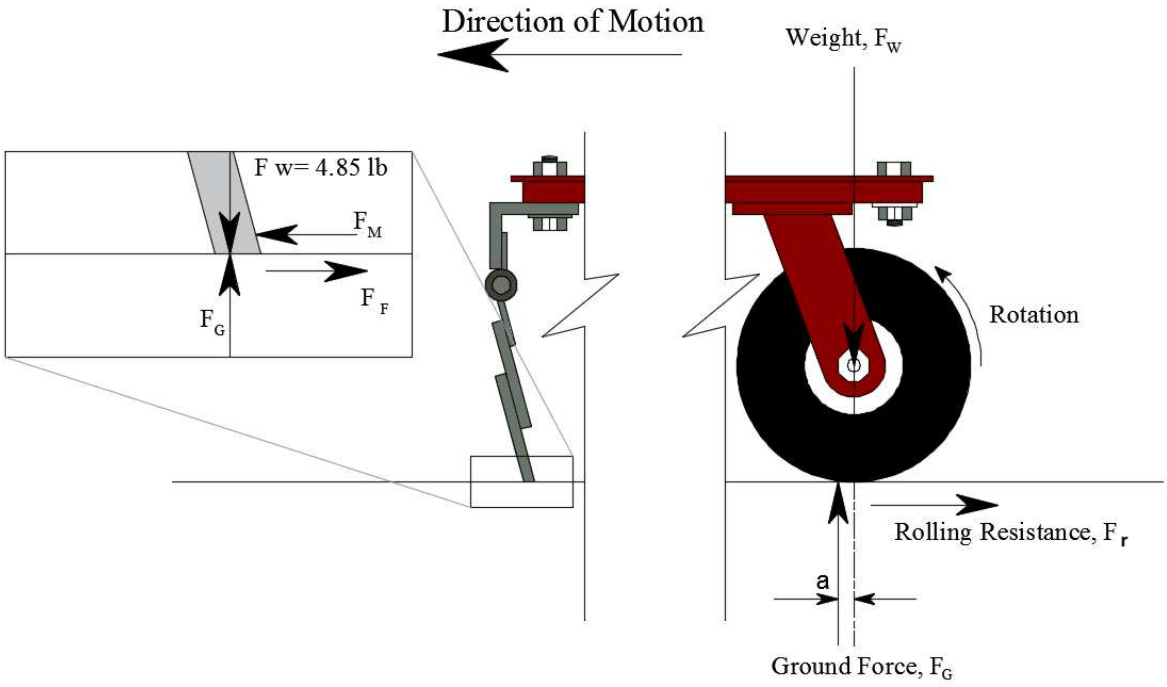

Figure 3.10: Free-body diagram of the snowplow simulator on a dry surface

The moment about the wheel axis when disregarding wheel-bearing resistance can be mathematically described as:

Equation 5: Moments about the TWPD wheel axis

$$(F_G * a) - (F_R * r) = 0 \quad (5)$$

$$F_R = (a/r) * F_G$$

$$F_R = (a/r) * F_W$$

where: *a/r* is the friction coefficient. Both *a* and *r* vary with tire design, tire weight, speed, braking degree, and effect of contamination. In dry conditions and rigid horizontal surfaces, the rolling resistance typically ranges from 0.5% to 3% of the carried weight (Hall et al. 2009).

3.2.3.2.Lateral Frictional Forces

As part of the TWPD, the pneumatic tires move in a circular direction around the center of the turning table. This moving action is similar to when a vehicle changes direction, changes lanes, or steers around a curve. Thus, lateral friction forces will develop. Figure 3.11 shows how the side-force friction acts to counter centripetal force when the TWPD tires are

executing a lateral motion. The mathematical relationship between the TWPD tire and the substrate forces can be estimated based on pavement-tire steering/cornering forces and by Equation 6 (Hall et al. 2009):

Equation 6: The mathematical relationship between the TWPD tire and the substrate forces

$$F_S = (V^2/15R)\text{-}e \quad (6)$$

where: F_S = friction force between the TWPD pneumatic tire and substrate surface, V = tire speed (mi/hr), R = radius of the path (ft), and e = pavement super-elevation, ft/ft (which is zero for the TWPD case since the surface is flat).

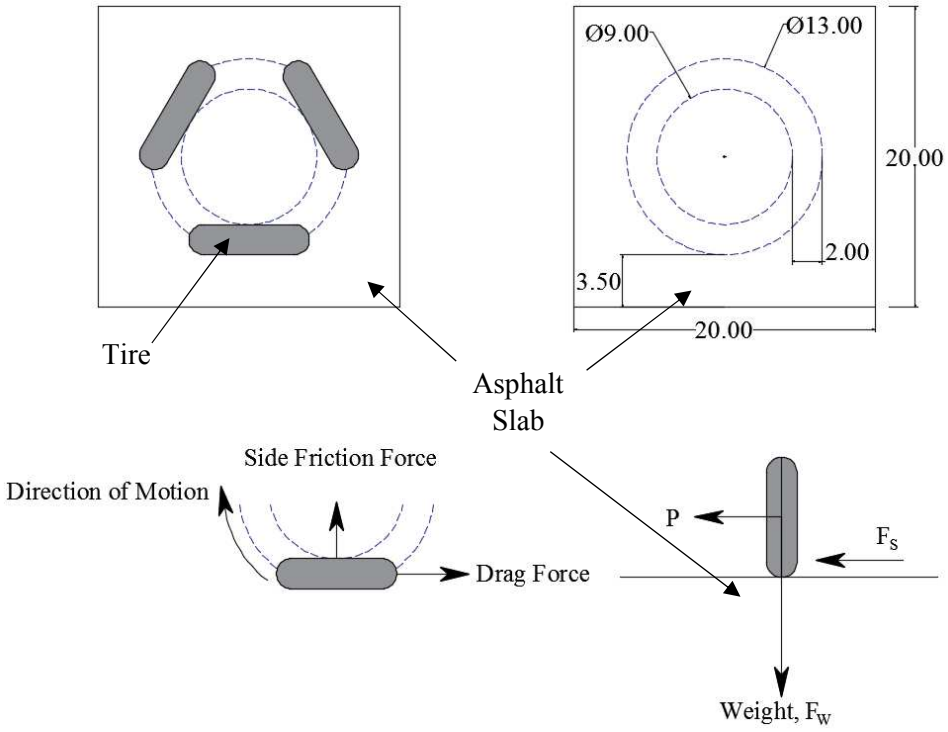

Figure 3.11: TWPD lateral frictional forces

3.2.3.3.Friction Forces on Wet Surfaces:

Under the TWPD's pneumatic tires the water is confined on the pavement substrate surface. This water film acts like a lubricant between the two surfaces and separates some of the tire contact area from the substrate surface. Figure 3.12 shows a free-body diagram of a free rolling tire on a wet surface. The ground reaction force (F_G) and resultant dynamic fluid lift force (F_L) are carrying the TWPD weight (F_W). The variables a and b are the eccentricity distance of the ground force and the eccentricity distance of the fluid lift force, respectively.

The horizontal water lifting reaction force (F_{LG}) is the resultant force of F_G and F_L while F_{DG} represents the reaction force in the tire–surface area due to the water displacement drag that resulted from the displacement drag force (F_D) and F_G.

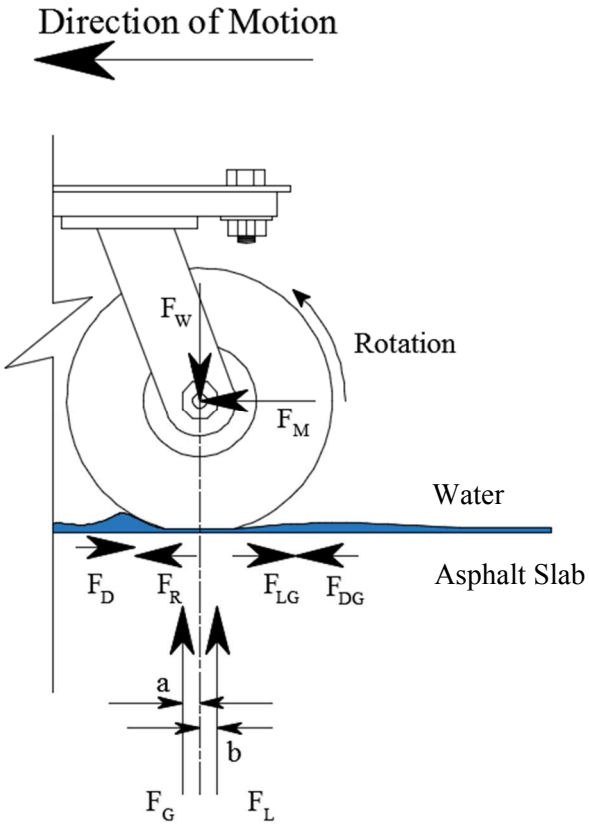

Figure 3.12: Friction forces on wet surfaces

Adding other materials such as abrasive or anti-icing chemicals when testing pavement markings will affect the friction process. For this study, a base case was proposed and implemented without the use of abrasive or anti-icing chemicals. The effect of adding such materials should be investigated in future research.

3.3.Developing an Accelerated Laboratory Procedure to Simulate Pavement Markings Degradation Due to Weathering

Pavement markings are naturally exposed to various conditions including a wide spectrum of electromagnetic radiation from the sun, moisture, snow, and humidity. The exposure of pavement markings to such conditions changes their physical (e.g.,

retroreflectivity, color, and appearance) and chemical properties. Several studies used artificial weathering under different types of weatherometers to study retroreflectivity deterioration, color change, and durability of many highway products (e.g., retroreflective sheets, and traffic signs), but to date there has not been a defined technique to study and evaluate the retroreflectivity deterioration of different pavement marking materials (Mohan et al. 2012). For this reason, there is value in developing an accelerated laboratory-based procedure that can replicate weathering of pavement marking materials and gauge performance in a shorter amount of time.

The duration of the field endurance test commonly used by the state DOTs today is a crucial factor that impacts pavement markings testing procedures. For example, the test deck requires up to three years to precisely evaluate a pavement marking material. Using the accelerated weathering chamber, the long-term environmental exposure can be reproduced as quickly as a few days. In the second phase of this study, accelerated weathering tests were conducted in a weatherometer to simulate the environmental impacts that contributed to pavement marking material deterioration. Sunlight, heat, and moisture are the most important factors that negatively impact the service life of pavement markings. As described earlier, a weatherometer was used to replicate the deterioration caused by sunlight and rain in the laboratory in previous studies.

The Q-sun Xe-1 xenon arc chamber (XAC) simulates a full spectrum of sunlight, including ultraviolet (UV), visible light, and infrared radiation (IR). Inside the chamber, moisture can be controlled by a reprogrammable sprayer which can operate either during light or dark conditions. It also has a black panel temperature sensor to control the temperature inside the chamber. To replicate sunlight, the XAC uses a single xenon arc lamp which sits on the upper side of the chamber. To replicate moisture, a water spray under the lamp is applied to specimens near-horizontally mounted on a tilted shelf in the chamber. Figure 3.13 shows the XAC components and a sample configuration.

Figure 3.13: XAC components and sample configuration

Solar power is theoretically measured by irradiance, which is defined as the rate at which solar energy falls on top of a surface. Irradiance is represented by power per unit area (watt /m^2). Before testing, the on-board solar eye irradiance sensor was calibrated using a CR20 calibration radiometer, and the black panel temperature sensor was calibrated using a CT202 thermometer (see Figure 3.14). Thereafter, two types (waterborne and thermoplastic) and two colors (white and yellow) of pavement markings were subjected to the accelerated weathering procedure using the recommended test cycle specifications used for XAC exposure testing of paints and related coatings per ASTM D6695.

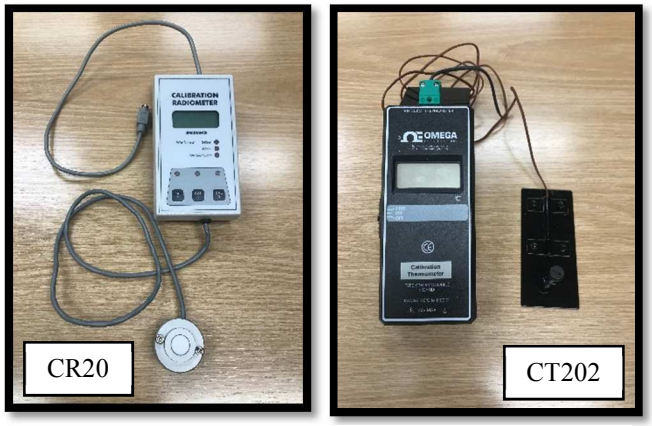

Figure 3.14: Calibration radiometer and the black panel temperature sensor

Retroreflectivity and color measurements were collected between exposure times of 0 and 2,000 hours. Consecutive 12-hour cycles were divided into two conditions: a light condition of 8 hours with an average irradiance of 0.55 w/m^2 at 340 nm and a chamber temperature of approximately 70 °C and a dark condition with water spray of 4 hours at 24 °C. This cycle was designed to ensure that the physical and chemical properties of the material changed due to the exposure to artificial sunlight and moisture.

The effects of the accelerated weathering on the visual appearance of the waterborne and thermoplastic pavement markings were investigated. A digital microscopy analysis was conducted before and after weathering using a handheld digital microscope (HDM) to address the problem of color change and monitor change in surface texture such as cracking, peeling, blistering, and changes to the embedment depth of the glass beads in the pavement marking material. HDM is a microscope wired to the computer using a USB and combined with an integrated 0.3-megapixel digital camera. This microscope provides two standards of magnification (20X and 400X), and the sample was lit using an LED illuminator source. Figure 3.15 shows the HDM connected to a computer in the laboratory.

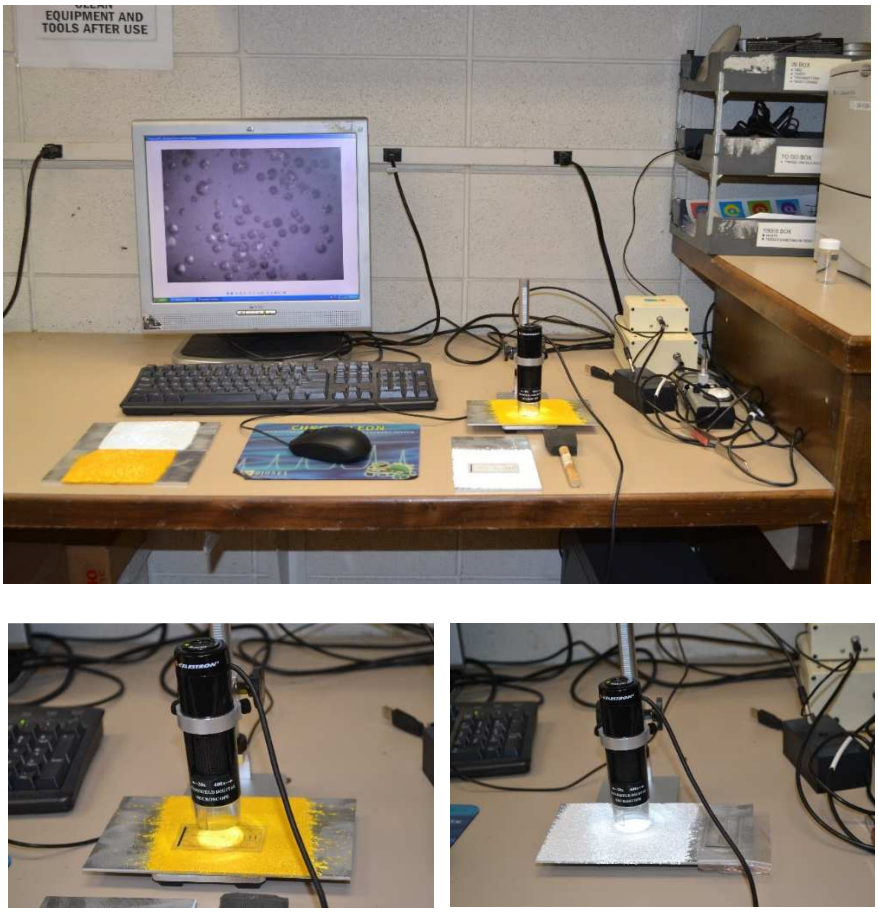

Figure 3.15: Handheld Digital Microscope (HDM)

3.4.Performance Measures

Any material degradation analysis must incorporate performance measures to evaluate its failure. The performance measures of the pavement markings change over time due to either internal and/or external impacts. Each performance measurement and the equipment used in the evaluation procedure is addressed in the following section.

3.4.1. Retroreflectivity Measurements:

All measurements were conducted to address the retroreflective characteristics of the horizontal marking material containing glass beads over time or cycle interval. A portable retroreflectometer (MX30) was placed on the specimen to measure retroreflection ($mcd/m^2/lx$) at a prescribed geometry (Figure 3.16).

Figure 3.16: MX30 portable retroreflectometer

A total of three evaluation locations were chosen on the asphalt substrates. Two locations were along the wheel path of the TWPD (location 1 and 2), and one location was in the middle (location 3), outside of the wheel path, and used as a reference point. Three measurements per each retroreflectivity condition (i.e. dry, recovery, and continuous wetting conditions) were conducted and averaged at each location after each cycle interval of the TWPD (see Figure 3.17). Measurements at location 1 and 2 were conducted in the direction of motion. Six readings were conducted and averaged after each time interval of the XAC (see Figure 3.18).

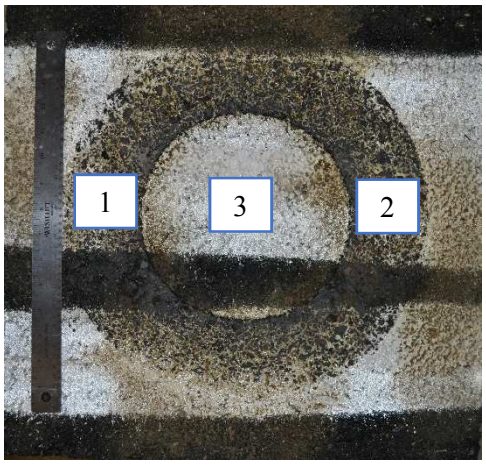

Figure 3.17: Measurements locations on asphalt substrate

Figure 3.18: Retroreflectivity measurement on aluminum substrate

The retroreflectivity was measured separately for dry, recovery, and continuous wetting conditions. For all measurements, the retroreflectometer was placed directly over the pavement marking material to ensure that the measurement area of the retroreflectometer fit within the width of the reduced area. After the completion of each cycle interval the specimen was wetted because of the TWPD water spray system, so measuring the wet condition first was appropriate. The following steps describe the retroreflectivity measurement procedure:

- First, the retroreflectivity under wet or recovery conditions (coefficient of retroreflected luminance, R_{L1}) was conducted in accordance with ASTM E-2177-18 standards. R_{L1} measurements were collected after forty-five seconds from pouring water on top of the marking specimen. This condition represented pavement marking retroreflectivity after rainfall, from dew, or humidity in the field. The recovery method or bucket method are commonly used names to describe this measuring method. To standardize wet retroreflectivity measurements, a platform with a five percent slope was used to facilitate drainage during all wet retroreflectivity measurements. While newly installed marking materials might reject wetting because of its natural surface tension, older marking materials may not exhibit this phenomenon. Generally, hydrophobic conditions are mitigated by exposure to the environment and wear of

traffic. Thus, to avoid the effect of this phenomenon, all TWPD tests were conducted 14 days after marking installation.

- Second, measurements during continuous wetting condition (coefficient of retroreflected luminance, R_{L2}) was conducted in the laboratory in accordance with ASTM E2176-08 standards. R_{L2} simulates rainfall conditions but excludes the effects of rain between the vehicle and the marking (Pike 2007). The following step-by-step procedure describes the wetting measurement process:
    a. A slope of 2% was standardized for recovery condition measurements to provide a drainage gradient so that water would run off the marking surface.
    b. The wetting device was constructed to supply a consistent and uniform continuous wetting condition. The wetting device consisted of: a garden pump sprayer with capacity size of 1 gallon, lab holder to carry the nozzle, and a sheet of aluminum to protect the retroreflectometer. Figure 3.19 shows the continuous wetting device and the placement of the retroreflectometer on a pavement marking sample.
    c. The wetting rate of the device was calibrated prior to performing any measurements. To achieve the required continuous wetting rate, the operating pressure and nozzle angle were adjusted properly. The water volume was estimated in ml/min according to the Volumetric Method in ASTM E2832-12 standards. The required wetting rate is 2.0 ± 0.2 in/hr.

$$\text{Wetting Rate (in/hr)} = (\text{VPM/area}) * 0.394\ (\text{in/cm}) * 60\ (\text{min/hr}) \quad (8)$$

where: VPM = volume per minute, in mL/min and area = container opening area, in cm^2.

Figure 3.19: Continuous wetting device

d. The wetting device was placed on the test specimen and checked to make sure that the wetting area was aligned with the pavement marking area receiving the retroreflectometer light. The pump was then turned on after checking the pressure and verifying that the test sample uniformly wetted at a rate of 2.0 ± 0.2 in/hr.

e. To ensure specimen saturation, each specimen was wetted for at least 30 seconds before conducting any measurements. Once a steady-state condition was achieved, three readings were taken, and the minimum reading was chosen as the representative measurement.

- Third, the specimen was dried using an air dryer. Dry retroreflectivity measurements (coefficient of retroreflected luminance, R_L) were then taken and averaged in accordance with ASTM E1710-18.

3.4.2. Color Measurements

Color measurements of each surface were conducted using an NR200 high-quality portable colorimeter with an 8 millimeter diameter aperture in accordance with ASTM D-2244 (Figure 3.20). The CIELab color coordinates (D65 light source) were used to measure the retention of marking color. The CIELab color space was chosen for this research to monitor the color change of the pavement marking samples because it was designed based on a concept similar to the opponent color processes of human vision. The total change in color (ΔE_{ab}) and difference in lightness (ΔL) were calculated using **Error! Reference source not found.** and 2. Color retention was measured in accordance with ASTM D6628 while ASTM E1347, E1348, and E1346 were used as guidance documents to perform appropriate light and sample positioning conditions.

Figure 3.20: NR200 portable colorimeter

3.4.3. Presence Performance (Durability)

The durability of various pavement marking materials was evaluated as part of the accelerated wear testing. The ImageJ v.1.50i software was used to determine material loss or surface texture change using digital images taken by a high-resolution camera mounted on a stand in standard lighting conditions. An image analysis procedure was applied using a high-resolution camera and the software to measure the presence of marking material after each traffic loading interval using the TWPD. To standardize the imaging environment, the camera was mounted at a constant height in a fluorescent-light environment. After each designated number of wearing cycles, images were taken using a high-resolution camera. To be consistent, all images were taken from the same height and with the same resolution. Figure

3.21 show the camera stand and image analysis software interface. The images were processed and analyzed using the software to quantify the worn area of the pavement marking in terms of percent loss and surface change of the pavement markings. ASTM D6359-99 and ASTM D7585/D7585M were used as guidance to assess this performance measure (Dwyer et al. 2013). Each image was adjusted separately using the default thresholding method in accordance with the color space (L*, a*, and b*) to specify the worn area of the marking material based on the color difference (i.e., white or bright colors represented the marking material and black or dark colors referred to worn areas). A durability rating procedure was used to determine the remaining marking material percentage (where zero equated to complete material loss and 100 equated to all material still remaining) (Dwyer et al. 2013).

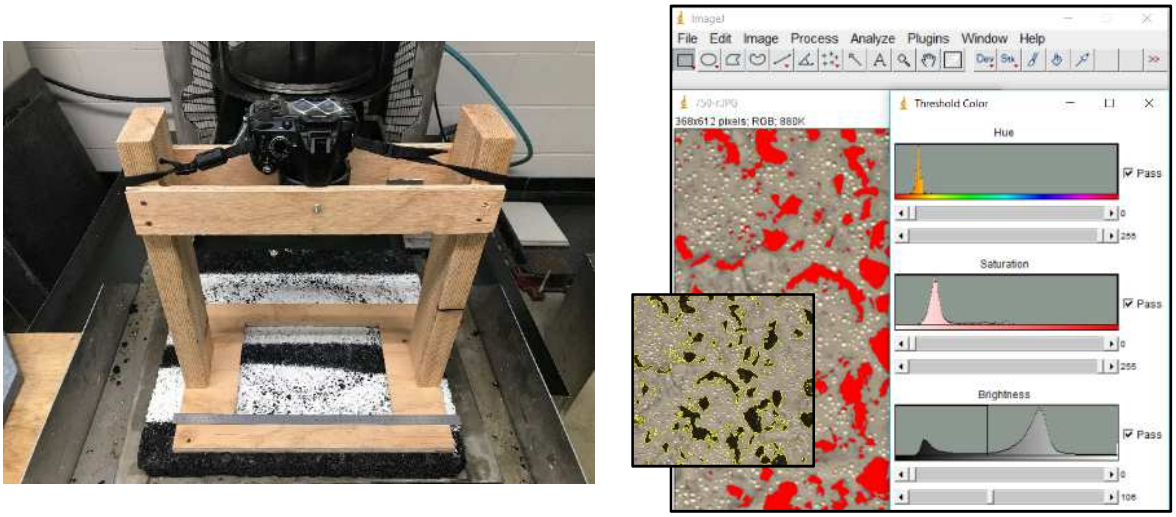

Figure 3.21: Camera stand and software interface

3.5.Experimental Design:

The TWPD was used to polish the asphalt substrates and to evaluate pavement marking materials under various loading conditions. Different wheelsets (pneumatic, steel, and a combination of pneumatic wheels and scraper blade) were mounted on the TWPD. To replicate traffic in a laboratory environment, the TWPD was used to accelerate the "wearing out action" of the pavement marking to study degradation. The TWPD polished a circular path using three caster wheels that tracked in a 11-inch diameter circle (abrasion wheel assembly) on top of the prepared slabs. Thus, the surface affected by the different wheelsets

was studied to determine pavement marking performance after each cycle interval since marking deterioration is significantly affected by repeated tire, blade, or steel wheel contact. The pneumatic wheelset simulates the normal tire effect that can be expected to occur in the field. The combination of pneumatic wheels with a scraper blade was developed and used to simulate snow removal activity and the steel wheelset was used to study more harsh effects (destructive) on the pavement markings. All pavement marking substrates were subsequently subjected to wet accelerated wear testing at room temperature (25°C, 77°F). Table 3.2 provides more details for the three wheelsets.

Table 3.2: Wheelset types and descriptions

Wheel Number	Wheelset description	Wheel dimensions		Capacity (lbs)	Approximate Weight of Wheels (lbs)	Normal Load (lbs)
		Diameter (in)	Tread Width (in)			
1	Pneumatic wheel	8	2.8	300	4.25	105
2	Payductile iron wheel, steel	8	3.0	5,000	20	105
3	Combination of pneumatic wheel and scraper blade	8	2.8	5,000	20	105

It should be noted that the idea of testing the effect of the combination of pneumatic wheels and scraper blade under cold conditions (–10°C or 14°F) was excluded because of the difficulty in obtaining appropriate performance measures. In particular, a frozen water film on top of the marking material directly affected the retroreflected light.

As part of the laboratory procedure, all samples were equally subjected to 100,000 cycles (with one TWPD cycle representing three tire contacts) at different speeds because of surface irregularity. The speed was 50 revolutions per minute (rpm) when using the pneumatic wheelset, 30 rpm when using steel wheels, and 20 rpm when using the combination of the pneumatic tires and scraper blade. The weight above the wheels was maintained at 15 kilograms (33 pounds or three standard No. 10 circular plates). The tire pressure of the pneumatic tires was maintained at 345 kilopascals (50 psi) during laboratory testing.

3.5.1. Reduced Measurement Area

To evaluate pavement marking performance over time, the surface affected by the wheel path of the TWPD was studied. The retroreflectometer captured a 4-inch by 3.5-inch (10-centimeter by 9-centimeter) area. Since the wheel path for the pneumatic wheels only covered an area 1.57-inch by 3.15-inch (4-centimeters by 8-centimeters), retroreflectivity readings were taken within a consistently framed area; the readings were then multiplied by an adjustment factor to be corrected. A similar adjustment was made for the steel wheelset (2.36-inch by 3.15-inch or 6-centimeter by 8-centimeter) and pneumatic with steel wheels and scraper blade (1.57-inch by 3.15-inch or 4-centimeter by 8-centimeter) tests, and these correction factors were applied to the dry, recovery, and continuous wetting readings for each wheelset. Table 3.3 shows the calculation of the correction factors for the 1.57-inch by 3.15-inch (4-centimeter by 8-centimeter) reduced area. Three slabs were evaluated at each measurement condition (dry, recovery, and continuous wetting), and five retroreflectivity measurements were calculated and then averaged for each sample, with and without the reduced area.

Table 3.3: Estimation of the reduced measurement area correction factor

Measurement Condition	Slab Number	Average Full Retroreflectivity Measurement (mcd)	Average Reduced Area (4 cm x 8 cm) Retroreflectivity Measurement (mcd)	Percent Reduction	Average Percent Reduction	Correction Factor
Recovery	S1WW	125	90	28.00%	44.10%	1.441
	S9TW	102	48	52.94%		
	S8TW	111	54	51.35%		
Continuous Wetting	S1TW	51	20	60.78%	57.69%	1.577
	S9TW	77	32	58.44%		
	S8TW	78	36	53.85%		
Dry	S1WW	314	140	55.41%	56.60%	1.566
	S2WW	303	141	53.47%		
	S3WW	307	120	60.91%		

3.5.2. Initial Accelerated Wearing and Weathering Test

An initial test was undertaken to establish a suitable procedure with appropriate interval cycle spans. This test also determined an appropriate weight value to be placed on the turning table to ensure a gradual degradation pattern of the pavement marking without exhausting machine parts. To put it simply, a slab striped with waterborne pavement markings was polished using the pneumatic wheelset until reasonable retroreflectivity deterioration was noticed. Thereafter, performance measures were conducted to gauge the deterioration due to abrasion. Intervals were set at: 100, 500, 1,000, 5,000, 10,000, 30,000, 50,000, and 100,000 cycles. All slabs were subjected to the same number of cycles and compared with each other and field data.

Wet testing was initially conducted instead of dry testing because when the rubber pneumatic wheels lost contact with the slab surface due to a reduction in slab height the test was stopped. This reduction in tire height resulted from tire abrasion. The tire pressure for the pneumatic tires was maintained at 50 psi which represented an average pressure for all traffic as it is lower than typical truck tire pressure but higher than automobile tire pressure. The

National Center for Asphalt Technology Report 06-06 was used as guidance during initial testing of the TWPD (Vollor and Hanson 2006).

The TWPD executed 100 maximum cycles per minute. If the TWPD was set to execute axle loads for 24 hours per day over a period of 7 days, then about 1 million axle loads could be executed in one week. This number of cycles is approximately equal to that provided by the AETEC, BASt, and MMLS. When studying pavement markings, 100,000 cycles was sufficiently causing a significant amount of retroreflectivity deterioration for a waterborne pavement marking sample under the pneumatic tires.

The effect of the accelerated weathering on the visual appearance (physical characteristics) of the waterborne and thermoplastic pavement markings was investigated. During the accelerated weathering procedure, the dry, recovery, continuous wetting retroreflectivity, and color retention measurements for each specimen were measured every 24 hours of exposure for the first 20 days (480 hours) and every 100 hours afterward. The total test duration was 2,000 hours. The durability was not measured under the accelerated weathering protocol because samples were not subjected to dynamic forces. Since the area of the markings striped on the aluminum substrates were larger than the area captured by the retroreflectometer, the reduced area technique was not used in the accelerated weathering procedure. In the initial test, no significant changes were observed when applying an average irradiance of 0.35 W/m^2 at 340 nm with a chamber temperature of approximately 63 °C. Therefore, condition settings were updated as described later in chapter 4. Table 3.4 presents the testing matrix for the evaluation procedure where, R_L, R_{L1}, R_{L2}, represent the retroreflectivity in dry, recovery, and continuous wetting, respectively, and C and D represent color and durability.

Table 3.4: Testing matrix for the evaluation procedure

Testing Procedure	**Device**	**Instrument**	**Marking Material**	**Waterborne Markings**		**Thermoplastic Markings**	
			Marking Color	White	Yellow	White	Yellow
Accelerated Loading Testing	**Three-Wheel Polisher Device (TWPD)**	**Pneumatic Tires**	**Applied Performance Measures**	$R_{L,1,2}$+C+D	$R_{L,1,2}$+C+D	$R_{L,1,2}$+C+D	$R_{L,1,2}$+C+D
		Steel Wheels		$R_{L,1,2}$+C+D	$R_{L,1,2}$+C+D	$R_{L,1,2}$+C+D	$R_{L,1,2}$+C+D
		Scraper Blade		$R_{L,1,2}$+C+D	$R_{L,1,2}$+C+D	$R_{L,1,2}$+C+D	$R_{L,1,2}$+C+D
Accelerated Weathering	**Xenon Arc Chamber (XAC)**	**Chamber**		$R_{L,1,2}$+C	$R_{L,1,2}$+C	$R_{L,1,2}$+C	$R_{L,1,2}$+C

CHAPTER 4: LABORATORY PROCEDURE RESULTS AND ANALYSIS

This chapter presents the analysis and results of the laboratory-based procedure described in Chapter 3 and is organized to: present the findings of the pavement marking performance measures under accelerated load testing (i.e. retroreflectivity, color change, and durability) and accelerated weathering (i.e. retroreflectivity, and color change).

4.1. Pavement Marking Performance under Accelerated Load Testing

4.1.1. Retroreflectivity Deterioration

Based on the procedure described in the previous chapter, the change in percent of pavement marking retroreflectivity under three conditions (R_L, R_{L1}, and R_{L2}), for two colors (white and yellow) of waterborne and thermoplastic materials, and under different operating conditions (i.e., steel wheels, pneumatic wheels, scraper blade) was determined (see Figure 4.1 to Figure 4.3). Percent retroreflectivity lost after each loading interval was calculated and plotted against the number of cycles. In general, a significant drop in percent retroreflectivity was observed in the first 1,000 cycles for all tests and then leveled out as the number of cycles increased. Based on this observation, a logarithmic scale was used to highlight the range before the first 1,000 cycles to measure the changes in retroreflectivity. All pavement marking retroreflectivity models and R^2 under each TWPD wheelset are provided in Table 4.1.

Figure 4.1 a and b show the percent retroreflectivity reading for dry conditions (R_L) versus the number of cycles for different loading wheelsets and for the white and yellow markings, respectively. The figures show how the retroreflectivity equations correlate to actual laboratory data; the graphs display the deterioration based on percent retroreflectivity lost and the initial retroreflectivity corresponds to x equal to 1 in Table 4.1. For example, to illustrate the graphical representation and Table 4.1 for white waterborne markings, Figure 4.1 a shows the percent R_L for the different loading or blade types versus the number of cycles. The coefficient of determination, R^2, for the pneumatic, steel, pneumatic with scraper blade, and scraper blade were 0.90, 0.97, 0.80, and 0.99 respectively, with the section where the pneumatic and scraper blade passed over having the least deterioration.

As expected, the retroreflectivity for all samples dropped with an increasing number of cycles. It was observed that the drop was significant over the first 1,000 cycles. A relatively

small reduction in percent retroreflectivity was noticed between 10,000 to 100,000 cycles as the test was completed. This is similar to what happens in the field, as retroreflectivity dramatically decreases the first few months after installation then stabilizes before the end of service life (Kopf 2004). In the state of Idaho, the reduction in retroreflectivity after the first few months of installation is mainly due to snowplowing activities and traffic exposure on specific locations (e.g., centerlines which are abraided by car tires during passing and on shoulder-lines located on curved roads). In the dry condition setup, the marking sample was placed on a standard flat surface. For pneumatic wheelsets, the retroreflectivity dropped 75% and 90% from the initial R_L for white and yellow waterborne markings after 100,000 cycles, respectively. On the other hand, pneumatic wheelsets did not cause any deterioration for the thermoplastic markings up to 100,000 cycles. The steel wheelset deteriorated 71% of the R_L of the white waterborne markings after just 10,000 cycles and the test was terminated due to severe changes in the marking surface texture. In contrast, thermoplastic markings lasted up to 100,000 cycles and lost 83% of its initial R_L. After 100,000 cycles with the scraper blade, the R_L for the thermoplastic was higher than the waterborne, and their values were 40% and 20%, respectively, of the original for the white markings, and 36% and 25%, respectively, for the yellow markings.

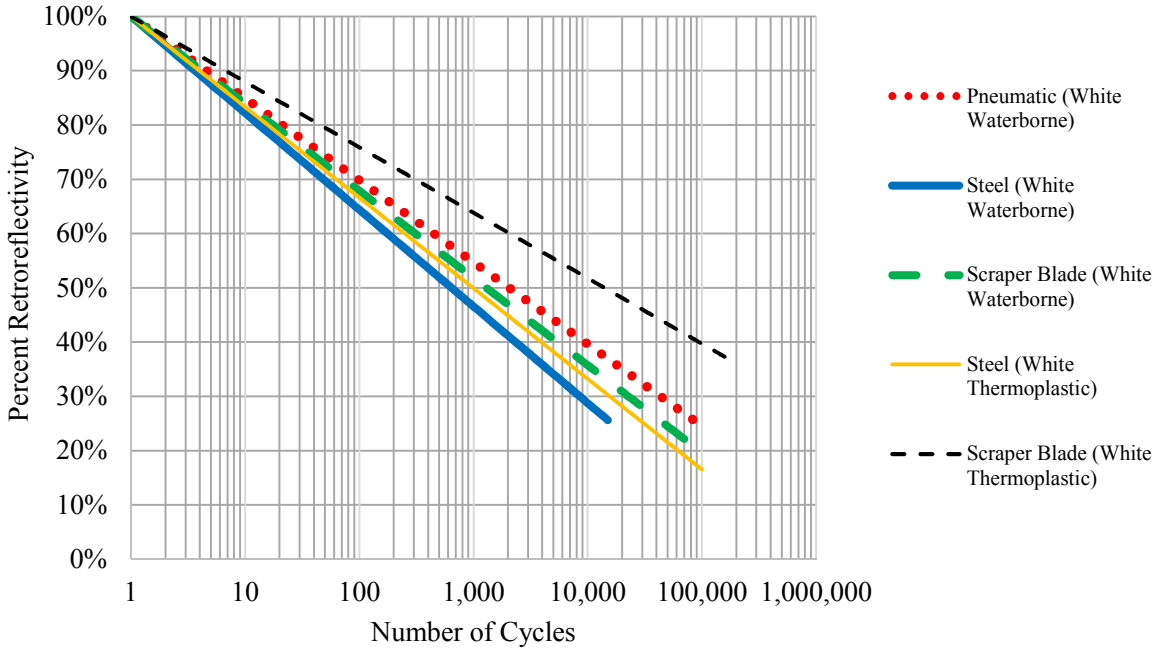

(a)

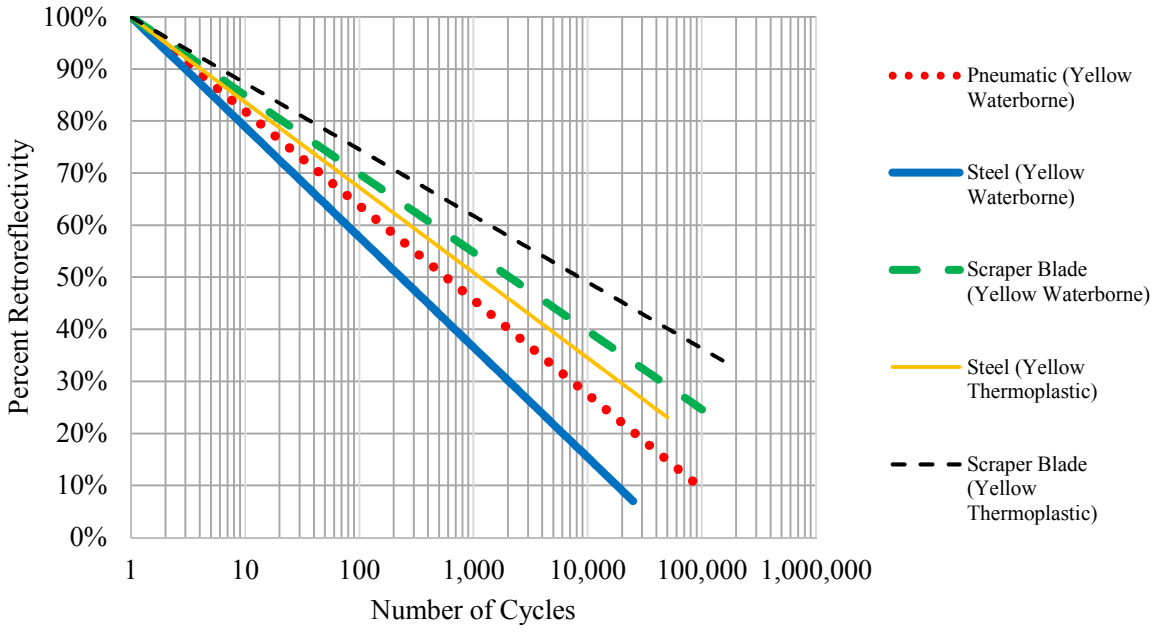

(b)

Figure 4.1: Dry percent retroreflectivity (R_L) for white (a), and yellow (b)

Table 4.1: Pavement marking retroreflectivity models and R^2 under each TWPD wheelset

Wheelset Type (Marking type and Color)	Dry Condition		Recovery Condition		Continuous Wetting	
	Equation	R^2	Equation	R^2	Equation	R^2
White Pavement Marking						
Pneumatic (White Waterborne)	y =-24.94ln(x) + 380.52	0.90	y = -16.63ln(x) + 247.18	0.86	y = -8.31ln(x) + 101.62	0.81
Steel (White Waterborne)	y =-22.55ln(x) + 291.52	0.97	y = -15.84ln(x) + 173.9	0.77	y = -4.10ln(x) + 54.72	0.90
Scraper Blade (White Waterborne)	y = -19.66ln(x) + 281.78	0.99	y = -16.37ln(x) + 259.84	0.9	y = -9.41ln(x) + 156.10	0.85
Pneumatic with Scraper Blade (White Waterborne)	y=-14.87ln(x) + 369.09	0.80	y=-10.35ln(x) + 299.18	0.75	y=-11.76ln(x) + 175.15	0.73
Pneumatic (White Thermoplastic)	y = -16.35ln(x) + 596.08	0.7	y = -4.65ln(x) + 196.80	0.66	y = -4.63ln(x) + 112.32	0.78
Steel (White Thermoplastic)	y = -63.22ln(x) + 871.90	0.83	y = -18.32ln(x) + 268.48	0.65	y = -7.70ln(x) + 116.06	0.75
Scraper Blade (White Thermoplastic)	y = -25.89ln(x) + 494.48	0.68	y = -13.03ln(x) + 177.18	0.89	y = -4.27ln(x) + 67.89	0.72
Yellow Pavement Marking						
Pneumatic (Yellow Waterborne)	y = -12.60ln(x) + 160.12	0.72	y = -8.42ln(x) + 103.17	0.83	y = -5.17ln(x) + 64.45	0.72
Steel (Yellow Waterborne)	y = -20.58ln(x) + 224.11	0.9	y = -14.05ln(x) + 143.68	0.98	y = -8.83ln(x) + 91.29	0.96
Scraper Blade (Yellow Waterborne)	y = -9.83ln(x) + 150.19	0.97	y = -6.98ln(x) + 104.28	0.87	y = -4.56ln(x) + 66.95	0.88
Pneumatic (Yellow Thermoplastic)	y = -7.92ln(x) + 285.03	0.49	y = -3.10ln(x) + 85.15	0.74	y = -1.18ln(x) + 41.60	0.78
Steel (Yellow Thermoplastic)	y = -18.72ln(x) + 263.30	0.95	y = -3.44ln(x) + 63.48	0.29	y = -1.14ln(x) + 21.96	0.82
Scraper Blade (Yellow Thermoplastic)	y = -15.90ln(x) + 201.83	0.94	y = -1.72ln(x) + 30.09	0.51	y = -1.85ln(x) + 24.14	0.96

Figure 4.2 a and b show the change in R_{L1} of the white and yellow markings, respectively, versus the number of cycles of the different wheelsets. This condition represented the marking retroreflectivity performance in situations where dew was present, or after rain. During the recovery setup, measurements were directly taken after 45 seconds of applying the water on top of the marking material in accordance with ASTM E-2177-18, so the remaining water film contributed to reducing R_{L1}. A reduction in R_{L1} due to loading followed the same logarithmic trend as R_L with lower retroreflectivity values.

The coefficient of determination (R^2), for the white waterborne markings for the pneumatic, steel, pneumatic with scraper blade, and scraper blade were 0.86, 0.77, 0.75, and 0.90, respectively. These coefficients were less than the dry readings due to the variability caused by taking readings when the pavement markings were wet. The water surface contributed more light dispersion in all directions rather than retroreflecting it directly back. The scraper blade had the lowest rate of degradation while the steel wheels had the highest rate. Another observation from this data set was that the pneumatic wheels and scraper blade, when testing the white waterborne material, had very similar rates of degradation. All yellow waterborne tests had higher deterioration rates than yellow thermoplastic (see Figure 4.2 b).

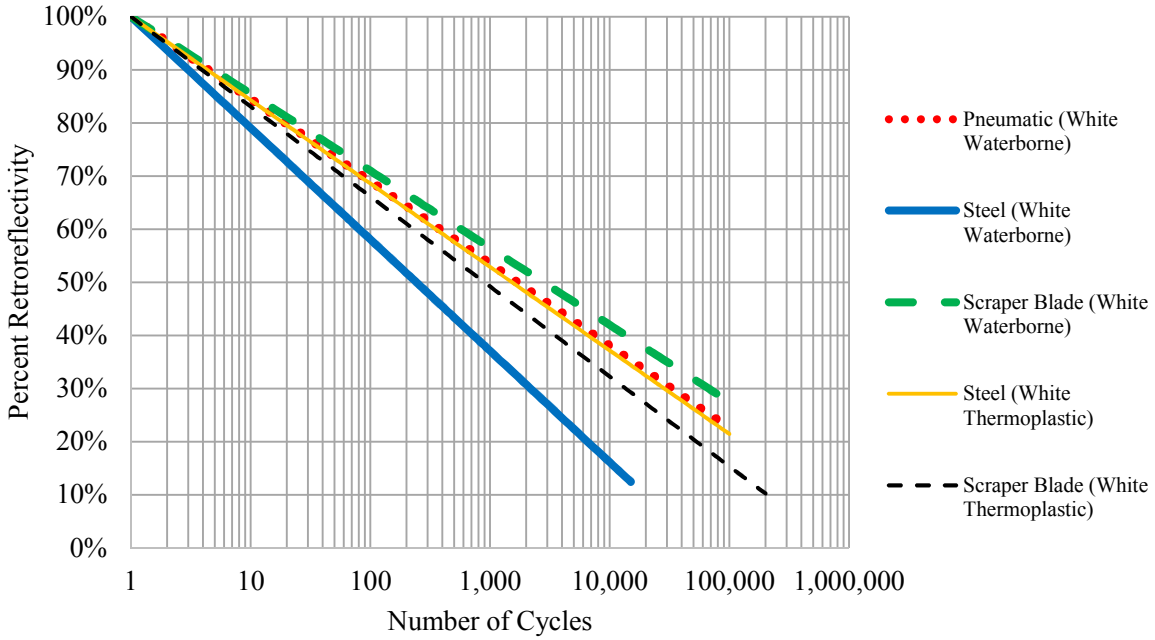

(a)

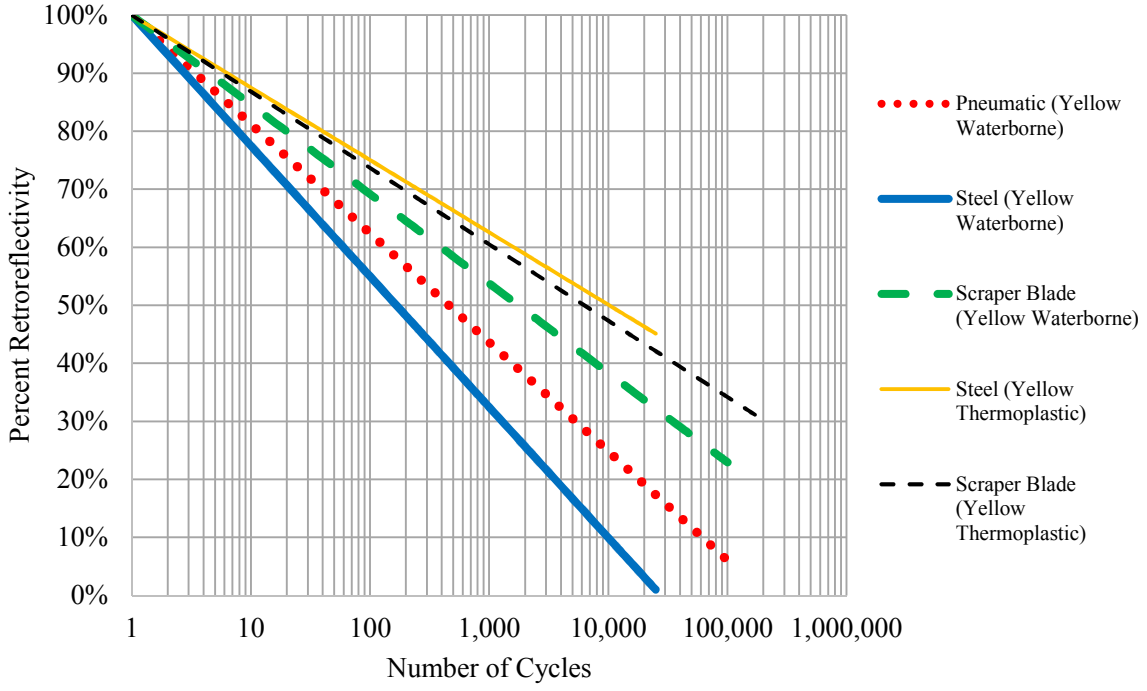

(b)

Figure 4.2: Recovery percent retroreflectivity (R_{L1}) for white (a), and yellow (b)

Figure 4.3 a and b show the R_{L2} percent retroreflectivity readings versus the number of cycles under continuous wetting conditions. This condition represented marking retroreflectivity performance during rain. Similar to the R_{L1} setup, a slope of 2% was maintained for the R_{L2} setup. A reduction in R_{L2} due to loading followed the same logarithmic trend as R_{L1} with lower percent retroreflectivity values.

The coefficients of determination for the white waterborne markings under the pneumatic, steel, pneumatic with scraper blade, and scraper blade were 0.81, 0.90, 0.73, and 0.85, respectively. Based on laboratory testing observations, the voids on top of the pavement surface were filling with water and affecting the continuous wetting readings for each tested condition. The change in percent retroreflectivity of the different wearing methods under the continuous wetting condition had closer trends as shown in Figure 4.3.

After 1,000 cycles of testing the white waterborne markings, it was observed that the scraper blade had decreased the pavement marking retroreflectivity by 0.194 mcd for the dry, 0.161 for the recovery, and 0.041 for the continuous wetting readings. In other words, if the deterioration of a pavement marking retroreflectivity by a snowplow completing one pass was available, the field data could be divided by these values in order to determine a relationship between the lab and field data. This number could then be multiplied by the number of snow plowing events in a year to predict marking deterioration over the course of a winter season.

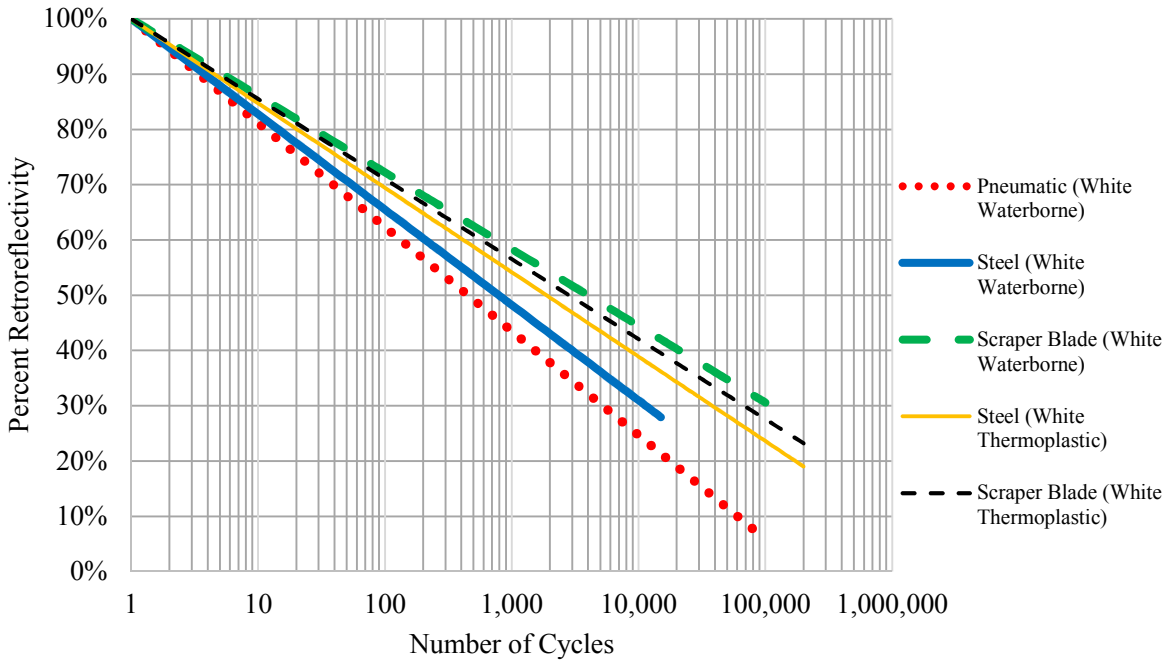

(a)

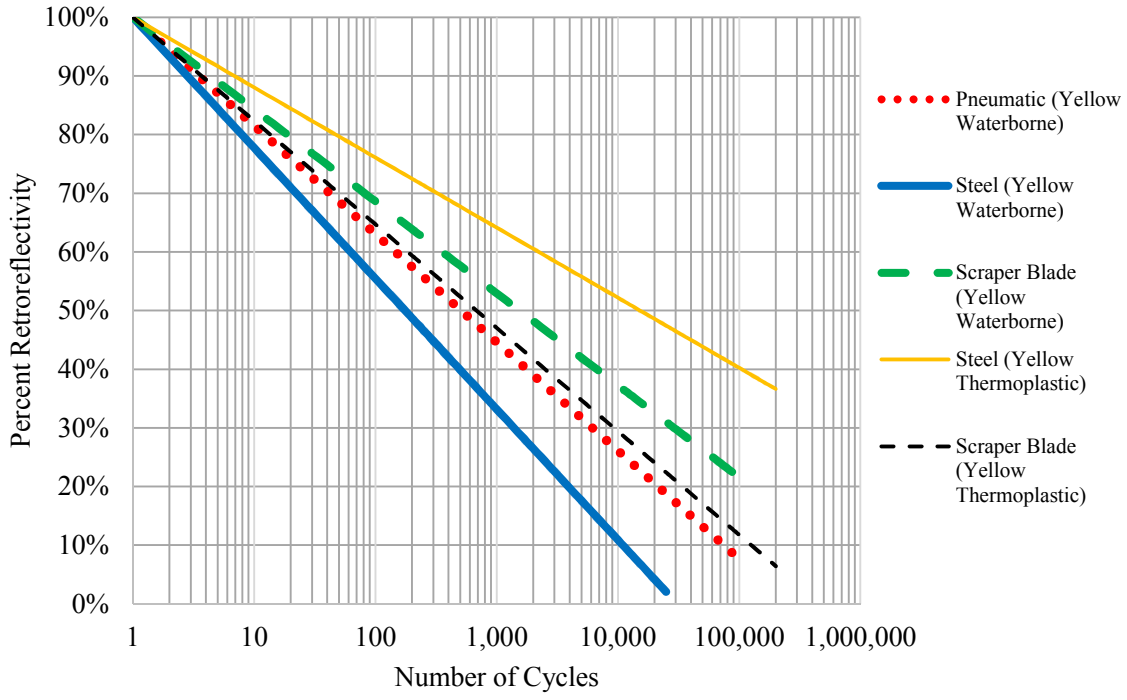

(b)

Figure 4.3: Continuous wetting percent retroreflectivity (R_{L2}) for white (a), and yellow (b)

The thermoplastic marking retroreflectivity performance under both wet conditions (R_{L1} and R_{L2}) showed better performance than waterborne with steel wheelset loadings. In contrast, most scraper blade loading cases showed that the performance of waterborne markings was better than the thermoplastic markings. This could be attributed to two reasons. First, the surface texture of the pavement marking had a strong impact on drainage during the R_{L2} readings. To illustrate, waterborne markings were more permeable than thermoplastic markings, thus water easily passed to the asphalt pavement layer. This reduced the water film on the glass beads which in turn increased the retroreflectivity of the waterborne markings. Second, the blade was scraping the upper peaks of the surface texture, extracting and crushing glass beads located there while some glass beads were secured in the lower peaks (cavities). Thus, because of the flatter surface of the thermoplastic compared to the waterborne material, fewer glass beads were secured, and may have led to lower retroreflectivity. For further details, tables showing retroreflectivity measurements in the laboratory are provided in Appendix A.1.

Various models including linear, exponential, and logarithmic were examined to assess retroreflectivity decay with the number of performance cycles. The logarithmic model was found to provide the highest coefficient of determination (R^2) value for the test data. In addition, among all models, it was found that the logarithmic model had the ability to represent the severe reduction in retroreflectivity during the first 1,000 cycles. The model shown in Equation 7 represents the retroreflectivity decay function:

Equation 7: General pavement markings retroreflectivity decay function

$$y = - m * \ln(x) + r_{initial} \quad (7)$$

where: y equals the predicted retroreflectivity value, m is the slope, x is the number of cycles and $r_{initial}$ is the initial retroreflectivity value.

Figure 4.4 a, b, and c show the imprints of the pneumatic wheels, steel wheels, and combination of pneumatic wheels with scraper blade used in the experiment, respectively. Figure 4.4 c shows the two paths (A and B) evaluated on the pavement marking sample that were polished by the pneumatic wheel and scraper blade combination. This combination had the least percent retroreflectivity deterioration compared to the other wheel sets and the

pneumatic wheel alone caused little rutting on the track (Path A). It should be noted that the slight difference in elevation between the slab surface and the bottom surface of the scraper impeded the wearing action by the scraper along Path A; in other words, there was no direct contact between the surface of the slab and scraper at this location. However, there was direct contact between the scraper and the surface of the slab, away from the wheel, along Path B (see Figure 4.4 d). For this reason, Path B provided a more reliable snowplowing simulation than Path A. As a reminder, the steel wheel test was terminated after 10,000 cycles since the asphalt surface was completely polished and had changed from its original state to a smooth compacted state.

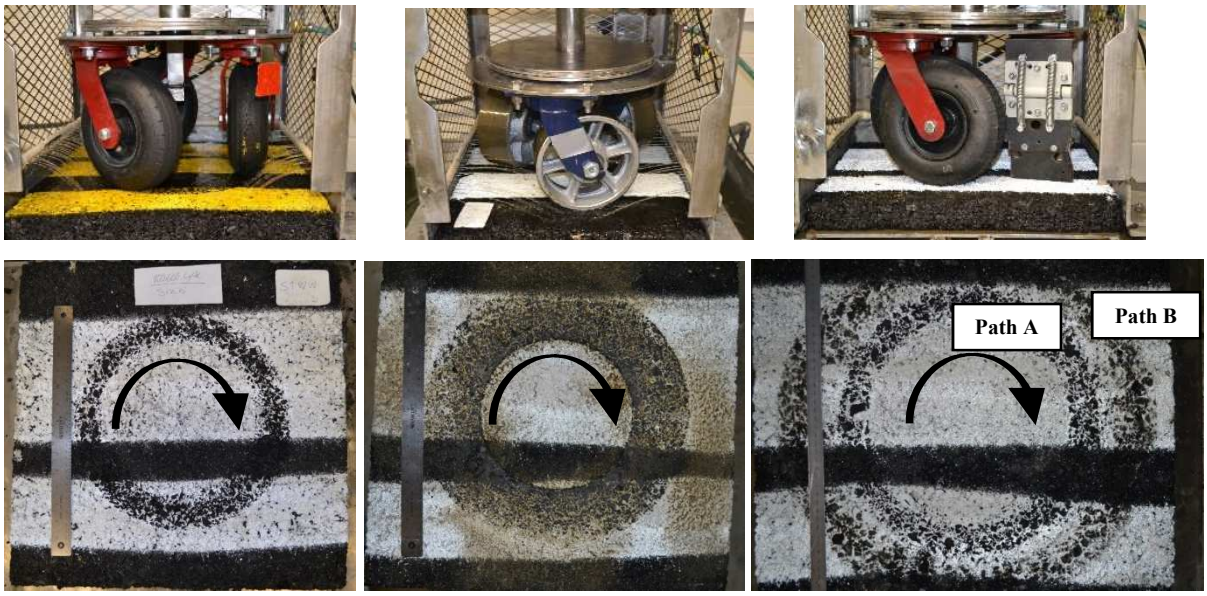

(a) (b) (c)

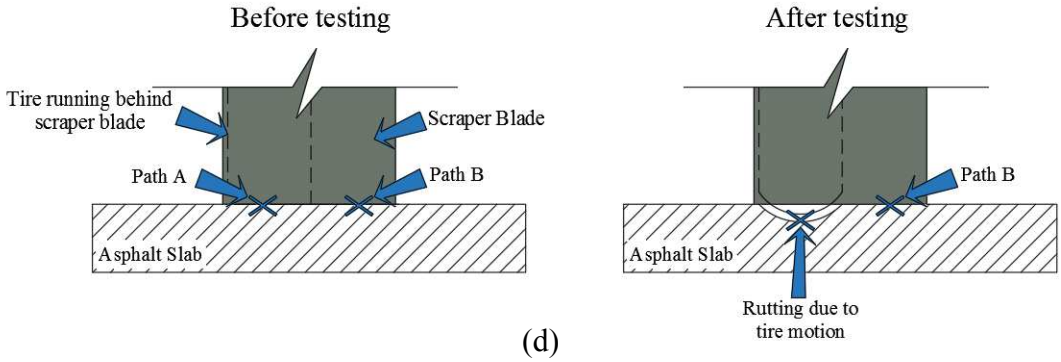

(d)

Figure 4.4: Waterborne markings polished imprints, (a) pneumatic wheelset, (b) steel wheelset, (c) combination of the pneumatic wheels and the scraper blade, and (d) front view section showing the drawback due to overhanging of the scraper blade and tire on path A

Based on the TWPD testing, each wheelset type reduced the retroreflectivity of the pavement marking material in different ways. For example, Figure 4.5 visually describes how the white color for both materials deteriorated under different wheelsets. The pneumatic tires abraided large paint flakes which were holding the glass beads (Figure 4.5 a) but no significant changes were noted in the surface texture of the thermoplastic markings (Figure 4.5b). The steel wheelset crushed and removed most of the glass beads of the waterborne material (Figure 4.5c) but crushed and extracted fewer glass beads from the thermoplastic material (Figure 4.5d). The blade only scraped the waterborne paint located on top of the upper peaks (hills) of the pavement texture but could not reach the lower peaks (valleys) so the lower peaks still retained marking material (Figure 4.5e). The existence of untouched glass beads in the lower peaks explained the retroreflectivity results after 10,000 cycles. In contrast, the blade scraped most of the glass beads from the thermoplastic marking because of the flatter surface (Figure 4.5f). In fact, all of these phenomena also occur in the field when tires and snowplow blades contact the pavement marking surface.

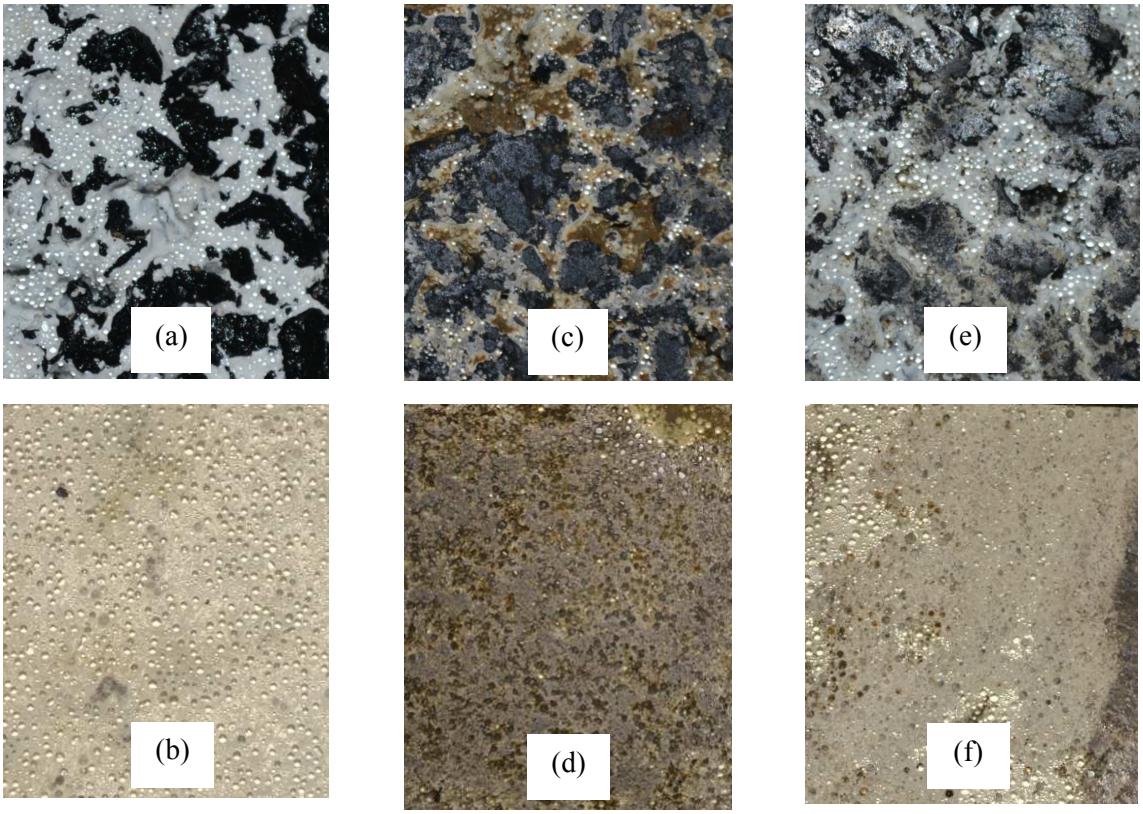

Figure 4.5: Light micrographs of (a and b) waterborne and thermoplastic texture change due to the pneumatic wheelset, (c and d) steel wheelset, and (e and f) scraper blade.

4.1.2. Color Change Analysis

Figure 4.6 to Figure 4.9 show the comparisons between the total color change (ΔE_{ab}) and the changes in lightness (ΔL) of the white and yellow waterborne and thermoplastic surfaces at different loading conditions. No change in color was observed when using pneumatic tires on the thermoplastic markings while a logarithmic change was observed in both ΔE_{ab} and ΔL of the waterborne markings. The steel wheelset had the highest ΔE_{ab} and ΔL after loading, a likely result caused by compaction rather than wearing in addition to the accumulation of color materials on top of the marking surfaces. The ΔE_{ab} and ΔL of the waterborne and thermoplastic markings resulting from the scraper blade had a similar trend but with higher values for waterborne markings. This explains the increased darkness in the waterborne surface after exposure to the same number of cycles.

From Figure 4.6 to Figure 4.9, it can be observed that after loading, the yellow color of both materials experienced greater color change than the white color, while the change in lightness of the white color was higher. In reference to percent retroreflectivity, initial traffic loading of the marking surfaces resulted in dramatic color darkening and further traffic loading caused stability in color and lightness. In other words, when the number of cycles increased the color of the marking materials darkened. These results were consistent with other trials of the same material under similar conditions. Initial traffic loading of waterborne marking surfaces resulted in color darkening and further traffic loading caused stability in color and no significant change in color was observed. The running wheels essentially polished the pavement markings located on the upper peaks of asphalt texture while the lower peaks still retained marking material.

During the waterborne testing, the asphalt background played a major role in darkening the marking surface color while the accumulation of dark abraided particles on the top surface had the same role with thermoplastic markings. The main reason the markings lost lightness and experienced a darkened color was due to a combination of tire wearing and the appearance of the asphalt background. When the tire rotated over the pavement surface, the rubber on the outside of the tire scraped off and onto the pavement surface. As a result, the color analysis revealed a relationship between retroreflectivity and color change. When the markings approached the black color, the markings retroreflected less light.

For the white waterborne markings, the ΔL and ΔE_{ab} results from the pneumatic, pneumatic with scraper blade, and scraper blade only were similar in their ΔE_{ab} which ranged from 35 to 40 after applying 100,000 cycles; however, the steel wheelset reached this level within 10,000 cycles. In other words, the steel wheelset was more abrasive than other wheelsets. A gradual change in ΔL and ΔE_{ab} was observed throughout the experiment. ΔL for the pneumatic, pneumatic with the scraper blade, and scraper blade followed the same trend as that of ΔE_{ab} at 10,000 to 100,000 cycles of exposure. Both ΔL and ΔE_{ab} increased for all wheelsets up to 10,000 cycles for the steel wheels and 100,000 cycles for the others, and the logarithmic scale showed a drastic increase in ΔL and ΔE_{ab} between 10,000 and 100,000 cycles of exposure.

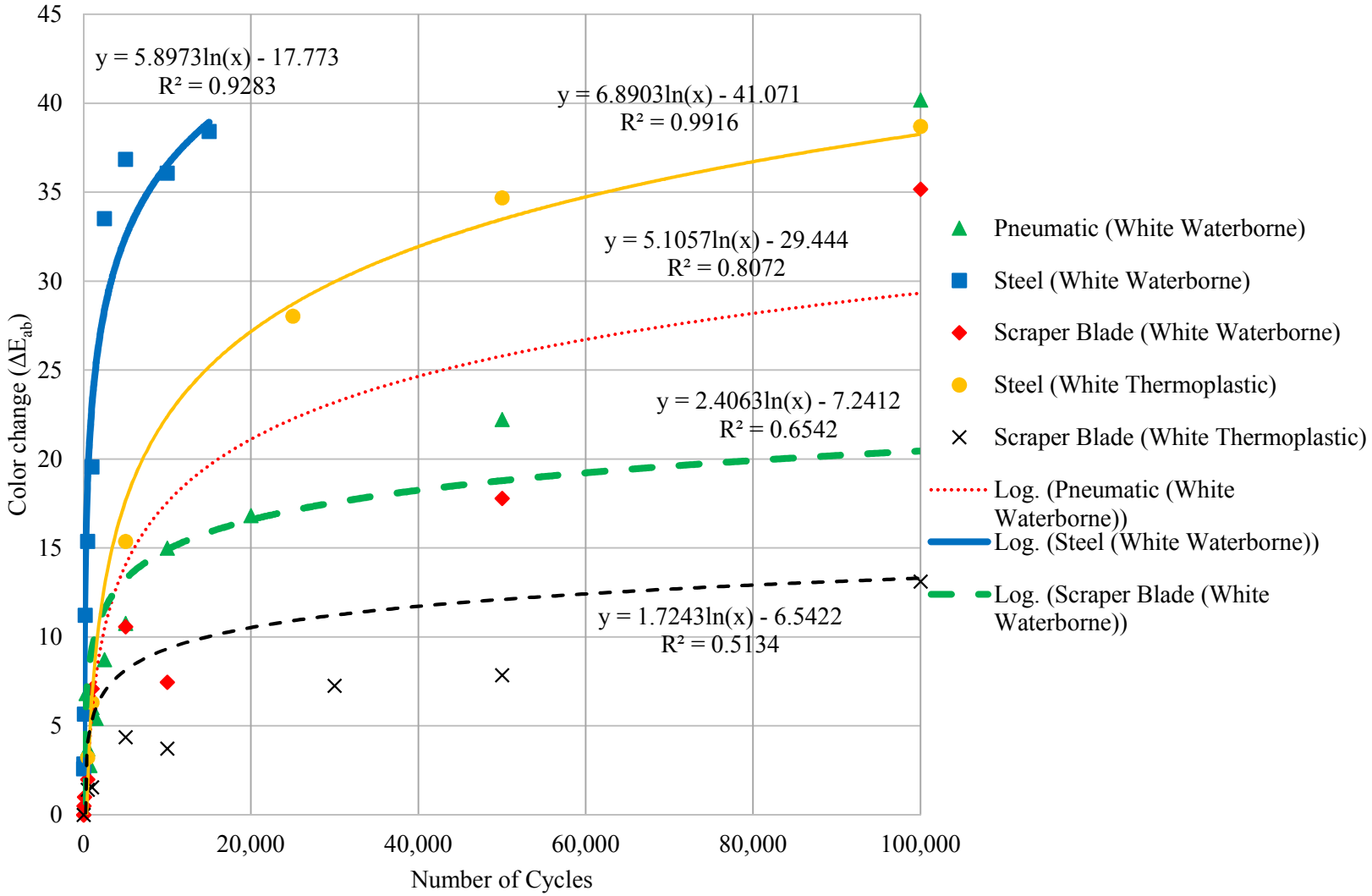

Figure 4.6: ΔE_{ab} vs. number of cycles for white waterborne and thermoplastic

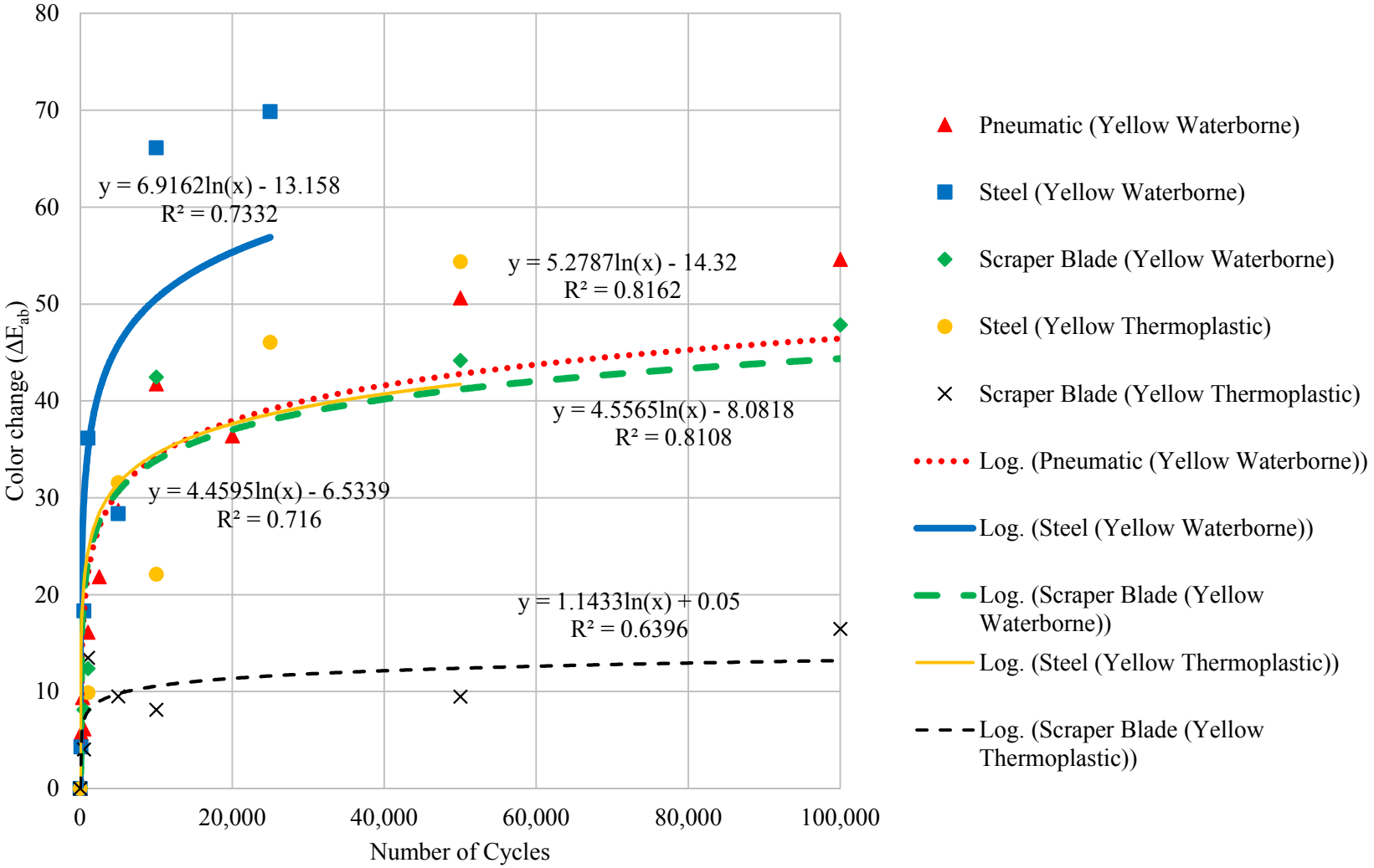

Figure 4.7: ΔE_{ab} vs. number of cycles for yellow waterborne and thermoplastic

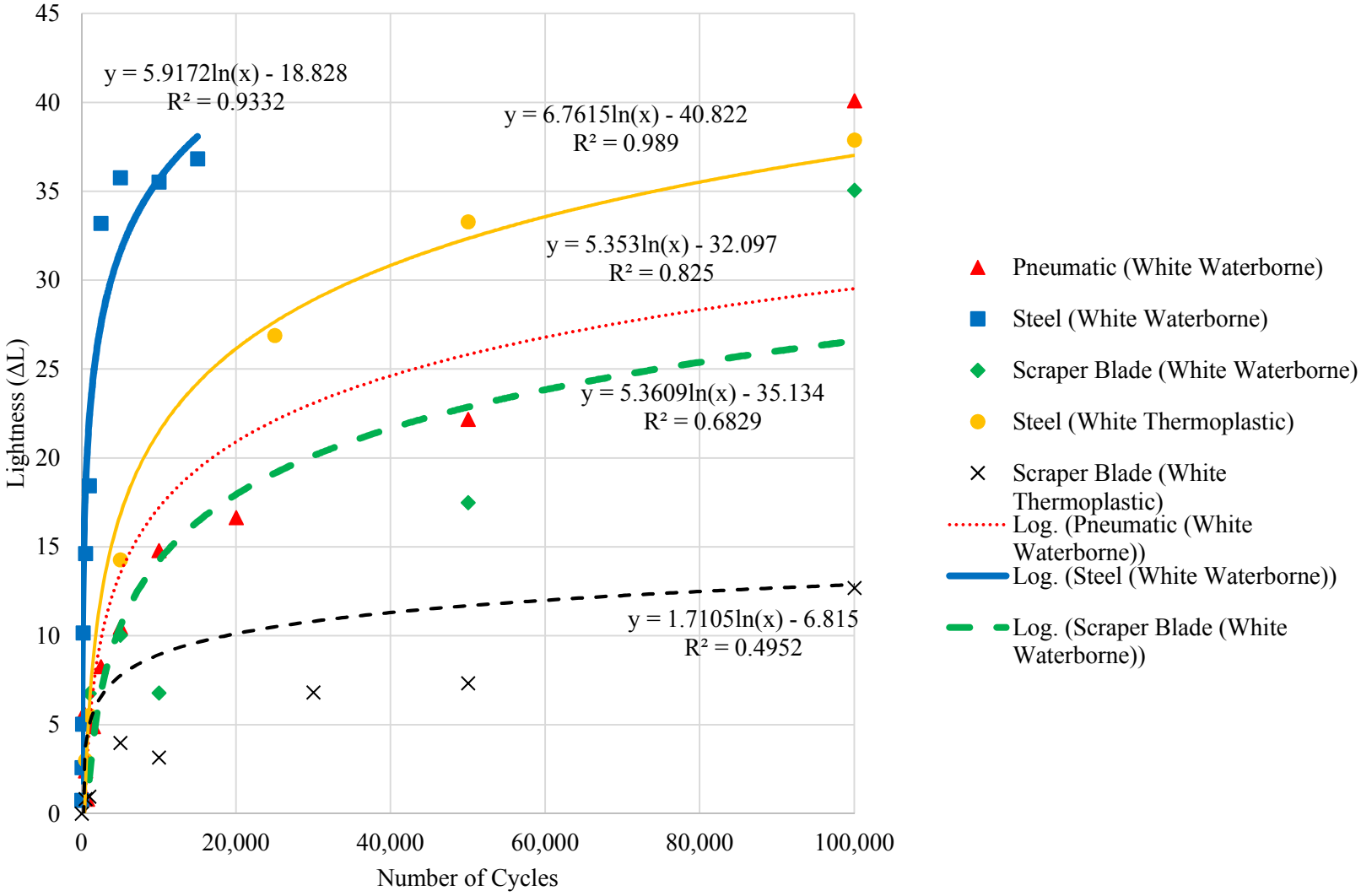

Figure 4.8: ΔL vs. number of cycles for white waterborne and thermoplastic

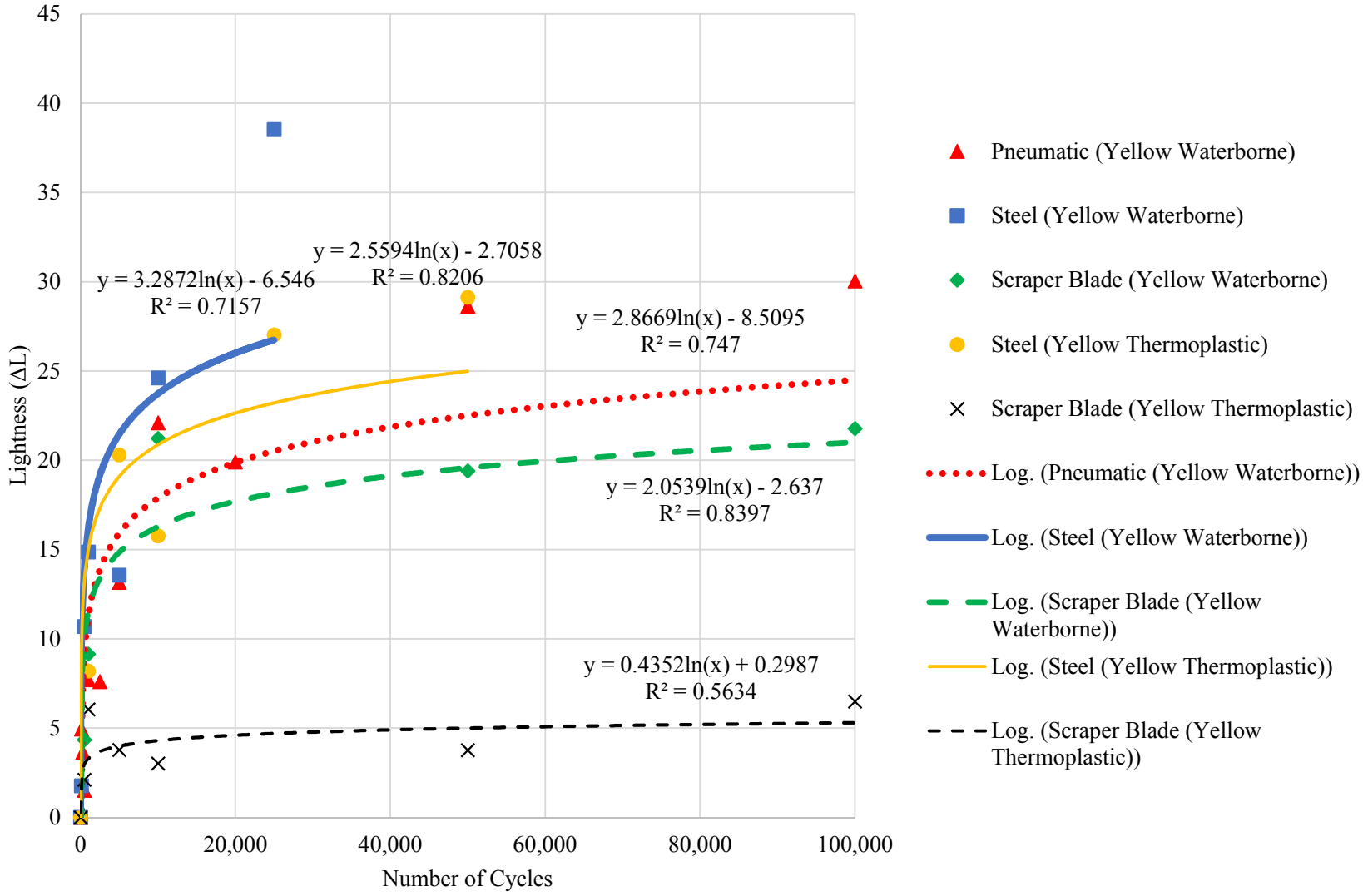

Figure 4.9: ΔL vs. number of cycles for yellow waterborne and thermoplastic

4.1.3. Percent Loss Analysis

Figure 4.10 and Figure 4.11 show the results of the image analysis for the durability comparisons between the white and yellow colors of waterborne and thermoplastic under different TWPD loading conditions. It was observed that the waterborne marking material percent loss due to loading followed a logarithmic function while the eroded thermoplastic marking surface followed a linear function. Because of the different behavior in the surface change of both materials due to the same loading, durability was calculated differently. The waterborne markings peeled off from the asphalt surface, but the thermoplastic material remained on the surface and developed a darker color due to surface abrasion. Therefore, durability for waterborne markings was calculated based on the percent material loss and for thermoplastic markings on the percent of the abraided areas. As a result, thermoplastic markings endured more TWPD loadings than waterborne markings. This performance of thermoplastic markings with regard to retroreflectivity, color change, and durability is similar to field performance as thermoplastic markings generally last longer than waterborne markings.

For the white waterborne markings, the coefficients of determination for the pneumatic, steel, and scraper blade were 0.92, 0.92, and 0.92, respectively. The waterborne marking started to experience material loss after 200 cycles under the pneumatic wheelset. As expected, the steel wheels caused the most rapid deterioration with a 75% loss after only 10,000 cycles. The scraper blade, on the other hand, caused the least percent loss and was attributed to the blade dragging along the surface; as the blade drug over the marking, the markings wore off quicker than any other wheelset but after completely removing all of the top markings, a small change in retroreflectivity was observed after 10,000 cycles. The rutting from the pneumatic, steel, and pneumatic with scraper blade resulted in an increase in percent loss compared to just the scraper blade.

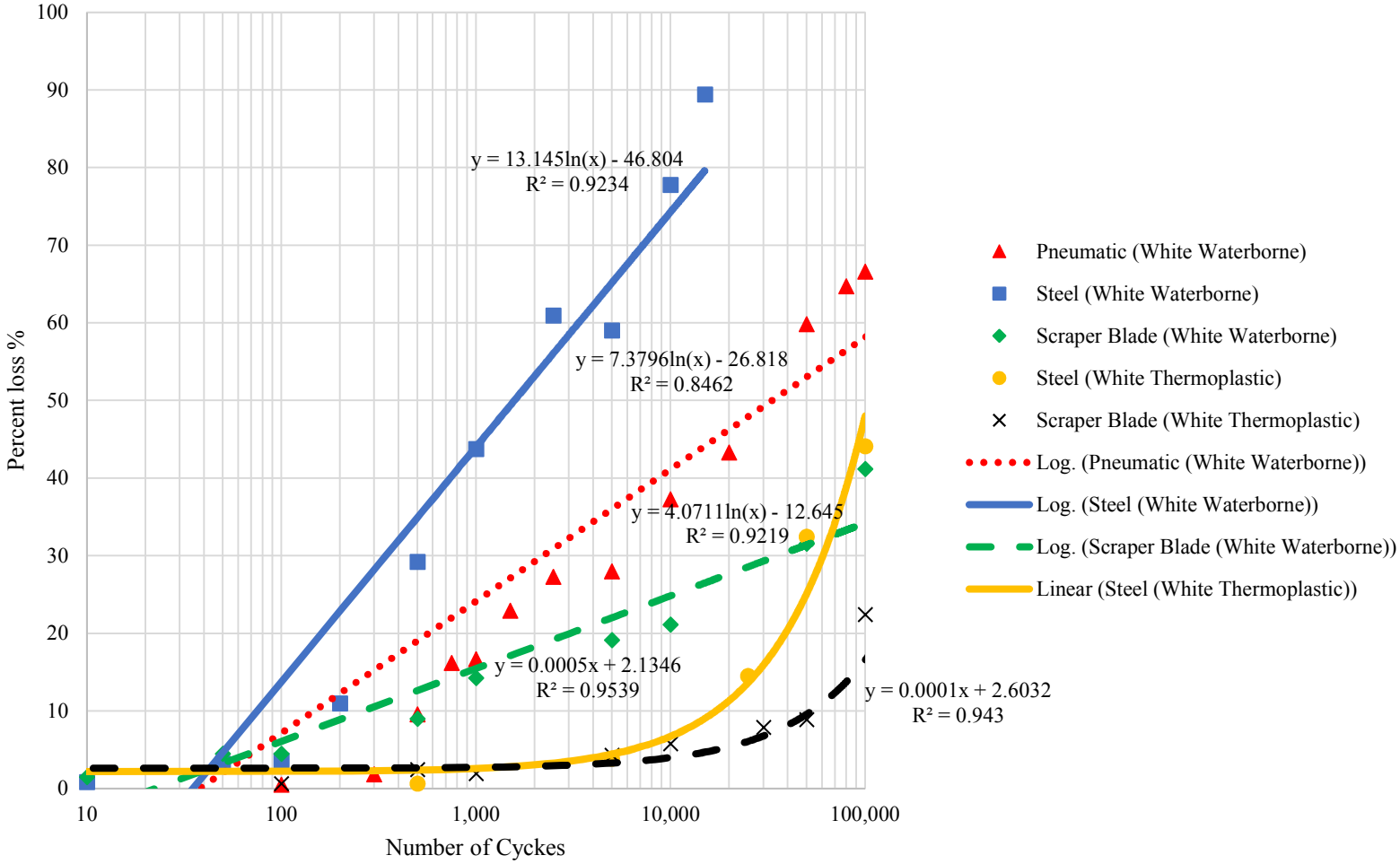

Figure 4.10: Durability Comparison between White Waterborne and Thermoplastic

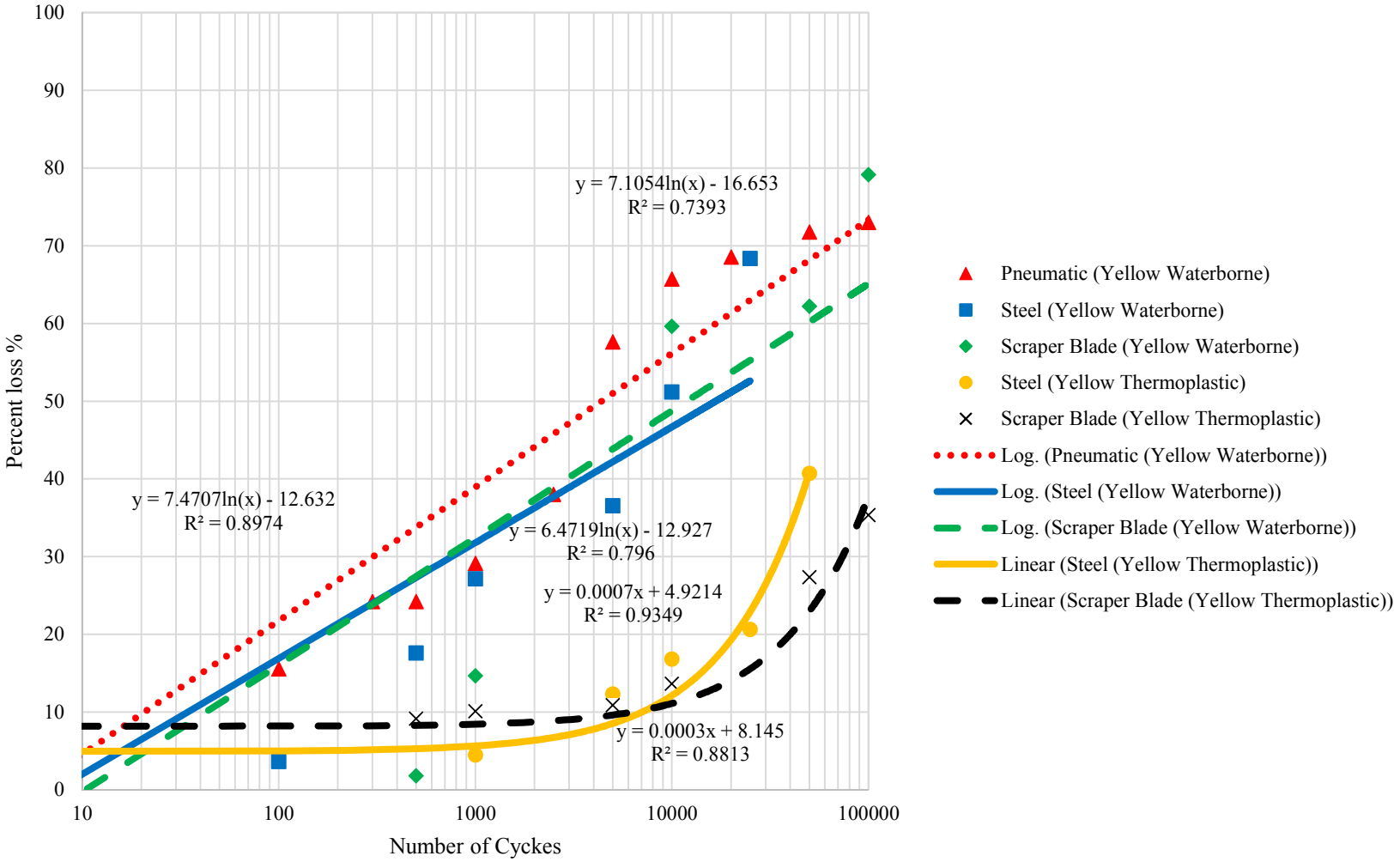

Figure 4.11: Durability Comparison between Yellow Waterborne and Thermoplastic

4.2. Pavement Marking Performance under Accelerated Weathering

4.2.1. Retroreflectivity Deterioration

The percent retroreflectivity after dry (R_L), recovery (R_{L1}), and continuous wetting (R_{L2}) conditions versus exposure time for the two colors of waterborne and thermoplastic markings were determined based on the accelerated weathering experiment (see Figure 4.12). All weathering tests in this study were conducted in isolation from mechanical interference to understand and study the physical effect of weathering on pavement markings in the laboratory, even though influences caused by traffic loadings would occur and affect the marking surface in the field. Unlike the mechanical loading exposure results using the TWPD, an increase in the percent retroreflectivity was observed in all pavement marking samples after the accelerated weathering exposure. This increase in retroreflectivity also occurred in the field immediately after the first few days of installation (Craig et al. 2007), and could be attributed to several reasons:

- After exposure to artificial sunlight, moisture, and high temperature in the weatherometer, the yellow markings faded and became lighter than before testing. When a color closely resembles white, the sample retroreflects more light.
- After weathering exposure, the marking's binder became more brittle and the embedment depth decreased to uncover more glass beads.
- The transmittance of the glass beads increased due to continuous washing of the samples, which in turn contributed to an increase in percent retroreflectivity. This is exactly what happens in the field when pavement markings show an increase in retroreflectivity in the early time period. This results from mechanical wear due to weathering (air blowing) and removal of excess marking material from the top and sides of beads.

All pavement marking retroreflectivity models and the corresponding R^2 under different exposure times in the weatherometer are provided in Table 4.2. A linear relationship between retroreflectivity and the age of the marking materials was examined. Under dry conditions, both thermoplastic marking colors displayed a higher percent retroreflectivity than waterborne markings. By comparison, thermoplastic markings in the field commonly have the ability to retain higher retroreflectivity than waterborne markings. Under the recovery and

continuous wetting conditions, the white waterborne markings showed a higher percent retroreflectivity than the thermoplastic markings while similar trends were experienced with the yellow color. During the recovery and continuous wetting measurements, the surface texture of the pavement markings and the water film thickness were major factors that impacted retroreflectivity values. For further details, tables showing retroreflectivity measurements in the laboratory are provided in Appendix A.2.

Table 4.2: Pavement marking retroreflectivity models and R^2 under accelerated weathering

Measurement condition, color, marking type	Equation	R^2
Dry Retro. White Waterborne	y = 0.0599x + 413.71	0.8397
Recovery Retro. White Waterborne	y = 0.1201x + 53.983	0.8449
Continuous Wetting Retro. White Waterborne	y = 0.0512x + 26.767	0.9871
Dry Retro. White Thermoplastic	y = 0.0782x + 264.71	0.9364
Recovery Retro. White Thermoplastic	y = 0.0373x + 45.719	0.7311
Continuous Wetting Retro. White Thermoplastic	y = 0.0139x + 26.287	0.7306
Dry Retro. Yellow Waterborne	y = 0.0365x + 143.6	0.8071
Recovery Retro. Yellow Waterborne	y = 0.0216x + 45.305	0.5313
Continuous Wetting Retro. Yellow Waterborne	y = 0.0087x + 23.893	0.9513
Dry Retro. Yellow Thermoplastic	y = 0.0888x + 137.07	0.9589
Recovery Retro. Yellow Thermoplastic	y = 0.0248x + 50.576	0.792
Continuous Wetting Retro. Yellow Thermoplastic	y = 0.0109x + 31.821	0.9381

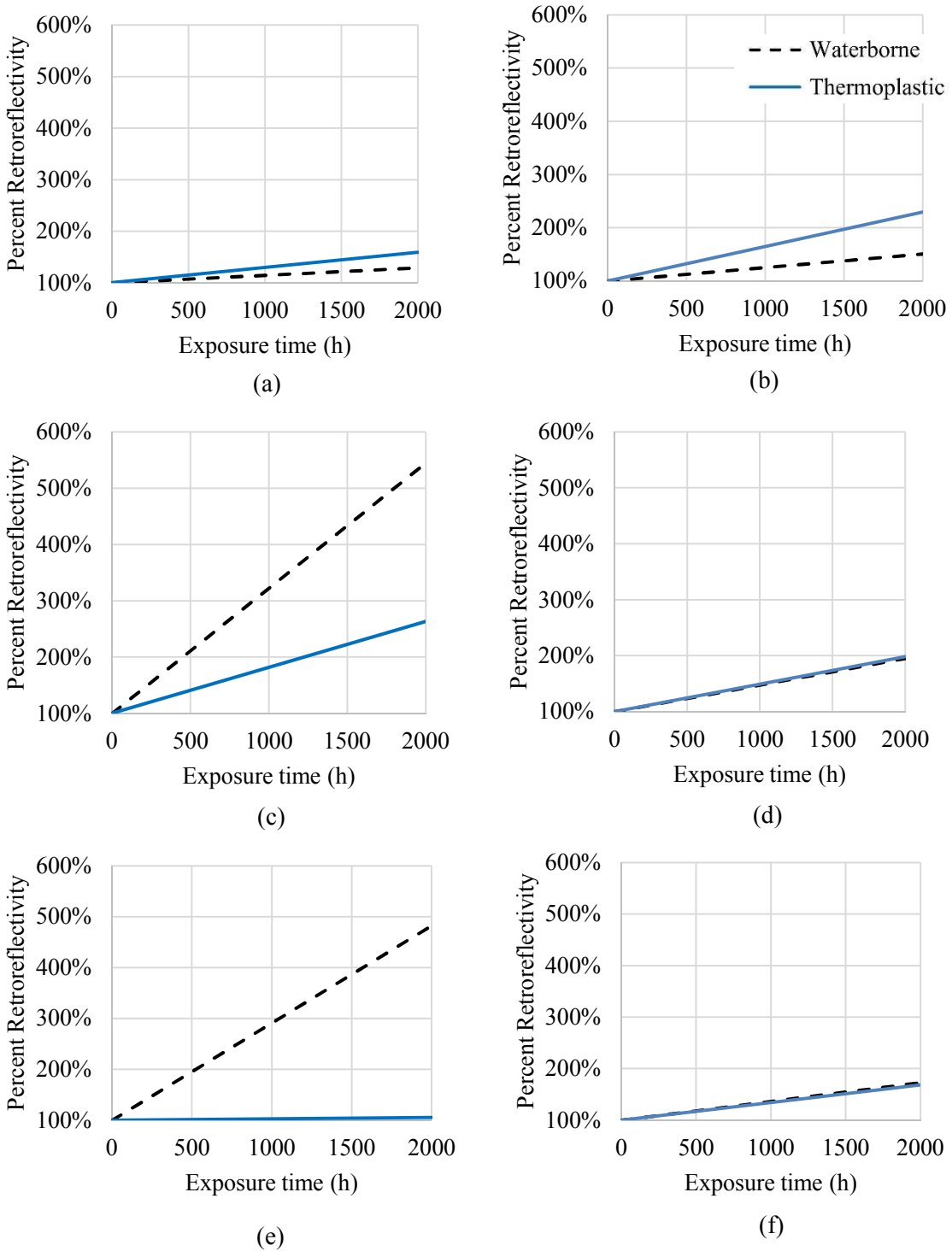

Figure 4.12: Percent retroreflectivity change due to accelerated weathering and conditions against time: R_L (a) white, (b) yellow, R_{L1} (c) white, (d) yellow, and R_{L2} (e) white, (f) yellow.

4.2.2. Color Change Analysis

Figure 4.13 and Figure 4.14 show the ΔE_{ab} and ΔL due to weathering for the white and yellow colors of the waterborne and thermoplastic markings versus exposure times. For waterborne and thermoplastic markings, ΔL and ΔE_{ab} increased upon weathering until 2,000 hours for the XAC and all samples followed a linear function. After 2,000 hours of exposure in the weatherometer, the white markings of both marking materials slightly darkened (ΔE_{ab} increased from 1 to 6.5) while the yellow markings sharply faded (ΔE_{ab} increased from 0 to 40). It can be observed from Figure 4.13 that the ΔE_{ab} value for the yellow waterborne and thermoplastic linearly increased from close to zero change to about 40 and 20, respectively, while a smaller change was noticed in the white color markings. The ΔL followed a same linear trend as that of ΔE_{ab} during the period of exposure. The white color samples were losing illumination (L) while a slight increase in L for the yellow markings was noticed (Figure 4.15).

A pigment reaction to high temperature, water, and sunlight depends on the chemical properties of the material. Longer exposure time in the XAC might completely deteriorate or burn the pavement marking samples. Thus, the difference in color change behavior between white and yellow pavement markings could be attributed to the difference in chemical compounds. To address this behavioral change a chemical analysis after artificial weathering is proposed as a topic for future research.

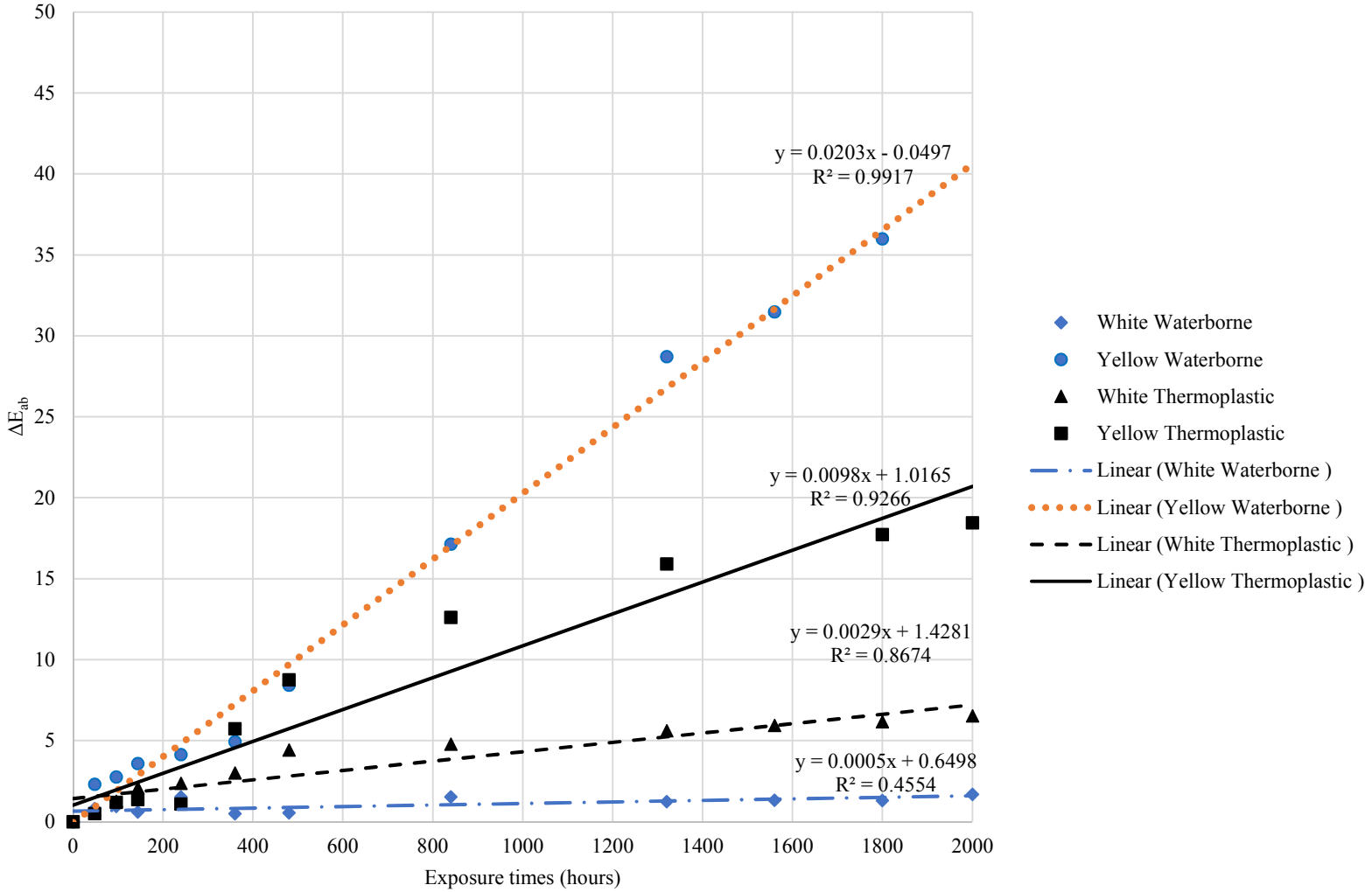

Figure 4.13: Color change (ΔEab) vs. exposure times

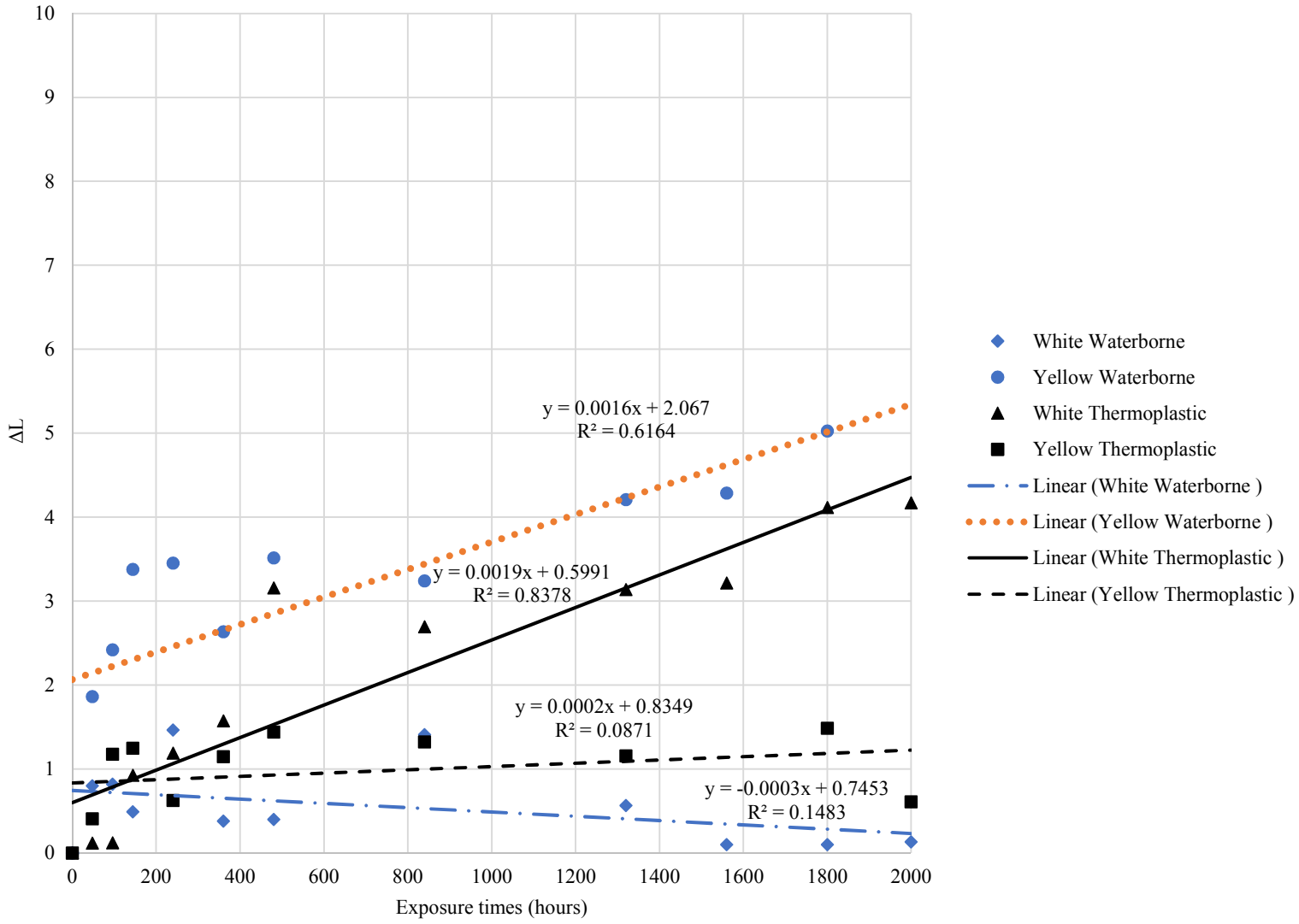

Figure 4.14: Change in lightness ΔL vs. exposure times

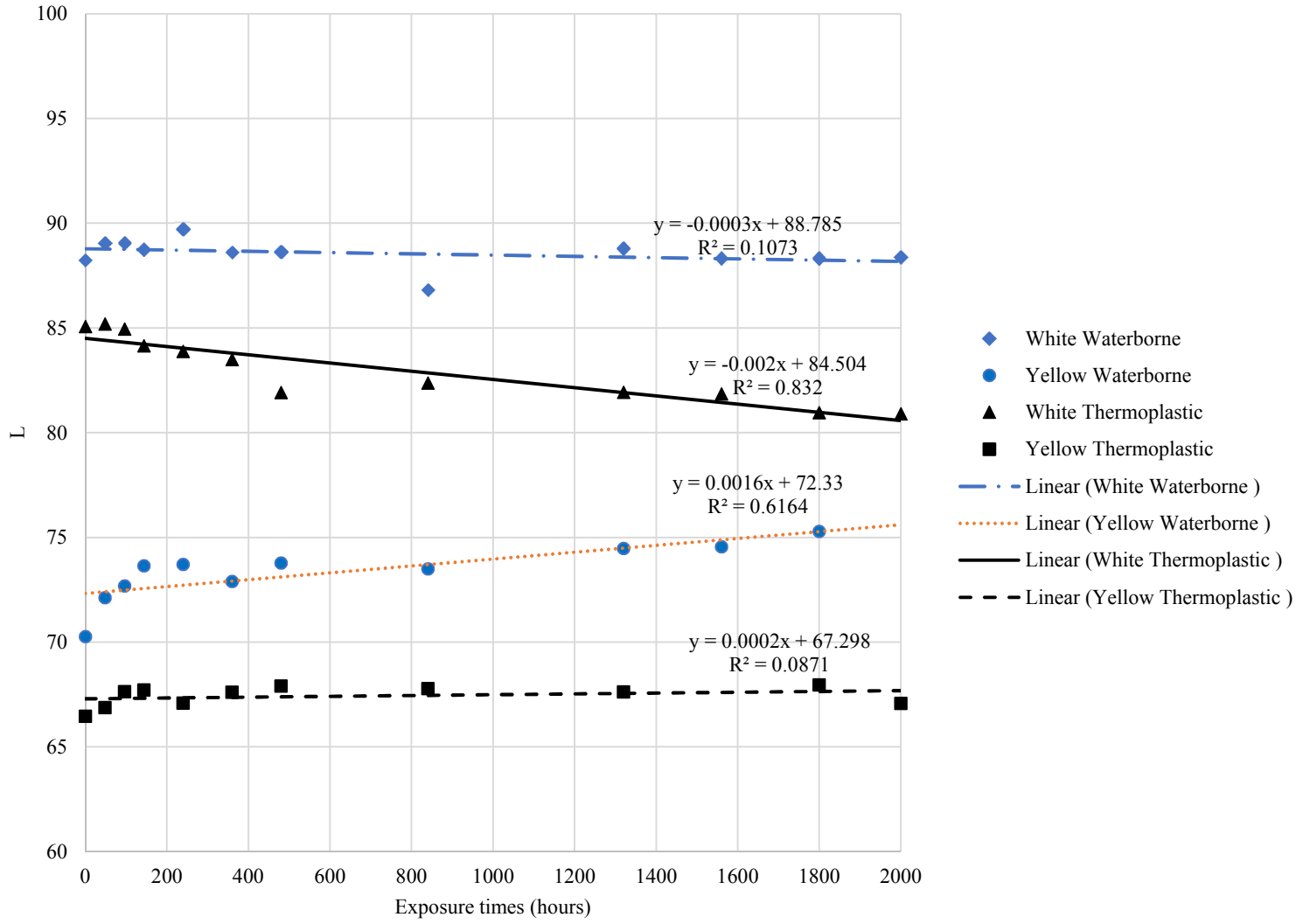

Figure 4.15: Average lightness (L) vs. exposure times

4.2.3. Durability

Figure 4.16 a and b show the yellow waterborne and thermoplastic marking samples before and after 2,000 hours of weathering exposure, respectively. After completing 2,000 hours of weathering, the diffused day color of all samples still satisfied the requirements of the FHWA CIE Chromaticity coordinates. In the field, the marking binder becomes brittle and cracks over time, resulting in bond failures and blow-offs. Under the accelerated weathering test, the same phenomenon was detected and both marking binders became brittle. The waterborne binder began to disband from the aluminum substrates due to small cracks that started to propagate from the top but did not entirely break the paint (Figure 4.16 c); no deep cracks appeared in the thermoplastic binder before 2,000 hours of exposure due to the thicker binder layer.

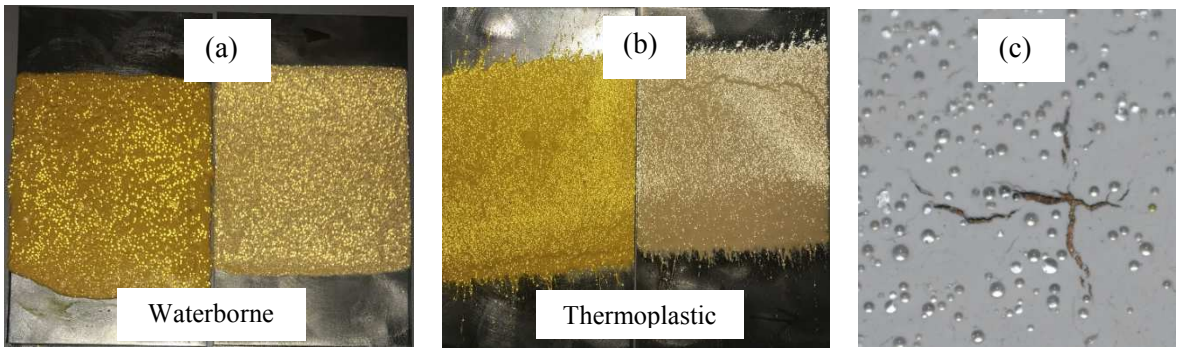

Figure 4.16: (a) photograph of thermoplastic markings, (b) photograph of waterborne markings, and (c) Photograph of cracks due to weathering, samples before and after 2,000 hr. of weathering

CHAPTER 5: FIELD RETROREFLECTIVITY DETERIORATION MODELS

5.1.Retroreflectivity Data Collection in the Field

To understand how the pavement marking changes over time in the field and correlate any changes to the proposed laboratory procedure, field data were collected from rural two-lane highways in Idaho (with respect to climatic change). The same performance measures (i.e. retroreflectivity, color change, and durability) were collected from the field and after which compared with laboratory results. In order to model pavement marking retroreflectivity deterioration in the field, a total of thirty-eight road segments on rural, two-lane highways in Idaho, corresponding to 343.4 miles (see Appendix B.2), were selected as test sites (see Figure 5.1). These test sections were chosen based on the: type of pavement markings (waterborne only), color of edgeline pavement markings (white only), location and climate (per district), pavement surface type (flexible pavements only), and traffic volume. Waterborne pavement marking is recommended to be used on low traffic volumes, therefore, segments of less than 4,000 vehicles per day were specifically chosen for this study.

Pavement marking striping activities in Idaho usually start at the end of March and continue through early August. White waterborne pavement markings in Idaho generally have a service life of one year, so data collection replicated this time period, though the exact timing of the restriping depended on the pavement marking condition, weather, and maintenance crew schedule. For quality assurance purposes, data collection trips were arranged to cover all targeted sites in sequential time periods throughout 2016 and 2017 (July 2016, November 2016, and April 2017) to monitor the degradation of the pavement markings at the test sites. All retroreflectivity measurements were manually collected using a handheld MX 30 retroreflectometer (see Figure 5.2). The data were collected by averaging three pavement marking measurements on three different spots at each mile marker of the targeted sites (nine total readings per marker) and then entered into a database.

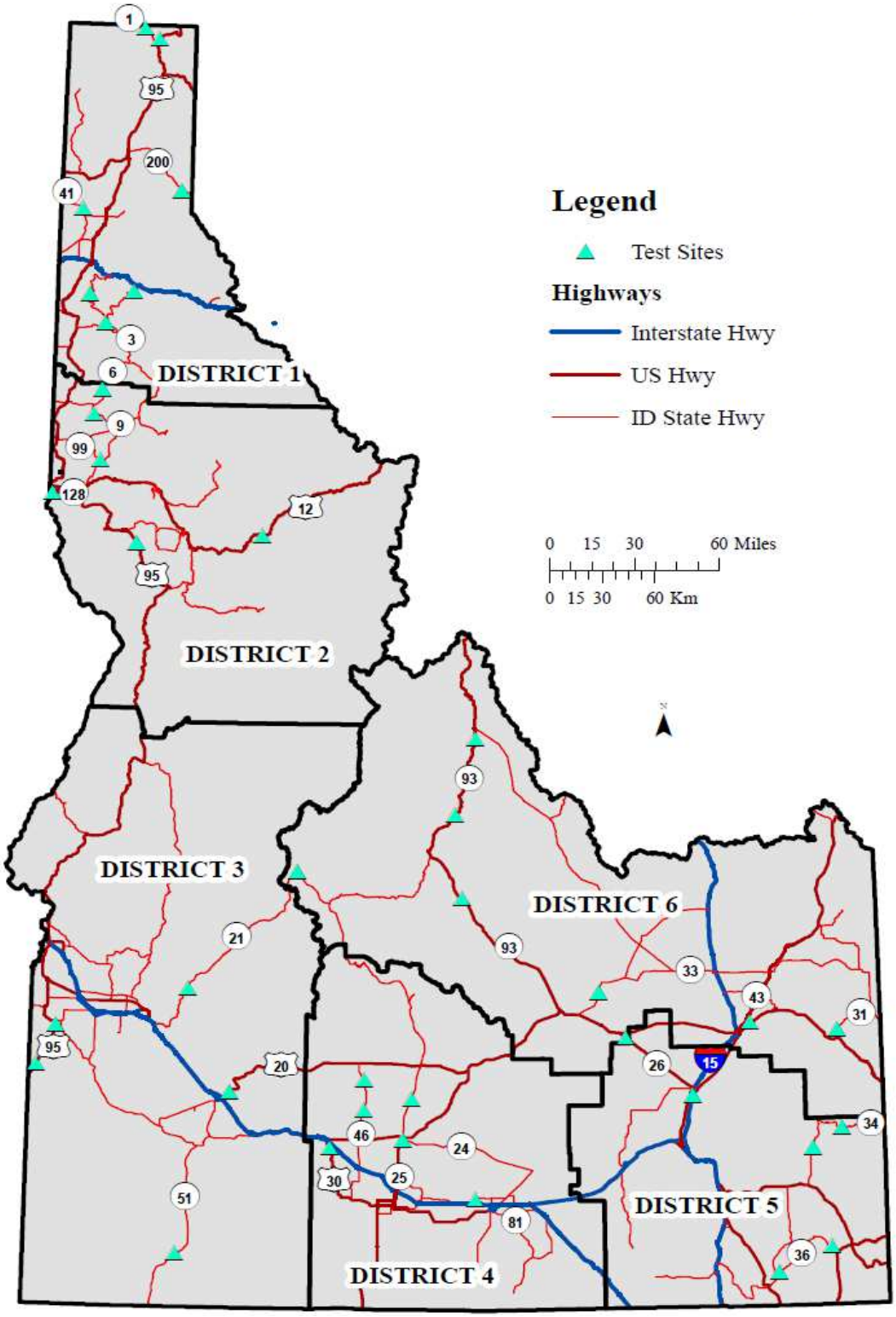

Figure 5.1: Test site locations along highways in Idaho

Figure 5.2: Measuring retroreflectivity at field test sites using MX 30 retroreflectometer

5.2.Field Data Analysis and Results

5.2.1. Idaho Retroreflectivity Deterioration Models

Retroreflectivity data from the Idaho field test sites were analyzed to study the deterioration of pavement markings in each district. Figure 5.3 a shows an example of the data collection results at a test section. In this example, the retroreflectivity measurements were collected right after 1, 5, and 11 months of painting. A logarithmic model was found to provide the highest r-squared for the relationship between pavement marking age and retroreflectivity loss and was used to capture the gradual change in retroreflectivity with time. Figure 5.3 b illustrates the relationship between pavement marking age and retroreflectivity loss for multiple test sections in one district (e.g., District 5) in Idaho. Since the decreasing retroreflectivity curves did not significantly over time vary between test sites an average deterioration curve of all test sites (shown as the dashed line) served as a cumulative representation for the entire district. In fact, an average curve was developed using the same method for the other five districts (see Figure 5.3 c). Table 5.1 shows the pavement marking retroreflectivity decay equations for each district (with x representing the number of months after painting). The constant value in each equation represents the initial value of the pavement marking retroreflectivity (i.e., when x = 1).

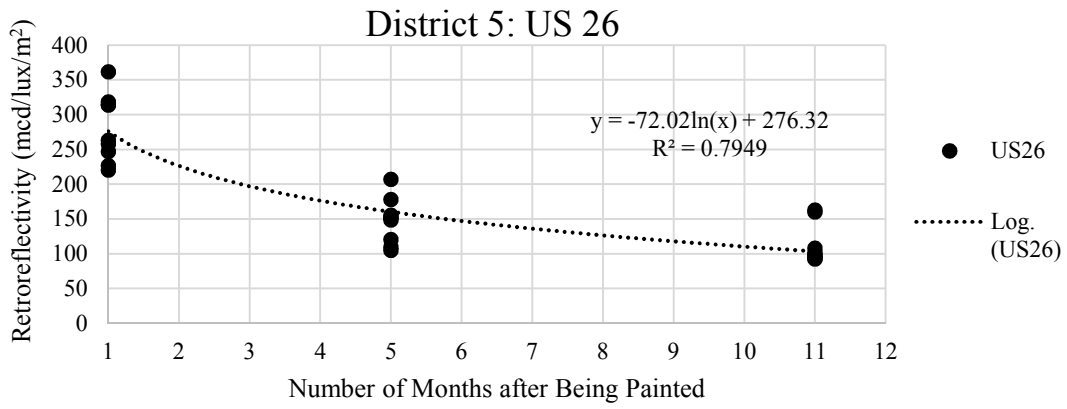

(a)

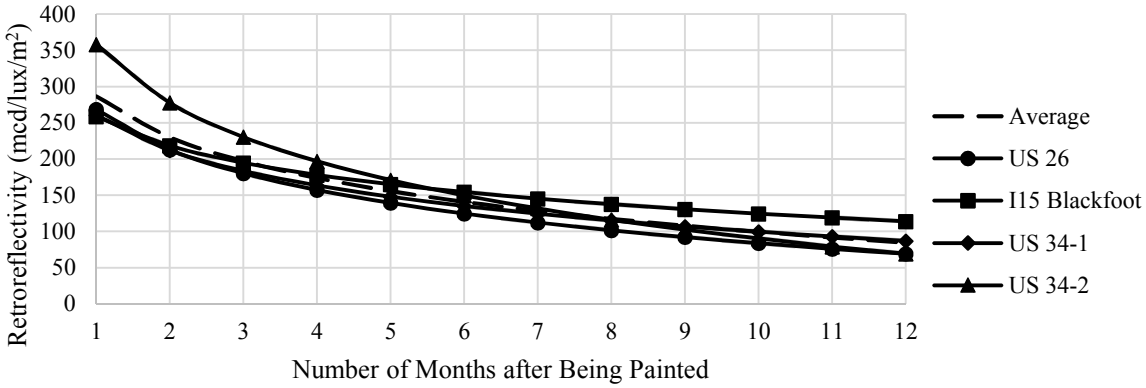

(b)

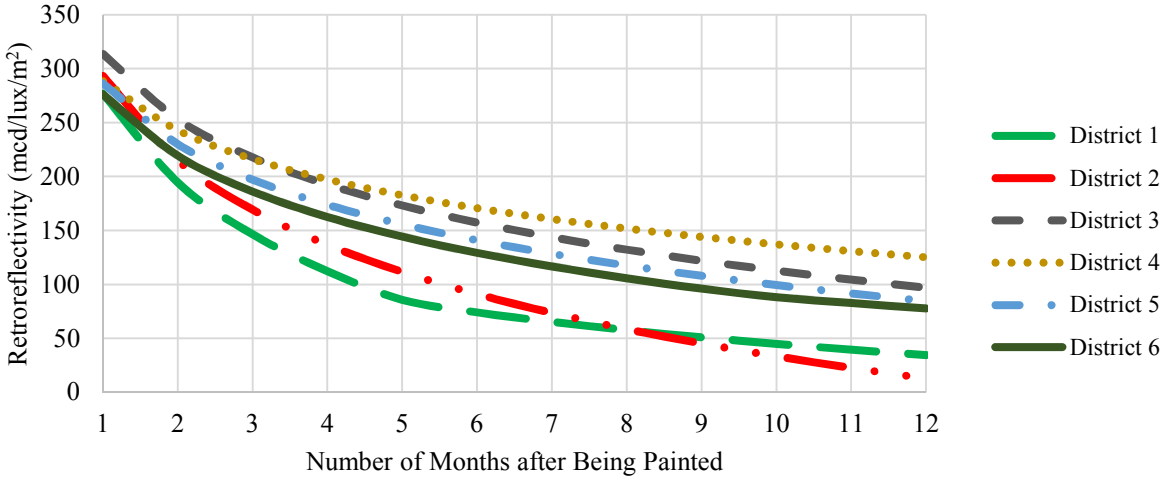

(c)

Figure 5.3: (a) An example of data collection, (b) change in retroreflectivity with time in District 5, and (c) retroreflectivity prediction per month after paint per district

Table 5.1: Monthly retroreflectivity decay equation per district

District	Equation
1	y = -96.25ln(x) + 258.99
2	y = -112.9ln(x) + 293.4
3	y = -87.22ln(x) + 313.67
4	y = -65.7ln(x) + 288.52
5	y = -81.2ln(x) + 286.50
6	y = -80.89ln(x) + 275.14

Figure 5.4 shows the normalized ground snow loads for Idaho based on the 2015 snow load map data (Al Hatailah 2015). Previous research has shown that pavement markings deteriorate at a higher rate in colder climates, and winter maintenance activities and harsh weather are the most dominant factors contributing to pavement marking deterioration (Mull 2011 and Cottrell, 1995). Figure 5.5 shows the relationship between the deterioration rate of pavement marking retroreflectivity and the weighted average normalized ground snow load (NGSL) for all districts for Idaho. This relationship illustrated that a higher NGSL caused greater deterioration (loss) in retroreflectivity, which was likely attributed to the increase in winter maintenance activities (e.g., snowplowing). The NGSL was calculated based on the snow load at each measurement site divided by the site elevation in feet to normalize the data to kilopascals per meter (Kpa/m) or pounds per square foot per foot (psf/ft). Districts 1 and 2 had higher NGSLs (3.26% to 4.18%) compared to Districts 3, 4, 5, and 6, (1.28% to 1.72%). The slope (which represents the deterioration rate of pavement marking retroreflectivity) was calculated from the logarithmic deterioration equation for each district. The normalized ground snow load (NGSL) for each district was calculated using ArcGIS 10.5.1. The resulting NGSL percentage was weighted for the area to be comparable between districts and averaged to be compared with other districts. Table 5.2 illustrates the method used for calculating the weighted NGSL (using District 1 as an example). It should be noted that this initial value varied from district to district and can be attributed to many factors related to the installation and/or pavement surface conditions. The weighted NGSL calculation for other districts is provided in Appendix B.1.

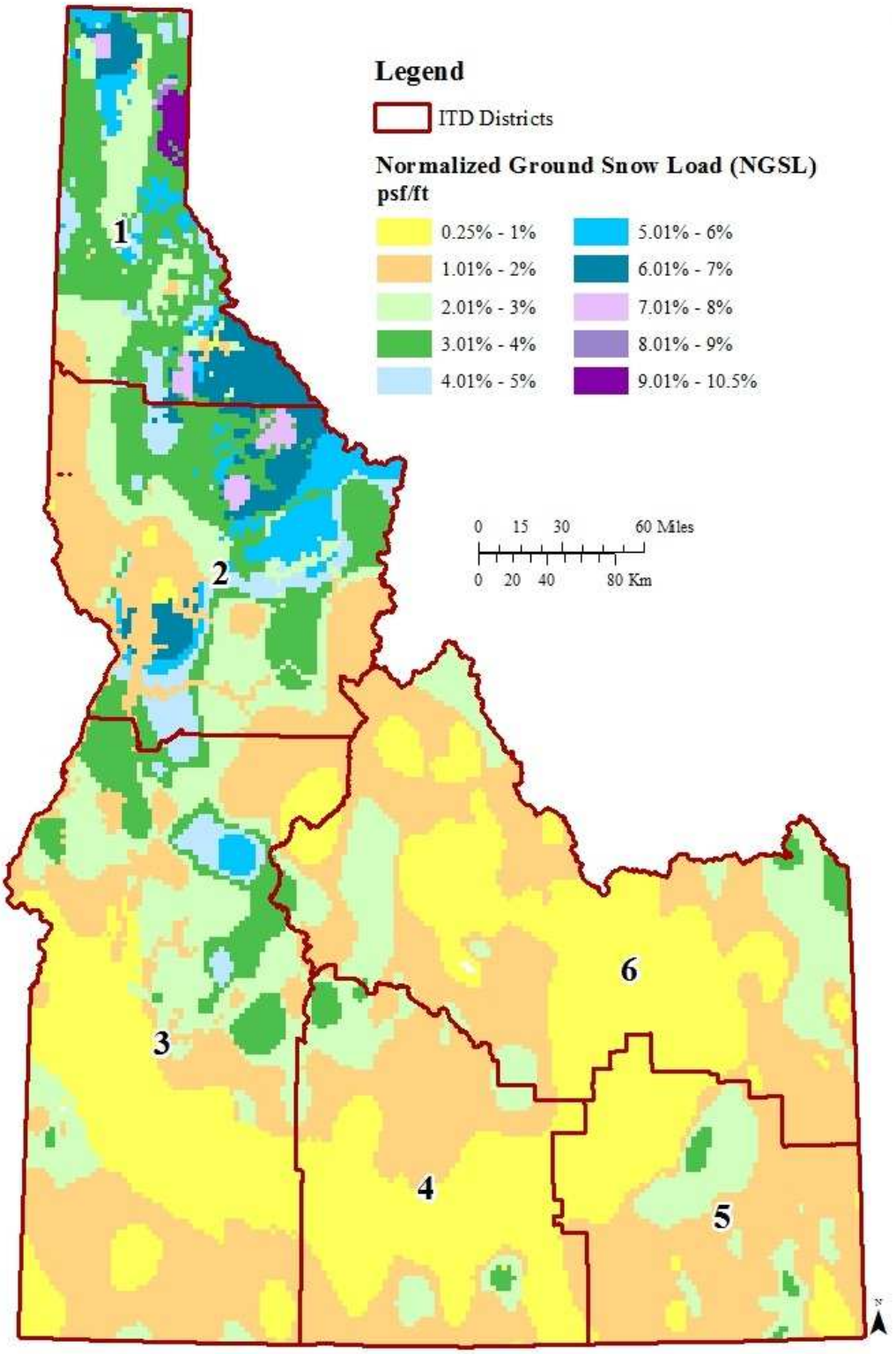

Figure 5.4: 2015 Normalized Ground Snow Loads for the State Idaho

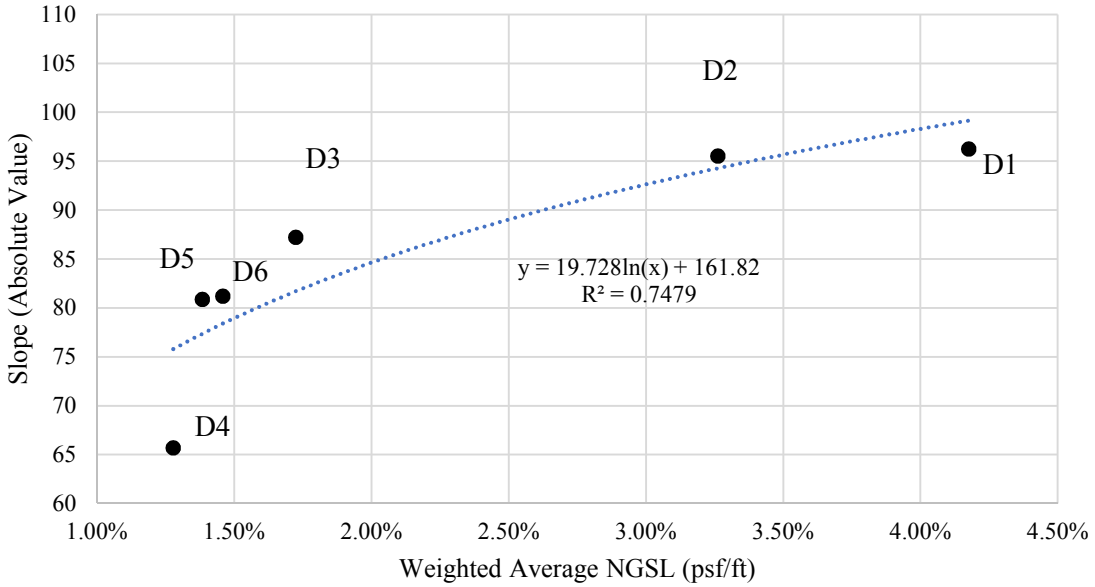

Figure 5.5: Correlation between NGSLs and deterioration rate of pavement marking retroreflectivity

Table 5.2: Weighted NGSL calculation for District 1

NGSL Range	Average NGSL Range	Area (Square Meter)	Area ratio	Weighted NGSL
0.25% - 1%	0.63%	36,000,000	0.18%	0.001%
1.01% - 2%	1.51%	715,020,105	3.48%	0.052%
2.01% - 3%	2.51%	4,293,927,703	20.90%	0.524%
3.01% - 4%	3.51%	8,077,350,365	39.32%	1.378%
4.01% - 5%	4.51%	1,840,010,040	8.96%	0.404%
5.01% - 6%	5.51%	1,534,724,366	7.47%	0.411%
6.01% - 7%	6.51%	2,925,204,689	14.24%	0.926%
7.01% - 8%	7.51%	441,000,000	2.15%	0.161%
8.01% - 9%	8.51%	72,000,000	0.35%	0.030%
9.01% - 10.5%	9.76%	607,774,897	2.96%	0.289%
Totals		**20,543,012,164**	**100.00%**	**4.18%**

5.2.2. Natural Exposure

After modeling the retroreflectivity deterioration based on field data from each of Idaho's six districts, natural weathering tests were conducted by monitoring two sites on two-way, two-lane rural road segments near the city of Moscow (US-95 and ID-8). The retroreflectivity, color change parameters, and durability (percent loss) of the edgeline (white) and the centerline (yellow) waterborne markings were analyzed. Figure 5.6 a shows the change in retroreflectivity during one full seasonal year (2017-2018). A logarithmic reduction in retroreflectivity was detected for both colors. The R^2 for the white and yellow were 0.98 and 0.90, respectively.

Since the pavement marking texture was not consistent over the targeted surface areas, high, middle and low readings were conducted and averaged to represent the color parameters. The results for the pavement marking color change over time are shown in Figure 5.6 b; the ΔE_{ab} for both colors rapidly increased during the first few months. With more exposure time, the white and yellow colors darkened because of the asphalt background which appeared due to the pavement marking peeling due to winter maintenance activities and dirt accumulating on top of the remaining marking. The white marking color change was similar to the artificial weathering which lost brightness (L) over time. In contrast, the yellow markings were more stable in brightness than the white markings but also darkened over time (Figure 5.6 c).

A logarithmic material loss pattern (durability) was observed in both waterborne marking colors. Figure 5.6 d shows that the yellow marking deteriorated more than the white markings; this could be attributed to vehicle passing behavior. The pavement surface texture played a major role in extending the life of the physical properties of the pavement marking. It has been observed that chip seals, seal coats, micro-surface treatments, and restriping over existing pavement markings negatively affects the bond between the asphalt surface and pavement marking. In other words, pavement markings do not perform efficiently in any of these cases.

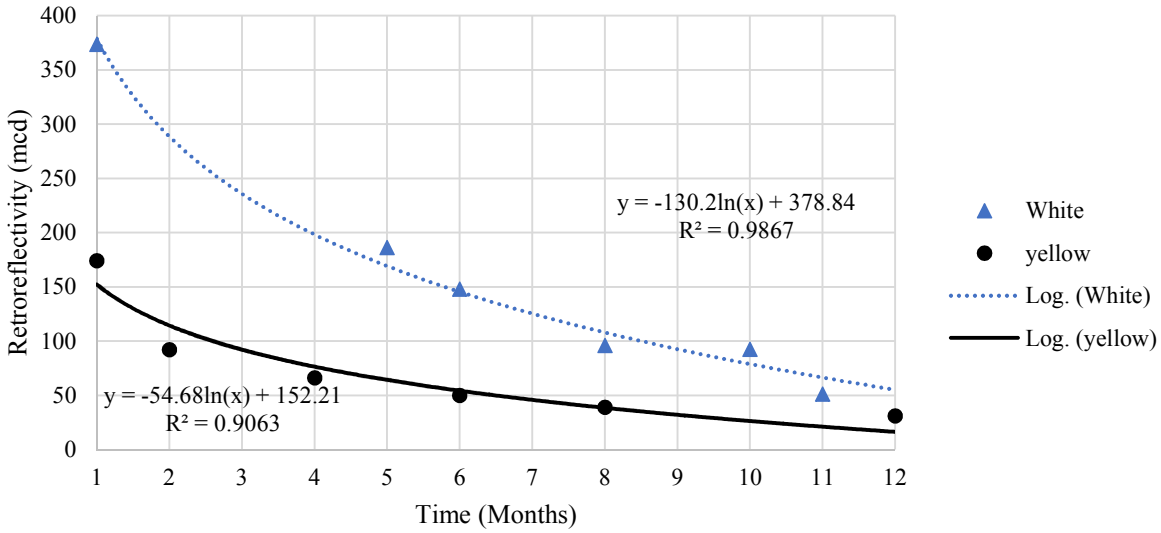

(a)

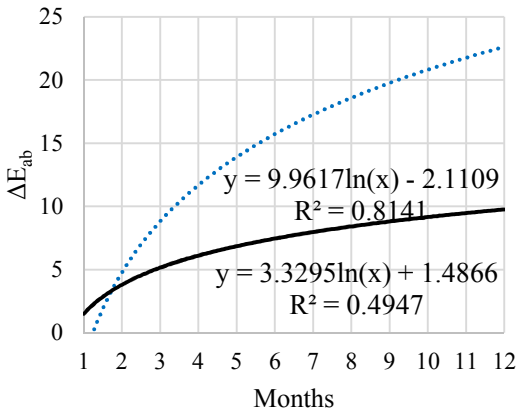

(b)

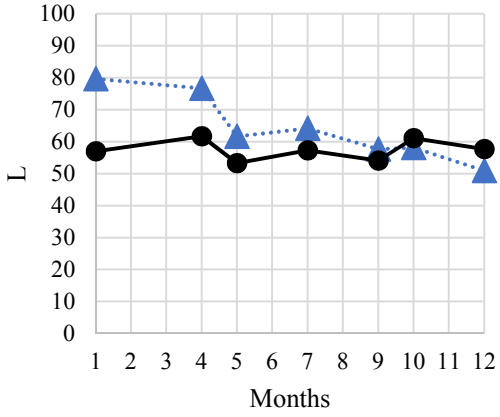

(c)

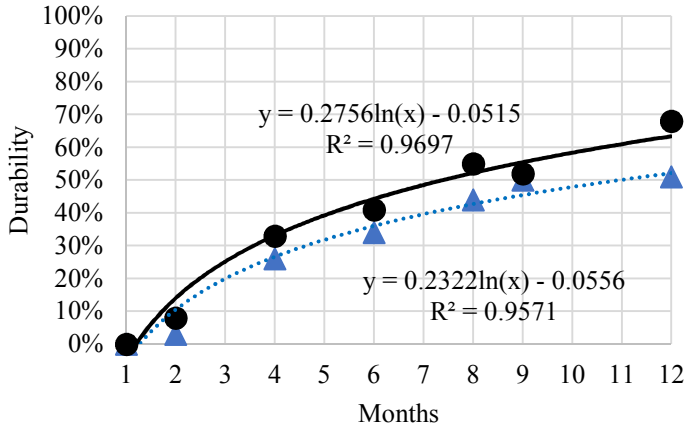

(d)

Figure 5.6: Natural exposure results (a) retroreflectivity, (b) ΔE_{ab}, (c) L, and (d) durability.

5.3.Correlation between Field and Laboratory

In order to correlate the retroreflectivity deterioration field models to the laboratory models, the cumulative number of traffic passes (CTP) in the field was compared with the estimated retroreflectivity from Figure 5.3 c (see Figure 5.7). CTP was calculated based on the cumulative AADT found from the ITD online traffic information maps. The pneumatic, steel, and scraper blade laboratory tests of the white waterborne markings were completed in an attempt to establish a relationship with white edgeline pavement markings. A similar trend between retroreflectivity versus CTP and retroreflectivity versus number of cycles from the TWPD with pneumatic wheels was observed. Based on the average field retroreflectivity value for each district after 100,000 CTPs and the dry pneumatic (R_L) results in the laboratory after 100,000 cycles, it was determined that 1.58 cycles of the TWPD was equivalent to one CTP in the field.

The scraper blade caused the pavement markings to deteriorate on the slab, similar to the act of snow plowing in the field causing deterioration to pavement markings. However, since field data capturing the number of snowplowing events on each segment was not available, the number of scraper blade passes in the lab could not be equated to an exact number of actual passes in the field. This relationship is recommended as an area for future study.

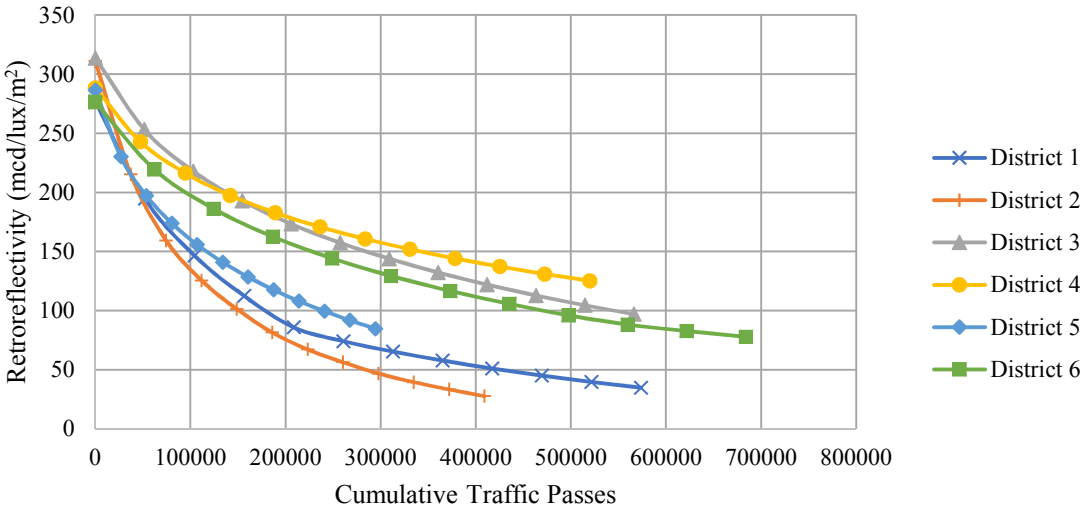

Figure 5.7: Retroreflectivity prediction per CTPs.

CHAPTER 6: RELATIONSHIP BETWEEN THE QUALITY OF EDGELINE PAVEMENT MARKING AND RUN-OFF-THE-ROAD CRASHES IN RURAL HIGHWAYS

The World Health Organization (WHO) states that around 1.35 million people die each year due to crashes. Although low and middle-income countries own 60% of the world's cars, about 93% of all fatalities occur in these countries. If there are no actions taken to overcome the challenge of increased road traffic crashes, these crashes will become the seventh leading cause of death by 2030 (WHO 2018). In the previous two decades, many safety-related studies have been carried out to investigate the relationship between vehicle crashes and highway characteristics. However, little attention has been paid to study the relationship between roadway departure crashes and longitudinal pavement markings. Pavement markings are considered to be one of the potential countermeasures that can be used to enhance road safety by providing continuous information to motorists to keep them in an appropriate lateral position on the roadway. The United States spends nearly $2 billion per year on pavement markings to provide safer roads, but a fatal crash still occurs every 21 minutes as a result of lane departure (Carlson et al. 2009). As stated by the Federal Highway Administration (FHWA) in 2005, more than 25,000 people died because drivers lost control and failed to keep an appropriate lateral lane position. Seventeen thousand of these deaths were caused by single-vehicle run-off-the-road (ROR) crashes, and a large number of the fatalities occurred on two-way, two-lane rural roads. In fact, seventy-five percent of all crashes around the globe occur on rural roads, with single-vehicle crashes comprising about 35% more than multi-vehicle crashes on rural fatalities (Peng et al. 2012).

Drivers instantaneously respond to their ever-changing surrounding environment, so even marginal changes in an environment can either positively or negatively impact a driver's behavior. For example, a marginal change in pavement marking quality or pattern could impact driving behavior. Roadway departure or run-off-the-road (ROR) crashes occur when a single-vehicle departs the roadway. Contributing circumstances may vary, such as a driver losing control or misjudging a roadway alignment. Rural highways in the United States account for approximately 91.4 billion vehicle-miles per year (32% of the total) and

contributes to a considerable number of ROR crashes (FHWA 2017). There are many countermeasures that are used to mitigate the severity of ROR crashes such as adding guardrails and removing dangerous fixed objects. For the same purpose, pavement markings are used to minimize the frequency of crashes by assisting road users to stay in appropriate lane positions. The objective of this part of the study was to examine the effect of retroreflectivity deterioration of pavement markings on traffic safety, particularly ROR crashes, and to determine how the use of highly-retroreflective edgeline markings affect crash rates.

6.1.Methodology

To assess the safety impact of edgeline deterioration on rural two-lane highways, retroreflectivity deterioration curves for the six Idaho districts were developed (see Chapter 4), and crash data were extracted from the Idaho Transportation Department (ITD) website (WebCARS). When a vehicle crash results in property damage of more than $1,500 per person or involves a personal injury and occurs on a public roadway in the State of Idaho, a vehicle collision report (VCR) must be filled out by a domestic law enforcement official and submitted to the ITD's Office of Highway Safety (OHS) who is responsible for maintaining the crash database. The database is available online and can be accessed and used with ITD's permission. For this study, crash data or the Automatic Traffic Recorders (ATRs) were downloaded from this database and identified by road segment and roadway geometry information (e.g., lane width, shoulder width, and shoulder type), while the AADT was extracted from online ITD maps and tables.

All delineation-related crashes were selected based on the Most Harmful Event (MHE), an accident form category that identified the "most contributing" reason behind the crash. For this research, only crashes that occurred because of low edgeline marking retroreflectivity were selected to be analyzed. The crash data were sorted based on the following factors:

- All crashes occurring on rural two-way, two-lane highways in the state of Idaho were included but crashes within city limits were not. The selection was based on two location boundaries: state district and roadway segment code.

- Only nighttime crashes were included, when marking retroreflectivity is a significant factor.
- Only single-vehicle crashes were used.
- No icy and snowy pavement surfaces were included.
- No intersection crashes or non-interchange segments were included.
- No animal-related collisions were included.
- All crashes associated with asleep, drowsy, and fatigued drivers were included, since they are strongly related to a driver losing vehicle control.
- All drunk or impaired driving, and careless or distracted driving crashes were not included.
- All hit-fixed objects and overturn crashes were included since they might have resulted from the driver losing control of a vehicle. These type of crashes were expected to occur due to vision deficiencies because they were single driver, during night time, and with dry pavement surface condition.

In the WebCARS database, the Most Harmful Event (MHE) parameter explains the most contributing reason behind the car crash. After the data sorting procedure, residual crashes related to nighttime vision and correlated to pavement markings were kept. These crash types as identified in the WebCARS database were:

- Bridge Rail
- Concrete Traffic Barrier
- Culvert
- Delineator Post
- Ditch
- Embankment
- Fence
- Guardrail End
- Guardrail Face
- Immersion
- Mailbox
- Other Non-Collision

- Other Object Not Fixed
- Overturn
- Parked Car
- Pedalcycle
- Pedestrian
- Traffic Sign Support
- Tree
- Utility Pole
- Utility/Light Support
- Other Fixed Object

Crash data from eight years (from 2010 to 2017) were downloaded, cleaned, and analyzed. The length of each selected segment was calculated based on the Idaho DOT segmentation system. Twenty different segments were selected representing a total of 3,017.13 miles and with AADT varying from 231 to 27,885 vehicles per day. After excluding all non-related crashes, 1,485 crashes were identified, including 145 fatal or serious injury crashes. Table 6.1 shows a summary of the data used in the crash analysis. Crash rate analysis was applied to the exposure data in the form of traffic volumes (AADT) and roadway mileage (length) to understand the relative safety compared to similar segments and districts. The equation used to calculate the crash rate was:

Equation 8: Crash rate

$$R = (100\ \text{million} * C)/(365 * N * V * L) \quad (8)$$

where: R represents the crash rate for the roadway segment expressed as crashes per one hundred million vehicle-miles of travel (VMT); C is the total number of crashes in the study period; N is the number of years of data; V is the number of vehicles per day for the two directions; and L is the length of the roadway segment in miles. Retroreflectivity data was ordered based on month and year.

Table 6.1: Data summary of the crash analysis

District	Segment Code	Length (Miles)	Average AADT (vehicle per day)	Total Crash Counts (2010-2017)	KA Crash Counts (2010-2017)
1	1610	33.24	3614	36	6
1	1540-1	166.329	12791	180	11
1	1590-1	76.225	6856	22	4
1	1590-2	63.334	1197	15	0
Total		339.128	-	253	21
2	1800	47.972	448	30	3
2	1870	53.5	10001	28	4
2	1910	163.97	2693	145	15
2	1540-2	188.887	3760	123	15
Total		454.329	-	326	37
3	1990	156	5230	135	11
3	2140	105	2856	39	2
3	1540-3	182	2016	102	6
3	2070-3	81.99	1901	41	4
Total		524.99	-	317	23
4	2230	84	12026	62	9
4	2040-4	93	3763	55	4
4	2220-4	144	5359	46	5
4	2240-4	73	1482	33	4
Total		394	-	196	22
5	1260	48	11052	16	0
5	2330	50.28	913	33	9
5	2350	122	1947	39	4
5	2380	44	1517	16	1
5	1330-5	111	19891	29	3
5	2040-5	125	2512	16	3
Total		500.28	-	149	20
6	2460	155	4997	44	6
6	1330-6	85	5064	12	0
6	2070-6	143	2320	68	3
6	2220-6	267.4	2530	65	6
6	2240-6	154	2052	55	7
Total		804.4	-	244	22

6.2.Analysis and Results

The sorted crash data were statistically analyzed using the R software to determine if there was a correlation between low pavement marking retroreflectivity and crash rate. A

scatter plot for edgeline retroreflectivity versus crash rate for the entire dataset (all six districts) is shown in Figure 6.1. Visually, no significant correlation between low edgeline retroreflectivity and crash rate is apparent. To isolate snow load effects in District 1 and 2, the dataset was split by district and analyzed to investigate if there was a relationship between a high NGSL occurrence and crash rate. In order to compare results across different subsets, edgeline retroreflectivity versus crash rate was plotted for each of the six districts in Idaho (see Figure 6.2).

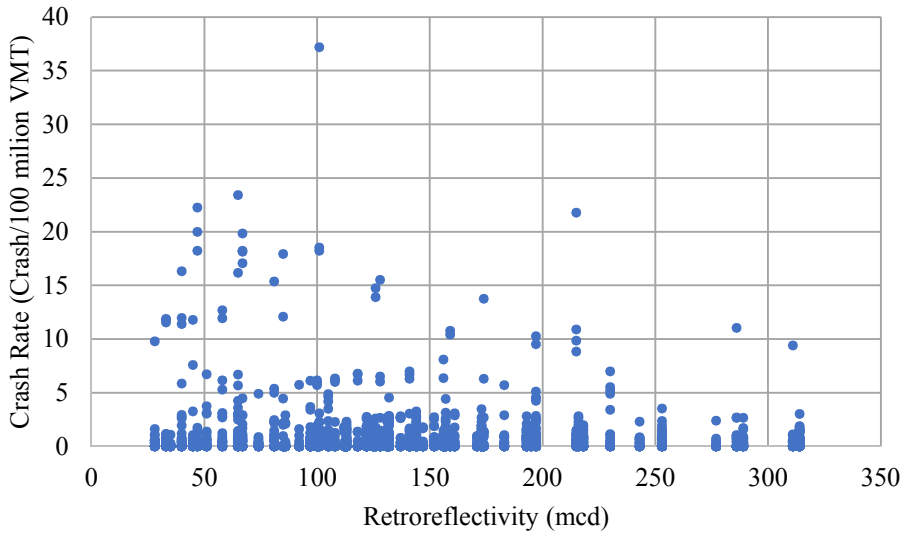

Figure 6.1: Pavement marking retroreflectivity vs. crash rate for all Idaho districts

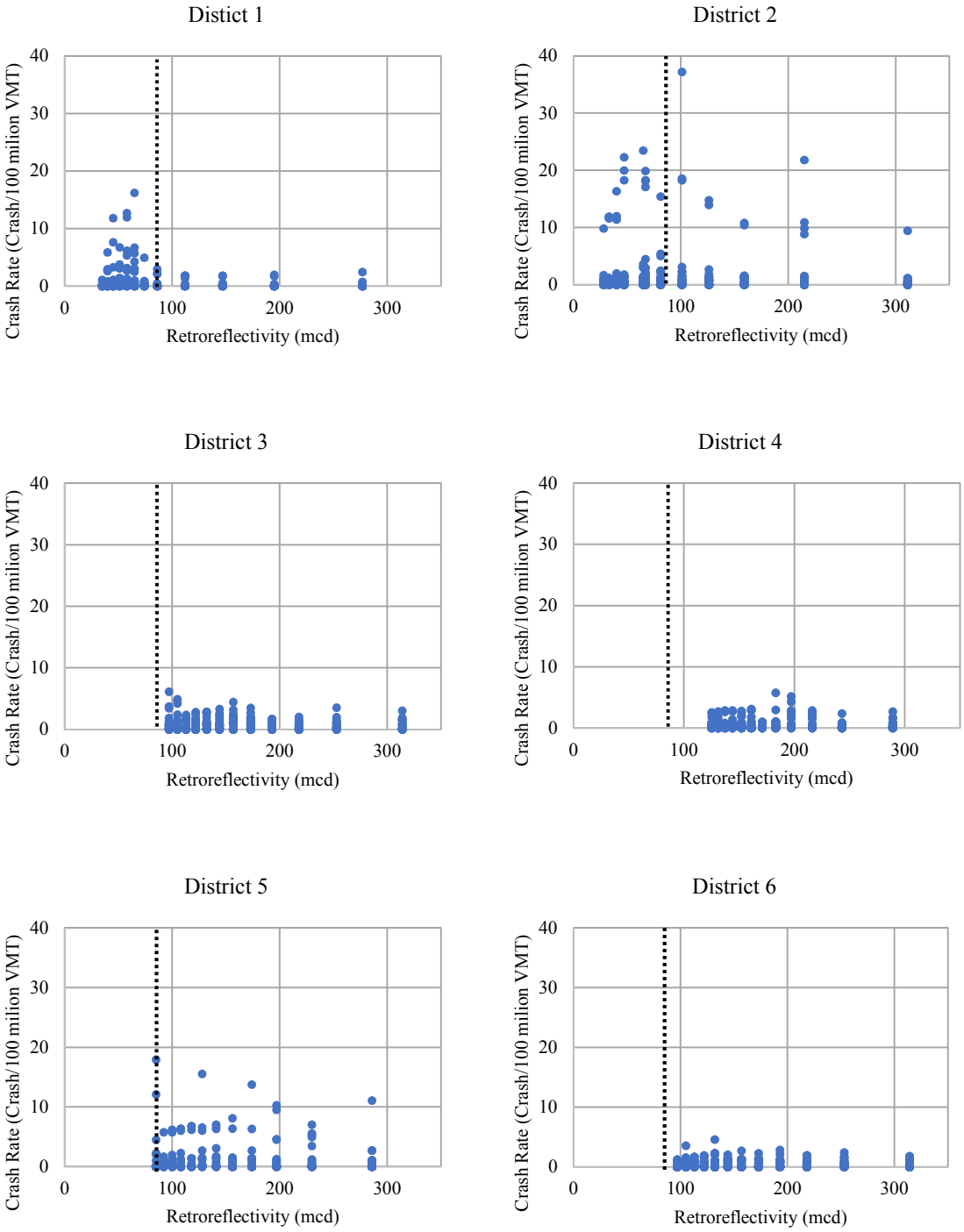

Figure 6.2: Retroreflectivity vs. crash rate per district

From the graphical representations, a clear pattern in District 1 was observed, where all high crash rates occurred at low retroreflectivity values. Therefore, a chi-square test of independence (X^2) was implemented (see Equation 9) to investigate whether crash rate distributions above and below a selected retroreflectivity value differed.

Equation 9: The chi-square formula

$$X^2 = \sum_{1}^{N} \frac{(Crash\ count\ below\ R_L\ value - Crash\ count\ above\ R_L\ value)^2}{Crash\ count\ above\ R_L\ value} \quad (9)$$

Where: N is the crash rate and R_L is the modeled dry retroreflectivity for each district. To set a dichotomization value, the lowest retroreflectivity value experienced in Districts 3, 4, 5, and 6 models was selected; this value was 85 mcd (see Figure 6.2). The null hypothesis was defined as the crash rate occurring below the selected retroreflectivity value being equal to the crash rate occurring above this retroreflectivity value. The null hypothesis would not be rejected if the chi-square statistic values differed from the critical chi-square statistic at a 95% confidence level. In other words, the null hypothesis would be rejected if the *p-value* was less than 0.05. A larger chi-square statistic indicates that there is something causing the differences in data, and in this case a low retroreflectivity value would be responsible for the difference in crash rates.

When the retroreflectivity values were dichotomized above and below 85 mcd, the chi-square test was conducted to test for the proportion of crashes in the two retroreflectivity groups. Table 6.2 and Table 6.3 show the general notation for a 2x2 contingency table for District 1 and District 2. As noted, the explanatory variables of this crash analysis were divided into two categories: crash occurrence in the targeted district (crash and no crash) and the selected threshold (<85 mcd and >85 mcd).

Table 6.2: Crash occurrence results in District 1

Variable	<85	>85	Total
No crash	137	87	224
Crash	117	43	160
Total	254	130	384

Table 6.3: Crash occurrence results in District 2

Variable	<85	>85	Total
No crash	123	101	224
Crash	76	84	160
Total	199	185	384

Based on the results of the chi-square test, the relationship was significant in District 1, X^2 (1, N = 384) = 5.4438, p <0.0196 but not significant in District 2, X^2 (1, N = 384) = 1.7669, p <0.1838. To illustrate, these results indicated that a large number of crashes occurred below a pavement marking retroreflectivity of 85 mcd in District 1. Knowing that District 1 experienced the highest deterioration rate and the highest ground snow load during the study period among all districts, this deterioration trend can be attributed to more frequent winter maintenance activities. A similar outcome could not be conducted for District 2; this may be due to the limitations of this research. One such limitation was that the retroreflectivity data were analyzed based on models that averaged several retroreflectivity readings, so some readings were above 500 mcd but averaging them reduced the absolute retroreflectivity value. Thus, lower initial retroreflectivity values may have impacted the dichotomization value (which was 85 mcd in this case). For these reasons, this methodology could not definitively conclude that an increased crash rate was associated with lower edgeline retroreflectivity.

CHAPTER 7: EFFECTS OF EDGELINE MARKINGS CONDITION ON DRIVER LANE DEVIATION

"Effects of longitudinal pavement edgeline condition on driver lane deviation." *Accident Analysis & Prevention, Elsevier, Vol. 128, 2019, pp. 87-93*

To improve pavement marking visibility during challenging driving conditions, the installation of wider pavement markings may be an appropriate solution. The MUTCD requires that standard longitudinal pavement markings be at least four inches wide. The usage of wider longitudinal pavement markings is expanding and Figure 7.1 depicts an updated state-of-the-practice inventory of wider pavement markings by state DOTs (Gates and Hawkins 2002 and Carlson and Wagner 2012). The primary objective of this part of the research was to study the effects of longitudinal edgeline pavement marking width with varying deterioration levels and to assess the driver's ability to maintain lane position.

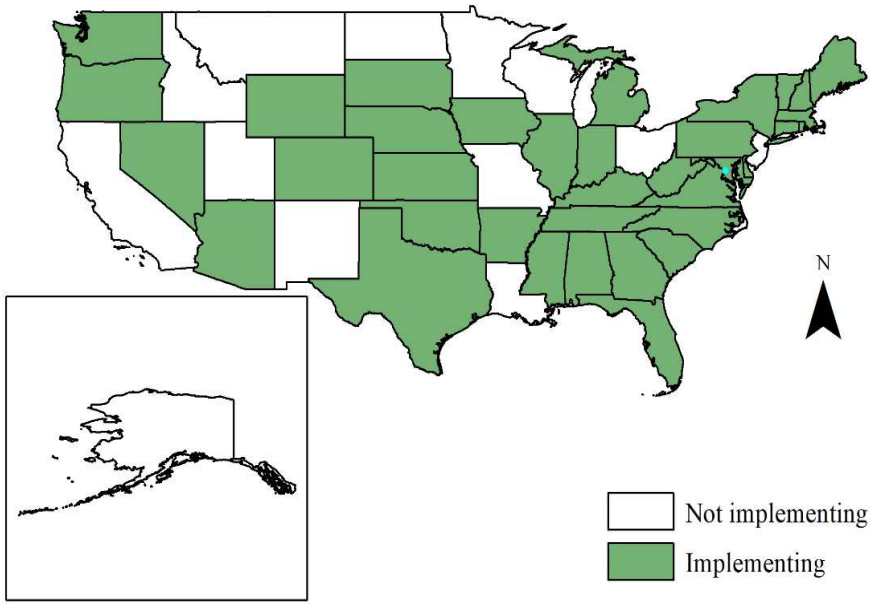

Figure 7.1: Use of wider markings among state DOTs in 2019

7.1.Pavement Markings and the Driving Task

A driver collects about 90% of the information needed to operate a vehicle through his or her sense of light. The human ability to see varies from one person to another, and many factors affect this ability. For example, visual acuity, contrast sensitivity, peripheral vision, movement in depth, and visual search are the most important vision skills that affect the driving task. Indeed, all of these factors assist drivers to discern pavement markings in direct or indirect ways, especially at nighttime and in harsh weather conditions. The human ability to detect small changes in the brightness of light (luminance) is expressed by contrast sensitivity; the higher the luminance of the pavement markings, the less contrast is needed to see it. Based on the Highway Safety Manual, contrast sensitivity has the largest impact on crash occurrence among all previously mentioned factors. Thus, contrast sensitivity can be a critical safety issue for non-reflective pavement markings or pavement markings with low retroreflectivity levels because of aging (Highway Safety Manual 2010).

7.2.Relationship between Pavement Markings and Safety

Previous studies have shown that the presence of longitudinal pavement markings yields benefits far greater than their costs and are feasible to increase road safety and reduce crashes (Miller 1991). However, the relationship between pavement marking retroreflectivity and road safety has yielded mixed results and counterintuitive findings (Carlson et al. 2013). For example, Bahar et al. (2006) concluded that there was no safety improvement providing higher retroreflectivity for longitudinal markings on non-intersection sites during nighttime (Bahar et al. 2006). On the other hand, a statistically significant correlation between pavement marking retroreflectivity and nighttime safety was detected using five years of data from rural roads in Michigan in a separate study (Avelar and Carlson 2014).

7.3.Lateral position effects

Several studies have focused on explaining the effect of edgeline pavement markings on a driver's lateral position. An early behavioral study investigated the impact of 4 inch edgelines on driver behavior and found that vehicle operators tended to shift toward the roadway centerline when no interference between vehicles was assumed (Sun and Tekell 2005). The tendency and change in magnitude of a motorist to move toward or away from an edgeline pavement marking depended on many factors such as lane width, operating speed,

time of day, frequency of heavy vehicles, pavement condition, roadway alignment (curvature), edge drop-off, and traffic volume of the opposite direction (Tsyganov et al. 2005). During normal operations, drivers often employed a curve-flattening strategy to overcome centrifugal force. For this reason, drivers tended to be closer to the centerline of the road while driving through left-hand curves and closer to the edgeline when driving through right-hand curves (Chrysler et al. 2009). Therefore, it is important to investigate the combined effect of pavement marking quality and width on vehicle lateral position.

7.4.Driving Simulation Study

Ramirez (2016) previously conducted a daytime driving simulation study to evaluate the safety effects of wider longitudinal edgeline pavement markings. Pavement marking deterioration, width, and roadway geometry were analyzed with respect to a car's lateral position and speed using the University of Idaho's driving simulator. No statistically significant differences were detected when introducing wider pavement markings during the daytime. The same study recommended to implementation of a nighttime environment for future research. Thus, a nighttime environment analysis was implemented as part of this study to study the effects of longitudinal edgeline pavement markings with varying deterioration levels and widths and to assess a driver's ability to maintain lane position.

7.5.Driving Simulation Methodology

7.5.1. Driving simulator experiment description

Forty-eight licensed drivers were hired to participate in this study. All participants were from the local community with valid driver's licenses and were recruited through online and bulletin board postings. A two-lane rural highway was simulated in the driver simulator. All participants drove at least two sessions for about 45 to 50 minutes per each session. Five minutes were set aside before the actual driving test to familiarize the participant with the system (e.g., gas pedal, brake pedal, and steering wheel) and minimize data anomalies due to the driver's lack of familiarity.

The simulation laboratory was equipped with a 2001 Chevrolet S10 pick-up truck cabin that was used by participants to drive all of the scenarios. The National Advanced Driving Simulator (NADS) MiniSim program was employed in this experiment to display the simulations and to collect and record the data.

Exactly half of all participants drove in daytime conditions (during the previous study), while the other half experienced nighttime conditions (during this study). Each participant drove 42½ miles of roadway simulation track; within the 42½ miles, 40 miles were driven at speeds close to 60 mph (posted speed limit). The roadway simulation track was divided into four parts: to reach the desired travel speed, one mile was set at the beginning of the track, 40 miles represented the experimental track, one half mile was set at the middle of the track to be used as a rest period, and one mile at the end of the track allowed the driver to gradually stop the vehicle.

The goal of each participant in this test was to control the vehicle as much as possible by keeping it centered at a safe position within the travel lane, just as in normal driving at the posted speed limit. All participants were instructed that they would be completing a 40 mile drive on a rural highway for each session and to imagine themselves returning from a weekend camping trip in rural Idaho. Every participant was assigned and completed sessions that consisted of a unique ordering of two different edgeline widths (4 and 6 inch). Further, each width was composed of four uniquely ordered edgeline deterioration percentages to minimize bias effects. Before a participant began the experiment, the simulator vehicle was reset and centered on the travel lane with no lane deviation. The lateral movement of the simulator vehicle was analyzed based on positive position values (deviating towards the edgeline) and negative position values (deviating towards the centerline) of the collected data.

The lateral position of the vehicle within the travel lane depended on each driver maneuvering to keep the vehicle in a stable position between the centerline and edgeline pavement markings. In this research, the lateral position of the vehicle was measured off of the centerline of the right lane per SAE International recommended practice (*SAE International* 2015).

7.5.2. Development of the Simulation Environment

Every scenario consisted of tiles which showed the roadway geometry and surrounding daytime or nighttime environment. The track tested in this study was a typical two-way, two-lane roadway of 12-foot lane widths, 10-foot shoulders, and no-passing zones with a level terrain. The paved roadway track consisted of straight and left or right horizontal curved segments, edgelines with different levels of deterioration and widths, and gravel

shoulders on both roadsides. The edgeline width and deterioration levels were adjusted along the roadway track to be later analyzed with respect to the lateral position of the vehicle. For this study, scenarios with four and six inch edgeline widths were developed based on discussions with Idaho Transportation Department staff, and any changes to the width were made on the shoulder side of the roadway. In other words, the lane width between the centerline and the travel side of the edgeline was maintained at a constant twelve feet for the duration of the study.

To develop the simulation environment, a multi-step method using several computer programs was implemented. The Autodesk 3ds Max was used to develop different pavement marking deterioration levels and widths; the Tile Mosaic Tool (TMT) and Interactive Scenario Authoring Tool (ISAT) were used to establish the roadway simulation tracks and import other visual objects such as cars, signs, and data collection points (triggers).

Based on the Annual Average Daily Traffic (AADT) reported data for two-lane rural highways in the state of Idaho (which averaged 3,200 vehicles per day statewide) and HCM 2010 guidance (with the proportion of AADT occurring in the peak hour, K, equal to 0.10 and the proportion of peak hour traffic in the peak direction, D, equal to 0.5), the Directional Design Hourly Volume (DDHV) for all scenarios in this study was calculated to be 160 vehicles. Twelve percent of this volume was heavy vehicles (e.g., semi-trucks and dump trucks). During the driving task, two vehicles were attached to the testing vehicle, with one preceding and the other following the targeted vehicle at the same distance (1,320 feet).

7.5.3. Description of scenarios created

Each participant drove through 64 triggers (which create epochs or logs) during their two sessions; these data points were collected for each of the 48 participants, resulting in a cumulative total of 3,072 possible data collection points. There were eight triggers for each edgeline deterioration percentage and since each width scenario was composed of four different edgeline deterioration percentages, thirty-two logs (epochs) were generated from each roadway simulation track: four logs representing the straight segments, two logs representing the gentle curved segments (turning left and right), and two logs representing the sharp curved segments (Table 7.1). Figure 7.2 shows a driver simulation scene during a

daytime environment and three pictures of different edgeline deterioration levels during a nighttime environment.

Table 7.1: Scenario distribution

Participant Driving Scenarios		
Marking Width	4 inch scenarios	6 inch scenarios
Deterioration Percentages	0% Scenario (8 logs)	0% Scenario (8 logs)
	25% Scenario (8 logs)	25% Scenario (8 logs)
	50% Scenario (8 logs)	50% Scenario (8 logs)
	75% Scenario (8 logs)	75% Scenario (8 logs)
Total Scenarios	8 Scenarios (64 logs)	

Figure 7.2: Driver simulation scene during daytime, and pictures of different edgeline deterioration levels at nighttime simulation

Figure 7.3 shows the representative difference between the four and six inch edgeline widths, while Figure 7.4 shows the difference between the 0%, 25%, 50%, and 75% edgeline deterioration percentages applied on the six inch edgeline width. The same design was applied to the four inch width but is not separately shown.

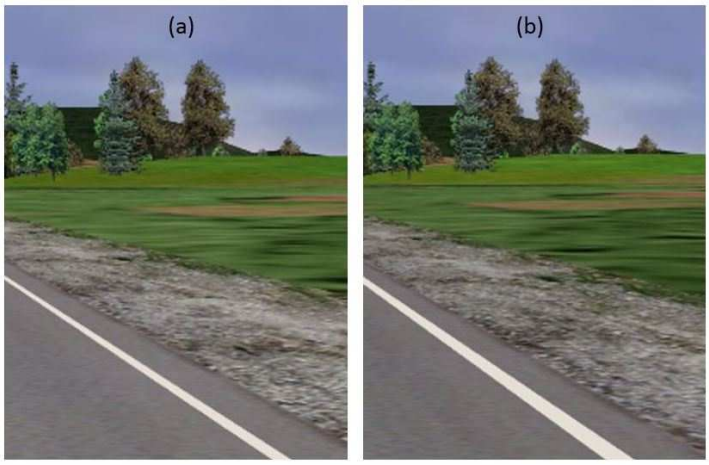

Figure 7.3: Driver simulation graphic of edgeline widths: (a) 4 inch and (b) 6 inch.

Figure 7.4: Driver simulation graphic of edgeline deterioration percentages (only 6 inch shown): (a) 0%, (b) 25%, (c) 50%, and (d) 75%

7.6.Driving Simulation Study Data Analysis and Results

Although forty-eight participants were initially selected for this study, preliminary analysis was only conducted using data from a reduced set of forty-four participants. This was due to the fact that some technical issues were encountered when converting the data format for three daytime participants and one nighttime participant; a fifth participant was identified as an outlier. Final data analysis was performed on the results from forty-three participants; there were twenty-eight male participants, and fifteen female participants. With regard to age, thirty-one participants were between eighteen and thirty years old, eight participants were

between thirty-one and forty-nine years old, and four participants were between fifty and seventy years old. The youngest participant was a nineteen year old female, while the oldest participant was a sixty-nine year old male (M = 29.5 years, SD = 12.8 years). The average years of driving experience among the participants was 13.4 years (SD = 12.7 years).

7.6.1. Lane Position (Vehicle Lateral Deviation)

The average participant performance based on lane deviation for the 4 and 6 inch edgeline width using the four deterioration scenarios (0 %, 25 %, 50 %, and 75 %) during nighttime conditions is plotted in Figure 7.5. The y-axis represents the lane deviation of the vehicle in feet (zero refers to no lateral movement where the vehicle would be in the center of the lane), while the negative and positive values indicate the vehicle's deviation towards the centerline and edgeline, respectively. The x-axis was divided into four sections based on the pavement marking degradation percentage (0 %, 25 %, 50 %, and 75 %), and each symbol represented a different pavement marking width (4 and 6 inches). Each section, as described earlier, consisted of eight data collection points that represented a differing roadway geometry option (see Table 7.2). For example, points 6, 14, 22, and 30 represented the lane deviation of each participant when traveling along the same gentler, left-hand curve segment section. Based on the visual analysis of Figure 7.5, it can be concluded that all drivers tended to move toward the edgeline of the right lane at night and increasingly shifted away from the centerline as edgeline deterioration worsened; this could be a factor in run-off-the-road crashes. For all pavement marking degradation levels, a left-turn through the gentle curve segments caused the highest positive values on the lane deviation axis; in other words, drivers deviated the most toward the edgeline under this roadway geometric condition versus all of the other roadway geometry options. Similar results were observed for drivers who experienced daytime conditions.

Table 7.2: Data collection points for specific geometry types

Geometry Type	Data Collection Points
Straight Segments	1, 3, 5, 7, 9, 11, 13, 15, 17, 19, 21, 23, 25, 27, 29, and 31
Gentle Curved Segment (Turning Left)	6, 14, 22, and 30
Gentle Curved Segment (Turning Right)	4, 12, 20, and 28
Sharp Curved Segments	2, 8, 10, 16, 18, 24, 26, and 32

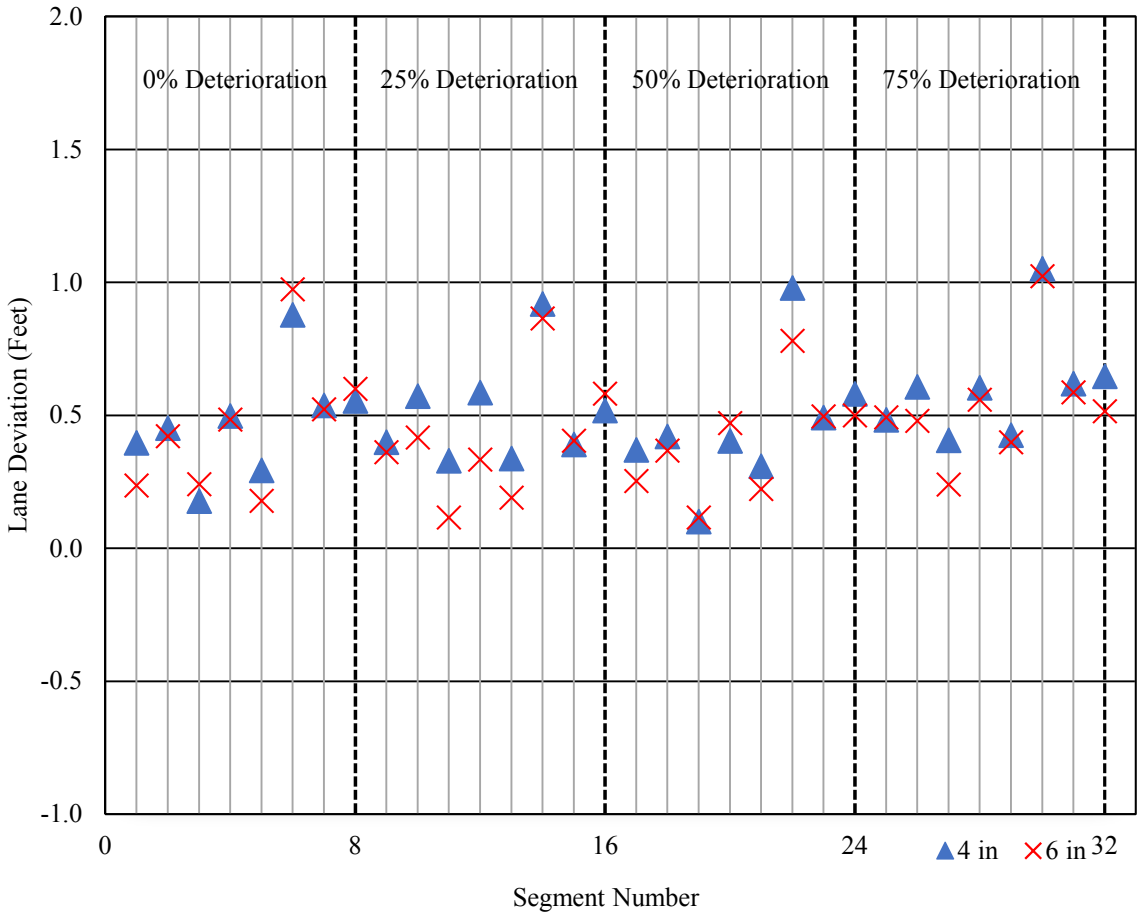

Figure 7.5: Effects of pavement marking deterioration and width on driver lane deviation.

A three-way analysis of variance (ANOVA) was conducted to understand and statistically describe the effect of edgeline width, deterioration percentage, and roadway geometry on vehicle lane deviation. Table 7.3 summarizes the results when data from all participants were included; due to the value placed on pavement markings for drivers at night, Table 3 isolates the results for this particular segment of the driver population (i.e., only those who experienced nighttime conditions). As shown in Table 7.3 and Table 7.4, the three-way ANOVA revealed significant differences only with the edgeline deterioration percentage (F (3, 2752) = 7.35, p = 6.6e-05 and F (3, 1472) = 3.30, p = 0.02) and roadway geometry (F (3, 2752) = 70.64, p < 2.2e-16 and F (3, 1472) = 42.27, p < 2E-16) on lane deviation at the 0.05 significance level (type I error); this implied that the lateral position of the vehicle was impacted independently by edgeline deterioration and roadway geometry. When nighttime drivers were isolated, marking width was added to the list of variables with statistically significant results (F (1, 1472) = 5.52, p = 0.02). For all cases, the simultaneous interactions between edgeline width and deterioration percentage, width and roadway geometry, and edgeline width and deterioration percentages and roadway geometry did not have a significant impact on lane deviation.

Table 7.3: Effect of edgeline width, deterioration percentage, and roadway geometry on vehicle lane deviation (all drivers).

Variable	**Degrees of Freedom**	**Sum of Squares**	**Mean Squares**	***F*-ratio**	***P*-value** *Pr(>F)*
Width (Edgeline)	1	1.29	1.287	2.7891	0.09502 .
Deterioration (Edgeline)	3	10.17	3.391	7.3521	6.61e-05***
Roadway Geometry	3	97.76	32.588	70.6448	< 2.2e-16***
Width : Deterioration	3	0.74	0.246	0.5328	0.65982
Width : Roadway Geometry	3	0.53	0.175	0.3802	0.76732
Deterioration : Roadway Geometry	9	1.3	0.145	0.3134	0.97092
Width : Deterioration : Roadway Geometry	9	0.76	0.084	0.182	0.99597
Residual	2752	1269.49	0.461		

(Note: significance level, *Pr(>F)*: 0 '***' 0.001 '**' 0.01 '*' 0.05 '.' 0.1 ' ' 1)

Table 7.4: Effect of edgeline width, deterioration percentage, and roadway geometry on vehicle lane deviation (nighttime drivers only).

Variable	Degrees of Freedom	Sum of Squares	Mean Squares	*F*-ratio	*P*-value *Pr(>F)*
Width (Edgeline)	1	2.23	2.2318	5.5232	0.0189*
Deterioration (Edgeline)	3	4.00	1.3349	3.3035	0.01961*
Roadway Geometry	3	51.25	17.0824	42.2747	< 2E-16 ***
Width : Deterioration	3	0.37	0.1244	0.3078	0.81974
Width : Roadway Geometry	3	0.04	0.0127	0.0314	0.99254
Deterioration : Roadway Geometry	9	0.45	0.0495	0.1224	0.99916
Width : Deterioration : Roadway Geometry	9	0.93	0.1033	0.2557	0.98567
Residual	1472	594.81	0.4041		

(Note: significance level, *Pr(>F)*: 0 '***' 0.001 '**' 0.01 '*' 0.05 '.' 0.1 ' ' 1)

Figure 7.6 a, describes the cumulative impacts that edgeline deterioration percentage had on lane deviation. As the edgeline deterioration percentage increased, lane deviation increased as well. When participants experienced 0% edgeline deterioration, the corresponding lane deviation ranged from 0.46 to 0.47 feet (14.0 to 14.3 centimeters) while at a 75% edgeline deterioration the lane deviation increased to between 0.54 and 0.61 feet (16.5 to 18.6 centimeters). This higher edgeline deterioration percentage did have an influence on lane deviation and was statistically significant. Figure 7.6 b, depicts a graphical representation of the influence of edgeline widths on lane deviation at specific roadway geometries. It can be observed that when the participants drove along the gentle curved segment (turning left), they experienced a higher lane deviation of 0.91 to 0.96 feet (27.7 to 29.3 centimeters) as compared to the other roadway geometries that had lane deviations from 0.32 to 0.54 feet (9.8 to 16.5 centimeters). Since the lane deviation values were universally positive, the results from this study implied that participants moved toward the edgeline for all roadway geometry types.

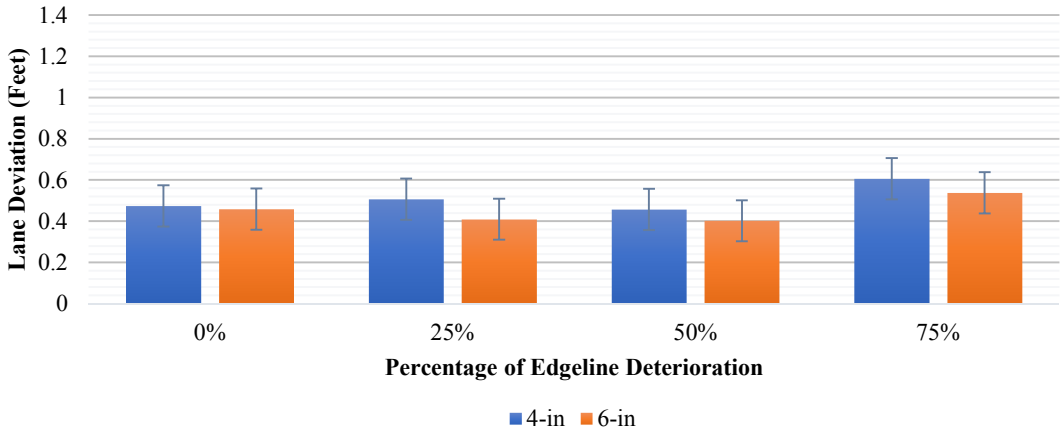

(a)

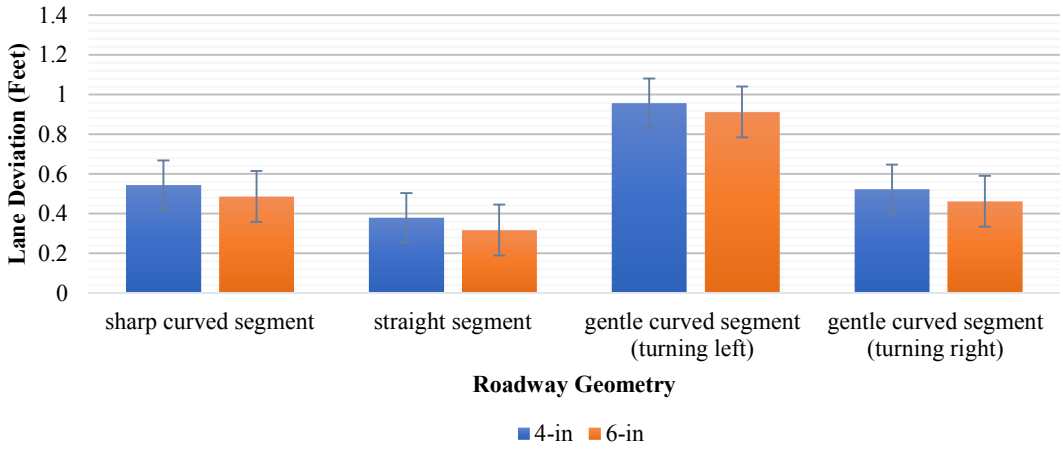

(b)

Figure 7.6: Lane deviation: (a) impact of edgeline deterioration and (b) impact of different roadway geometries

CHAPTER 8: CONCLUSIONS AND RECOMMENDATIONS

The existing practice of evaluating pavement marking performance is based on the NTPEP test-deck method. Although the testing deck provides an accurate performance evaluation of pavement markings under service conditions, it takes up to three years to complete and exposes technical staff to roadway risks while constructing test decks and conducting measurements; road closures are also possible. In this research, an accelerated laboratory-based evaluation procedure was proposed and assessed for its validity and feasibility to simulate the field performance of pavement markings while mitigating for existing drawbacks. In addition, to assess the safety performance of these traffic devices, separate crash analysis and driver simulation studies were conducted.

The performance of different marking materials and colors was evaluated in the laboratory. To simulate user actions (e.g., traffic and snowplowing) and weathering, a three-wheel polisher device and weatherometer were employed. The following conclusions were drawn:

- To assess and study pavement marking deterioration performance, the laboratory TWPD effectively replicated and accelerated traffic and snowplowing effects in the field.
- A logarithmic model was found to provide the highest r-squared for the relationship between pavement marking retroreflectivity loss and the number of cycles applied by the TWPD.
- Based on the average dry retroreflectivity (R_L) of the pneumatic tire results, 1.58 cycles of the TWPD is equal to one traffic pass on the roadway.
- The recovery (R_{L1}) and continuous wetting (R_{L2}) measurements were applied to observe the variability in retroreflectivity measurements when water was present. These retroreflectivity performance measures decreased with an increasing number of cycles, similar to the dry readings.
- An increase in pavement marking lightness (ΔL), overall color difference (ΔE_{ab}), and durability (percent loss) was directly correlated to a loss in retroreflectivity.

- The color analysis revealed an important relationship between pavement marking retroreflectivity and color change. After traffic loading, the faded markings retroreflected less light. In other words, the exposed black pavement caused less light to retroreflect.
- The XAC effectively simulated and accelerated the effect of sunlight, moisture, and temperature to assess and study pavement marking performance in an abbreviated time frame.
- A linear increase in the percent retroreflectivity was observed during all pavement marking samples tested under the accelerated weathering procedure (up to 2,000 hours).
- After artificially weathering pavement markings (up to 2,000 hours), the yellow colors faded and contributed to a dramatic increase in percent retroreflectivity. When the sample became whiter due to weathering, it retroreflected more light.
- The retroreflectivity of the white waterborne pavement markings (edgeline) was modeled using field data collected over a year from 38 targeted rural road segments in Idaho. The best fit curve to predict edgeline retroreflectivity deterioration in Idaho used a logarithmic decay function.
- There was a strong relationship between the pavement marking retroreflectivity degradation rate and the weighted average NGSL. In Idaho, the higher the NGSL, the quicker the degradation in retroreflectivity. This could be attributed to the increase in winter maintenance activities (e.g., snowplowing and use of anti-icing and deicing materials) in addition to the climatic impact.
- A direct correlation was found between models developed in the laboratory using the TWPD and field models in the state of Idaho. A reduction in percent retroreflectivity was detected during the initial part of the TWPD testing, and leveled out as the number of cycles increased. This degradation behavior is similar to what occurs on roadways, as retroreflectivity drops after the first few months of application and levels out in the long term.

Based on the results, the laboratory procedure can also be standardized and used as pre-qualifying testing for assessing different pavement marking products or selecting a

suitable material from a set of alternatives for a specific climate or operational condition. This procedure is considered to be flexible since it has room to test the pavement markings under different environments (e.g., cold, hot, rainy, or snowy) and types of traffic loads (e.g., different types of tires, steel wheels, and studded tires). It is also advantageous since it can be less expensive, easier to operate, and reduce the testing time from years to weeks.

After applying the crash analysis to investigate the correlation between pavement marking quality (represented by retroreflectivity) and crash occurrence, the statistical results indicated that no significant correlation between low edgeline retroreflectivity values and crash rate was detected, except in District 1, which was subjected to high ground snow loads. This suggests that more research is still required to investigate this relationship and avoid the shortcomings of this crash analysis.

The driver simulation study determined that longitudinal edgeline pavement marking width alone does not affect lane deviation but there is a correlation between deterioration level and increased lane deviation from the centerline across different roadway geometry types. For this study, drivers consistently maintained a lane position that slightly favored the edgeline side and increasingly shifted away from the centerline as edgeline deterioration worsened. The study examined the relationship between driver lane deviation and varying combinations of edgeline pavement marking widths and deterioration levels, and the simulated environment encountered by all participants represented daytime and nighttime driving conditions. During real-world conditions with visible light, external factors such as signage, trees, and the presence of guardrail may impact driver behavior, though these elements were not simulated as part of this research. However, testing during nighttime conditions when such cues are not visible and when pavement markings are more heavily relied upon did occur.

Edgeline deterioration is an expected event that occurs due to weathering, snowplowing, and wearing from recurrent vehicle tire loading. The results of this study have shown that there are subtle differences in driver behavior that occur at different deterioration levels and different widths. For public agencies who are responsible for the operations of these facilities, proper maintenance and upkeep of edgeline markings, regardless of width,

ensures that vehicle operators, under normal driving conditions, will be most likely to maintain lane position when visibility of these markings is highest.

The FHWA has funded several studies after the United States Congress called for the Manual on Uniform Traffic Control Devices (MUTCD) to set minimum pavement marking retroreflectivity standards for all highway types. As of this study, no final specifications have been published. This procedure has identified failure points and also addressed relationships between safety and color marking changes, along with marking durability over time, and established specifications for retroreflectivity, color ranges, and durability of various marking materials. This research opens more doors for future research opportunities. It is recommended that future research address:

- the color darkening and fading issue in pavement markings by studying surface chemical changes before and after testing;
- the effects of anti-icing and de-icing substances on pavement markings using different polishing agents during TWPD testing;
- how pavement markings affect skid resistance on the road surface;
- the effect of combining the accelerated weathering process using the weatherometer with accelerated loading under the TWPD; and
- the adhesion effects between marking materials and the pavement surface.

The TWPD can be equipped with a climatic chamber to test the effects of specified environmental conditions on different pavement marking materials to facilitate a more robust evaluation procedure. Collecting specific field snowplow information, such as an exact number of snowplow passes and amount of anti-icing material placed over specified time and roadway segments, could then be used to correspond this field data with laboratory data using the TWPD snowplow simulator.

REFERENCES

AASHTO-NTPEP. (2019). *Pavement Marking Materials (PMM)*. Washington, DC: AASHTO. http://www.ntpep.org/Pages/PMM.aspx

Abbas, A. R., Mohi, A., and Butterfield, J. (2009). *Long Term Striping Alternatives for Bridge Decks*. Ohio Department of Transportation Delaware.

Al Hatailah, H. 2015. *Ground snow loads for the state of Idaho, Idaho ground snow load interactive map.* Moscow, ID: Univ. of Idaho.

ASTM (American Society for Testing and Materials). (2008). *Standard test method for measuring the coefficient of retroreflected luminance of pavement markings in a standard condition of continuous wetting (RL-Rain), (Withdrawn 2013).* ASTM E2176-08. West Conshohocken, PA: ASTM.

ASTM (American Society for Testing and Materials). (2016). *Standard practice for calculation of color tolerances and color differences from instrumentally measured color coordinates.* ASTM D2244-16. West Conshohocken, PA: ASTM.

ASTM (American Society for Testing and Materials). 2017. *Standard practice for conducting road service tests on fluid traffic marking materials.* ASTM D713-12. West Conshohocken, PA: ASTM.

ASTM (American Society for Testing and Materials). (2018a). *Standard test method for measurement of retroreflective pavement marking materials with CEN-prescribed geometry using a portable retroreflectometer.* ASTM E1710-18. West Conshohocken, PA: ASTM.

ASTM (American Society for Testing and Materials). (2018b). *Standard test method for measuring the coefficient of retroreflected luminance (RL) of pavement markings in a standard condition of wetness. ASTM E2177-18.* West Conshohocken, PA: ASTM.

Al-Qadi, I. L., Loulizi, A., Flintsch, G. W., Roosevelt, D. S., Decker, R., Wambold, J. C., and Nixon, W. A. (2002). *Feasibility of using friction indicators to improve winter maintenance operations and mobility*. Transportation Research Board, National Research Council.

Avelar, R., and Carlson, P. (2014). “Link Between Pavement Marking Retroreflectivity and Night Crashes on Michigan Two-Lane Highways.” *Transportation Research Record: Journal of the Transportation Research Board*, 2404, 59–67.

Bahar, G., Masliah, M., Erwin, T., Tan, E., and Hauer, E. (2006). *Pavement Marking Materials and Markers: Real-World Relationship Between Retroreflectivity and Safety Over Time*. Transportation Research Board, Washington, D.C.

Bektas, B. A., Gkritza, K. and Smadi, O. (2016). “Pavement marking retroreflectivity and crash frequency: Segmentation, line type, and imputation effects.” *J. Transp. Eng.* 142 (8): 04016030. https://doi.org/10.1061/(ASCE)TE.1943-5436.0000863.

Benz, R. J., Pike, A. M., Kuchangi, S. P., and Brackett, Q. (2009). *Serviceable Pavement Marking Retroreflectivity Levels*. Texas Transportation Institute The Texas A&M University System.

British Standards Institution. (2018). *BS EN 1436:2018: Road marking materials. Road marking performance for road users and test methods.* https://shop.bsigroup.com/en/ProductDetail/?pid=000000000030373461.

Carlson, P., E. Park, and Andersen, C. (2009). “Benefits of pavement markings: A renewed perspective based on recent and ongoing research.” *Transp. Res. Rec.* 2107 (1): 59–68. https://doi.org/10.3141/2107-06.

Carlson, P., Park, E., and Kang, D. (2013). “Investigation of Longitudinal Pavement Marking Retroreflectivity and Safety.” *Transportation Research Record: Journal of the Transportation Research Board*, 2337, 59–66.

Carlson, P., and Wagner, J. (2012). “An Evaluation of the Effectiveness of Wider Edge Line Pavement Markings.”

Carlson, P., Park, E.,Pike, A., Porter, R., Miles, J. Boulanger, B., Smadi, O., Hawkins, N., Chalmers, S., Darmiento, F., Burde, A., Kuhn, B., Ealding, W. (2013)."Pavement Marking Demonstration Projects: State of Alaska and State of Tennessee." Project Rep. No. FHWA-HRT-12-048. TX: Texas Transportation Institute.

Dwyer, C., Vavrik, W., and Becker, R. (2013). *Evaluating Pavement Markings on Portland Cement Concrete (PCC) and Various Asphalt Surfaces Results of Year 1 Data Collection*. Project Report, Illinois Center for Transportation, Illinois.

Choubane, B., Gokhale, S., and Fletcher, J. (2006). "Feasibility of Accelerated Pavement Testing to Evaluate Long-Term Performance of Raised Pavement Markers." *Transportation Research Record: Journal of the Transportation Research Board*, 1948, 108–113.

Chrysler, S. T., Re, J., Knapp, K. S., Funkhouser, D. S., and Kuhn, B. T. (2009). "Driver response to delineation treatments on horizontal curves on two-lane roads." *Rep. FHWA/TX-09/0-5772-1, Texas Transportation Institute, Texas A&M Univ., College Station, TX*.

Chrysler, S. T., Schrock, S. D., and Gates, T. J. (2006). *Durability of Preformed Thermoplastic Pavement Markings for Horizontal Signing Applications*. National Technical Information Service.

Cottrell, B. H. (1995). *Investigation of the impact of snow removal activities on pavement markings in Virginia.* Rep. No. FHWA/VA-96-R3. Charlottesville, VA: Virginia Transportation Research Council.

Craig, W. N., Sitzabee, W. E., Rasdorf ,W. J., and Hummer, J. E. (2007). "Statistical validation of the effect of lateral line location on pavement marking retroreflectivity degradation." *Publ. Works Manage. Policy* 12 (2): 431–450. https://doi.org/10.1177/1087724X07308773.

Donnell, E., Chehab, G., Tang, X., and Schall, D. (2009). "Exploratory Analysis of Accelerated Wear Testing to Evaluate Performance of Pavement Markings." *Transportation Research Record: Journal of the Transportation Research Board*, 2107, 76–84.

Drschel, S. J. (2014). *Salt Brine Blending to Optimize Deicing and Anti-icing Performance and Cost Effectiveness, Phase II*. Minnesota Department of Transportation, Research Services & Library.

Elhouar, S., Dragoo, D., Khodair, Y., and Lee, Y.-S. (2015). *Performance Evaluation of Snow and Ice Plows*. Final Report, llinois Center for Transportation, llinois.

Fu, H., and Wilmot, C. G. (2012). "Evaluating alternative pavement marking materials." *Public Works Management & Policy*, 1087724X12451844.

Gates, T. J., and Hawkins, H. G. (2002). *The Use of Wider Longitudinal Pavement Markings*. Rep. No. FHWA/TX-02-0024-1. College Station, TX: Texas Transportation Institute.

Gates, T., Hawkins, G. and Rose, E. (2003). Effective pavement marking materials and applications for portland cement concrete roadways. Rep. No. FHWA/TX-03/4150-2. College Station, TX: Texas Transportation Institute.

Gibbons, R., Williams, B., and Cottrell, B. (2013). "Assessment of Durability of Wet Night Visible Pavement Markings: Visibility Experiment." *Transportation Research Record: Journal of the Transportation Research Board*, 2337, 67–73.

Hall, J. W., Smith, K. L., Titus-Glover, L., Wambold, J. C., Yager, T. J., and Rado, Z. (2009). "Guide for pavement friction." *Transportation Research Board of the National Academies, Washington DC, USA*.

Hawkins, N. R., Pike, A. M., Smadi, O. G., Knickerbocker, S., and Carlson, P. J. (2015). *Evaluating All-Weather Pavement Markings in Illinois: Volume 1*. Illinois Center for Transportation, Illinois.

Hawkins, N., and Smadi, O. (2011). *Pavement Marking Compatibility with Chip Seal and Micro Surfacing*. Minnesota Department of Transportation, Research Services Section.

Heitzman, M., and Erukulla, S. (2011). "Accelerated Laboratory Testing Protocol to Measure Asphalt Mixture Friction Characteristics."

Heitzman, M., Turner, P., and Greer, M. (2015). *High Friction Surface Treatment Alternative Aggregates Study*.

Hummer, J. E., Rasdorf, W., and Zhang, G. (2011). "Linear Mixed-Effects Models for Paint Pavement-Marking Retroreflectivity Data." *Journal of Transportation Engineering*, 137(10), 705–716.

Jiang, Y. 2008. *Durability and retro-reflectivity of pavement markings (synthesis study).* Rep. No. FHWA/IN/JTRP-2007/11. West Lafayette, IN: Purdue Univ.

Kassem, E., Awed, A., Masad, E., and Little, D. (2013). "Development of Predictive Model for Skid Loss of Asphalt Pavements." *Transportation Research Record: Journal of the Transportation Research Board*, 2372, 83–96.

Kopf, J. (2004). *Reflectivity of pavement markings: Analysis of retroreflectivity degradation curves*. Washington State Department of Transportation.

Lee, J.-T., Maleck, T. L., and Taylor, W. C. (1999). "Pavement marking material evaluation study in Michigan." *ITE Journal*, 69(7), 44.

Lopez, C. A. (2004). *"Pavement Marking Handbook."* <http://onlinemanuals.txdot.gov/txdotmanuals/pmh/manual_notice.htm> (Feb. 3, 2017).

Migletz, J., Graham, J., Harwood, D., and Bauer, K. (2001). "Service life of durable pavement markings." *Transportation Research Record: Journal of the Transportation Research Board*, (1749), 13–21.

Migletz, J., J. Graham, D. Harwood, and K. Bauer. 2001. "Service life of durable pavement markings." Transp. Res. Rec. 1749 (1): 13–21. https://doi.org/10.3141/1749-03.

Migletz, J., and J. L. Graham. 2002. Long-term pavement marking practices. NCHRP Synthesis, 306. Washington, DC: Transportation Research Board.

Miles, J. D., Carlson, P. J., Ryan Eurek, J. R., and Park, E. S. (2010). *Evaluation of Potential Benefits of Wider and Brighter Edge Line Pavement Markings*. Citeseer.

Miller, T. R. (1991). "Benefit-Cost Analysis of Lane Marking." *Transportation Research Record*, 38.

Mohan, S., Gangopadhyay, S., Singh, S., and Ahlawat, A. (2012). "Deterioration of Retro-Reflective Sheet Under Outdoor Weathering and Weather-O-Meter." *International Journal of Transportation Science and Technology*, 1(1), 61–72.

Molino, J. A., Kennedy, J. F., Beuse, P. A., Miller, C. C., Davis, W., and Andersen, C. K. (2013). *Daytime Color Appearance of Retroreflective Traffic Control Sign Materials*.

Moser, J., Jeff, M., Bruce, D., Wayne L. (2015). "MnDOT Pavement Marking Field Guide."

Mull, D. (2011). "Paint Pavement Marking Performance Prediction Model That Includes the Impacts of Snow Removal Operations." Air University.

Mull, D. M., and Sitzabee, W. E. (2012). "Paint Pavement Marking Performance Prediction Model." *Journal of Transportation Engineering*, 138(5), 618–624.

MUTCD. (2009). US Department of Transportation, Federal Highway Administration.

Onyango, M. A., Malyuta, D., Owino, J., and Chimba, D. (2014). "Verification of pavement marking degradation models using eastern tennessee pavement marking retroreflectivity data." *Science, Computing and Telecommunications (PACT), 2014 Pan African Conference on*, IEEE, 56–61.

Ozelim, L., and Turochy, R. E. (2014). "Modeling Retroreflectivity Performance of Thermoplastic Pavement Markings in Alabama." *Journal of Transportation Engineering*, 140(6), 05014001.

Parker, N., and Meja, M. (2003). "Evaluation of performance of permanent pavement markings." *Transportation Research Record: Journal of the Transportation Research Board*, (1824), 123–132.

Pendleton, O. (1988). "Field Studies of Temporary Pavement Markings at Overlay Project Work Zones on Two-Lane, Two-Way Rural Highways."

Peng, Y., Geedipally, S., and Lord, D. (2012). "Effect of Roadside Features on Single-Vehicle Roadway Departure Crashes on Rural Two-Lane Roads." *Transportation Research Record: Journal of the Transportation Research Board*, 2309, 21–29.

Pike, A. M. (2007). "An investigation into the predictive performance of pavement marking retroreflectivity measured under various conditions of continuous wetting." Texas A&M University.

Pike, A. M., and Songchitruksa, P. (2015). "Predicting Pavement Marking Service Life with Transverse Test Deck Data." *Transportation Research Record: Journal of the Transportation Research Board*, 2482, 16–22.

Ramirez, M, (2016), "Potential Impacts of Wider Longitudinal Edgeline Pavement Markings" thesis, presented to University of Idaho at Moscow, ID, in partial fulfillment of the requirements for the degree of Master of Science.

Sadid, H., Wabrek, R. M., and Dongare, S. (2010). *Material Acceptance Risk Analysis: Pavement Markings*. Final Report 07/27/07-08/30/10, Idaho Transportation Department, Idaho.

SAE International. (2015). J2944, Service Vehicle Recommended Practices.

Sasidharan, L., Karwa, V., and Donnell, E. T. (2009). "Use of Pavement Marking Degradation Models to Develop a Pavement Marking Management System." *Public Works Management & Policy*, 14(2), 148–173.

Sathyanarayanan, S., Shankar, V., and Donnell, E. (2008). "Pavement Marking Retroreflectivity Inspection Data: A Weibull Analysis." *Transportation Research Record: Journal of the Transportation Research Board*, 2055, 63–70.

Schalkwyk, I. van. (2010). *Enhancements to Pavement Marking Testing Procedures*. Final Report, Oregon Department of Transportation, Oregon.

Sitzabee, W. (2008). "A Spatial Asset Management Study Through an Analysis of Pavement Marking Performance." North Carolina State University.

Sitzabee, W. E., Hummer, J. E., and Rasdorf, W. (2009). "Pavement Marking Degradation Modeling and Analysis." *Journal of Infrastructure Systems*, 15.3, 190–199.

Smadi, O. (2013). *Predicting the initial retroreflectivity of pavement markings from glass bead quality*. NCHRP report, Transportation Research Board, Washington, D.C.

Sun, X., and Tekell, D. (2005). *Impact of Edge Lines on Safety of Rural Two-Lane Highways*. Final Report.

Taek, J., Maleck, T. L., and Taylor, W. C. (1999). "Pavement making material evaluation study in Michigan." *Institute of Transportation Engineers. ITE Journal*, 69(7), 44.

Thomas-Meyers, G., and Nagy, A. L. (2010). "Pavement marking color specifications." *Journal of Vision*, 3(12), 65–65.

Tsyganov, A. R., Machemehl, R. B., and Warrenchuk, N. M. (2005). *Safety Impact of Edge Lines on Rural Two-Lane Highways*. Technical Report, Texas Department of Transportation, Texas Department of Transportation.

Vollor, T. W., and Hanson, D. I. (2006). *Development of Laboratory Procedure for Measuring Friction of HMA Mixtures–Phase I*. National Center for Asphalt Technology, Auburn University, Alabama.

Wang, C., Wang, Z., and Tsai, Y.-C. (2016). "Piecewise Multiple Linear Models for Pavement Marking Retroreflectivity Prediction Under Effect of Winter Weather Events." *Transportation Research Record: Journal of the Transportation Research Board*, 2551, 52–61.

Wang, S. (2010). "Comparative Analysis of NTPEP Pavement Marking Performance Evaluation Results." University of Akron.

WSDOT, Design Manual. (2017). "WSDOT, Design Manual." <https://www.wsdot.wa.gov/Publications/Manuals/M22-01.htm> (Jan. 23, 2018).

World Health Organization. (2018). Road Traffic Injuries. https://www.who.int/news-room/fact-sheets/detail/road-traffic-injuries

Zhang, G., Hummer, J. E., and Rasdorf, W. (2009). "Impact of bead density on paint pavement marking retroreflectivity." *Journal of Transportation Engineering*, 136(8), 773–781.

Zhang, Y., and Wu, D. (2010). "Methodologies to predict service lives of pavement marking materials." *Journal of the Transportation Research Forum*.

APPENDICES

Appendix A: Laboratory Data

Glossary	
Symbol	Description
S	Slab
First letter W	Waterborne
Second letter W	White Color
Y	Yellow
T	Thermoplastic
Ret	Retroreflectivity analysis folder
Color	Color analysis folder
Image	Image analysis folder
✓	Implemented
x	Not implemented

Sample numbering and test management

Asphalt Slabs	Applied Test	Performance measures				
		Retroreflectivity			Color Retention	Presence
		Dry	Recovery	Continuous Wetting		
Waterborne White						
S1WW	Pneumatic wheelset	✓	✓	✓	✓	✓
S2WW	Steel Wheelset	✓	✓	✓	✓	✓
S3WW	Scraper Blade With Pneumatic Wheelset	✓	✓	✓	✓	✓
Waterborne Yellow						
S4WY	Pneumatic wheelset	✓	✓	✓	✓	✓
S5WY	Steel Wheelset	✓	✓	✓	✓	✓
S6WY	Scraper Blade With Pneumatic Wheelset	✓	✓	✓	✓	✓
Thermoplastic White						
S7TW	Pneumatic wheelset	x	x	x	x	x
S8TW	Scraper Blade With Pneumatic Wheelset	✓	✓	✓	✓	✓
S9TW	Steel Wheelset	✓	✓	✓	✓	✓
Thermoplastic Yellow						
S10TY	Steel Wheelset	✓	✓	✓	✓	✓
S11TY	Pneumatic wheelset	x	x	x	x	x
S12TY	Scraper Blade With Pneumatic Wheelset	✓	✓	✓	✓	✓

Aluminum Plates	Applied Test	Performance measures				
		Retroreflectivity			Color Retention	Presence
		Dry	Recovery	Continuous Wetting		
Waterborne White						
WW1	Accelerated weathering test	✓	✓	✓	✓	x
WW2	Reference	✓	✓	✓	✓	x
WW3		✓	✓	✓	✓	x
Waterborne Yellow						
WY1	Accelerated weathering test	✓	✓	✓	✓	x
WY2	Reference	✓	✓	✓	✓	x
Thermoplastic White						
TW1	Accelerated weathering test	✓	✓	✓	✓	x
TW2	Reference	✓	✓	✓	✓	x
Thermoplastic Yellow						
TY1	Accelerated weathering test	✓	✓	✓	✓	x
TY2	Reference	✓	✓	✓	✓	x

Appendix A.1: Waterborne White - Retroreflectivity

Dry RetroReflectivity												
Number of Cycles	Retroreflectivity measurements				Predicted model values				Percentage			
	Pneumatic, P	Steel, S	Pneumatic w/ Blade, P w SB	Scraper Blade, SB	P	**S**	P w SB	SB	P	**S**	P w SB	SB
1	346	307	335	335	381	292	369	282	100%	100%	100%	100%
10		271	320		323	240	335	237	85%	82%	91%	84%
50			318		283	203	311	205	74%	70%	84%	73%
100	288				266	188	301	191	70%	64%	81%	68%
200		175			248	172	290	178	65%	59%	79%	63%
300	277				238	163	284	170	63%	56%	77%	60%
500	195	169	307		226	151	277	160	59%	52%	75%	57%
750	216				215	142	271	152	57%	49%	73%	54%
1000	240		288	141	208	136	266	146	55%	47%	72%	52%
1500	191				198	127	260	138	52%	43%	71%	49%
2500		136			185	115	253	128	49%	39%	68%	45%
5000	187	112	231	127	168	99	242	114	44%	34%	66%	41%
10000		79	233	94	151	84	232	101	40%	29%	63%	36%
15000		41			141	75	226	93	37%	26%	61%	33%
20000	149				134	68	222	87	35%		60%	31%
50000	90		157	68	111	48	208	69	29%		56%	25%
80000	59				99	37	201	60	26%		55%	21%
100000	99				93	32	198	55	25%		54%	20%

Recovery RetroReflectivity												
Number of Cycles	Retroreflectivity measurements				Predicted model values				Percentage			
	Pneumatic, P	Steel, S	Pneumatic w/ Blade, P w SB	Scraper Blade, SB	P	**S**	P w SB	SB	P	**S**	P w SB	SB
1	212	189	277	277	247	174	299	260	100%	100%	100%	100%
10		185	249		209	137	275	222	85%	79%	92%	85%
50		81	296		182	112	259	196	74%	64%	86%	75%
100		62			171	101	252	184	69%	58%	84%	71%
200		58			159	90	244	173	64%	52%	82%	67%
300	192				152	84	240	166	62%	48%	80%	64%
500	169		252		144	75	235	158	58%	43%	79%	61%
750	143				137	69	231	151	55%	40%	77%	58%
1000	138		249	116	132	64	228	147	54%	37%	76%	56%
1500					126	58	223	140	51%	33%	75%	54%
2500		50			117	50	218	132	47%	29%	73%	51%
5000	111	43	224	111	106	39	211	120	43%	22%	71%	46%
10000		42	202	89	94	28	204	109	38%	16%	68%	42%
15000		42			87	22	200	102	35%	12%	67%	39%
20000	73				82		197	98	33%		66%	38%
50000	47		180	107	67		187	83	27%		63%	32%
80000	42				59		182	75	24%		61%	29%
100000			150	90	56		180	71	23%		60%	27%

Continuous Wetting RetroReflectivity												
Number of Cycles	Retroreflectivity measurements				Predicted model values				Percentage			
	Pneumatic, P	Steel, S	Pneumatic w/ Scraper Blade, P w SB	Scraper Blade, SB	P	S	P w SB	SB	P	S	P w SB	SB
1	109	54	155	155	102	55	175	156	100%	100%	100%	100%
10		44			82	45	148	134	81%	83%	85%	86%
50		37			69	39	129	119	68%	71%	74%	76%
100	91	36	142		63	36	121	113	62%	65%	69%	72%
200		33			58	33	113	106	57%	60%	64%	68%
300	41				54	31	108	102	53%	57%	62%	66%
500	35		110		50	29	102	98	49%	53%	58%	63%
750					47	28	97	94	46%	50%	56%	60%
1000	32	37	126	114	44	26	94	91	44%	48%	54%	58%
1500	25				41	25	89	87	40%	45%	51%	56%
2500		20			37	23	83	82	36%	41%	47%	53%
5000		19	62	59	31	20	75	76	30%	36%	43%	49%
10000		13	39	51	25	17	67	69	25%	31%	38%	44%
15000					22	15	62	66	21%	28%	35%	42%
20000					19		59	63	19%		34%	40%
50000	20			53	12		48	54	12%		27%	35%
80000	17				8		42	50	8%		24%	32%
100000	10			62	6		40	48	6%		23%	31%

Waterborne Yellow - Retroreflectivity

Dry RetroReflectivity									
Number of Cycles	Retroreflectivity measurements			Predicted model values			Percentage		
	Pneumatic, P	Steel, S	Scraper Blade, SB	P	S	SB	P	S	SB
1	124	204	144	160	224	150	100%	100%	100%
10				131	177	128	82%	79%	85%
50				111	144	112	69%	64%	74%
100		182		102	129	105	64%	58%	70%
200				93	115	98	58%	51%	65%
300	137			88	107	94	55%	48%	63%
500	112	89	99	82	96	89	51%	43%	59%
750				77	88	85	48%	39%	57%
1000	96	67	90	73	82	82	46%	37%	55%
1500				68	74	78	42%	33%	52%
2500	57			62	63	73	38%	28%	49%
5000	41	50		53	49	66	33%	22%	44%
10000	22	26	52	44	35	60	28%	15%	40%
15000				39	26	56	24%	12%	37%
20000	20			35	20	53	22%	9%	35%
25000		13		33	16	51	20%	7%	34%
50000	17		41	24		44	15%	0%	29%
80000				18		39	11%	0%	26%
100000	11		36	15		37	9%	0%	25%

Recovery RetroReflectivity									
Number of Cycles	Retroreflectivity measurements			Predicted model values			Percentage		
	Pneumatic, P	Steel, S	Scraper Blade, SB	P	S	SB	P	S	SB
1	96	141	97	103	144	104	100%	100%	100%
10				84	111	88	81%	77%	85%
50				70	89	77	68%	62%	74%
100		93		64	79	72	62%	55%	69%
200				59	69	67	57%	48%	65%
300	42			55	64	64	53%	44%	62%
500	75	50	83	51	56	61	49%	39%	58%
750				47	51	58	46%	35%	56%
1000	62	39	49	45	47	56	44%	32%	54%
1500				42	41	53	40%	28%	51%
2500	43			37	34	50	36%	23%	48%
5000	17	23		31	24	45	30%	17%	43%
10000	17	15	40	26	14	40	25%	10%	38%
15000				22	9	37	22%	6%	36%
20000	16			20	5	35	19%	3%	34%
25000		4		18	1	34	17%	1%	32%
50000	12		24	12		29	12%	0%	28%
80000				8		25	8%	0%	24%
100000	6		21	6		24	6%	0%	23%

Continuous Wetting RetroReflectivity									
Number of Cycles	Retroreflectivity measurements			Predicted model values			Percentage		
	Pneumatic, P	Steel, S	Scraper Blade, SB	P	**S**	SB	P	**S**	SB
1	57	86	61	64	91	67	100%	100%	100%
10				53	71	56	82%	78%	84%
50				44	57	49	69%	62%	73%
100		63		41	51	46	63%	55%	69%
200				37	45	43	57%	49%	64%
300	32			35	41	41	54%	45%	61%
500	52	35	50	32	36	39	50%	40%	58%
750				30	33	37	47%	36%	55%
1000	41	27	35	29	30	35	45%	33%	53%
1500				27	27	34	41%	29%	50%
2500	20			24	22	31	37%	24%	47%
5000	16	12		20	16	28	32%	18%	42%
10000	11	10	29	17	10	25	26%	11%	37%
15000				15	6	23	23%	7%	35%
20000				13	4	22	21%	4%	33%
25000	7	2		12	2	21	19%	2%	31%
50000			17	9		18	13%		26%
80000				6		15	9%		23%
100000			6	5		14	8%		22%

White Thermoplastic - Retroreflectivity

Dry RetroReflectivity									
Number of Cycles	Retroreflectivity measurements			Predicted model values			Percentage		
	Pneumatic, P	Steel, S	Scraper Blade, SB	P	S	SB	P	S	SB
1	540	763	400	596	872	494	100%	100%	100%
10				558	726	435	94%	83%	88%
50				532	625	393	89%	72%	80%
100				521	581	375	87%	67%	76%
200				509	537	357	85%	62%	72%
300				503	511	347	84%	59%	70%
500	539	527	389	494	479	334	83%	55%	67%
750				488	453	323	82%	52%	65%
1000	520	598	408	483	435	316	81%	50%	64%
1500				477	410	305	80%	47%	62%
2500				468	377	292	79%	43%	59%
5000	511	457	376	457	333	274	77%	38%	55%
10000			271	445	290	256	75%	33%	52%
15000				439	264	246	74%	30%	50%
20000				434	246	238	73%	28%	48%
25000	450	196		431	232	232	72%	27%	47%
30000			220	428	220	228	72%	25%	46%
50000	423	89	179	419	188	214	70%	22%	43%
80000				411	158	202	69%	18%	41%
100000	387	53	159	408	144	196	68%	17%	40%
150000	372		165	401		186	67%		38%
200000	344		108	397		178	67%		36%

Recovery RetroReflectivity									
Number of Cycles	Retroreflectivity measurements			Predicted model values			Percentage		
	Pneumatic, P	Steel, S	Scraper Blade, SB	P	**S**	SB	P	**S**	SB
1	184	216	152	197	268	177	100%	100%	100%
10				186	226	147	95%	84%	83%
50				179	197	126	91%	73%	71%
100				175	184	117	89%	69%	66%
200				172	171	108	87%	64%	61%
300				170	164	103	87%	61%	58%
500	178	202	128	168	155	96	85%	58%	54%
750				166	147	91	84%	55%	51%
1000	175	185	102	165	142	87	84%	53%	49%
1500				163	135	82	83%	50%	46%
2500				160	125	75	82%	47%	42%
5000	174	186	85	157	112	66	80%	42%	37%
10000			57	154	100	57	78%	37%	32%
15000				152	92	52	77%	34%	29%
20000				151	87	48	77%	32%	27%
25000	150	56		150	83	45	76%	31%	26%
30000			39	149	80	43	76%	30%	24%
50000	140	32	25	146	70	36	74%	26%	20%
80000				144	62	30	73%	23%	17%
100000	125	11	22	143	58	27	73%	21%	15%
150000			16	141		22	72%		12%
200000			5	140		18	71%		10%

Continuous Wetting RetroReflectivity									
Number of Cycles	Retroreflectivity measurements			Predicted model values			Percentage		
	Pneumatic, P	Steel, S	Scraper Blade, SB	P	**S**	SB	P	**S**	SB
1	105	101	57	112	116	68	100%	100%	100%
10				102	98	58	91%	85%	86%
50				94	86	51	84%	74%	75%
100				91	81	48	81%	69%	71%
200				88	75	45	78%	65%	67%
300				86	72	44	76%	62%	64%
500	88	83	49	84	68	41	74%	59%	61%
750				82	65	40	73%	56%	58%
1000	88	70	48	80	63	38	72%	54%	57%
1500				78	60	37	70%	51%	54%
2500				76	56	34	68%	48%	51%
5000	79	63	45	73	50	32	65%	43%	46%
10000			31	70	45	29	62%	39%	42%
15000				68	42	27	60%	36%	40%
20000				66	40	26	59%	34%	38%
25000	77	57		65	38	25	58%	33%	36%
30000			22	65	37	24	58%	32%	35%
50000	50	19	9	62	33	22	55%	28%	32%
80000				60	29	20	53%	25%	29%
100000	49	2	10	59	27	19	53%	24%	28%
150000				57	24	17	51%	21%	25%
200000				56	22	16	50%	19%	23%

Yellow Thermoplastic - Retroreflectivity

Dry RetroReflectivity									
Number of Cycles	Retroreflectivity measurements			Predicted model values			Percentage		
	Pneumatic, P	Steel, S	Scraper Blade, SB	P	S	SB	P	S	SB
1	256	274	213	285	263	213	100%	100%	100%
10				267	220	186	94%	84%	87%
50				254	190	167	89%	72%	78%
100			159	249	177	159	87%	67%	75%
200				243	164	150	85%	62%	71%
300				240	157	146	84%	59%	68%
500	258			236	147	140	83%	56%	66%
750				233	139	135	82%	53%	63%
1000	250	101	127	230	134	132	81%	51%	62%
1500				227	126	127	80%	48%	60%
2500				223	117	121	78%	44%	57%
5000	244	100		218	104	113	76%	39%	53%
10000	229	102	112	212	91	104	74%	35%	49%
15000				209	83	100	73%	32%	47%
20000				207	78	96	72%	30%	45%
25000	221	82		205	74	94	72%	28%	44%
30000				203	70	92	71%	27%	43%
50000	179	67		199	61	86	70%	23%	40%
80000				196		80	69%		38%
100000	142		74	194		77	68%		36%
150000				191		73	67%		34%
200000				188		69	66%		33%

Recovery RetroReflectivity									
Number of Cycles	Retroreflectivity measurements			Predicted model values			Percentage		
	Pneumatic, P	Steel, S	Scraper Blade, SB	P	S	SB	P	S	SB
1	77	53	29	85	63	30	100%	100%	100%
10				78	56	26	92%	88%	87%
50				73	50	23	86%	79%	78%
100				71	48	22	83%	75%	74%
200				69	45	21	81%	71%	70%
300				67	44	20	79%	69%	67%
500	75		24	66	42	19	77%	66%	64%
750				65	41	19	76%	64%	62%
1000	72	78	19	64	40	18	75%	63%	61%
1500				62	38	18	73%	60%	58%
2500				61	37	17	72%	58%	55%
5000	62	30	8	59	34	15	69%	54%	51%
10000	59	19	22	57	32	14	66%	50%	47%
15000				55	30	14	65%	48%	45%
20000				54	29	13	64%	46%	43%
25000	50	18		54	29	13	63%	45%	42%
30000				53		12	62%	0%	41%
50000	48		2	52		11	61%	0%	38%
80000				50		11	59%	0%	35%
100000	42		16	49		10	58%	0%	34%
150000				48		10	57%	0%	32%
200000				47		9	56%	0%	30%

Continuous Wetting RetroReflectivity									
Number of Cycles	Retroreflectivity measurements			Predicted model values			Percentage		
	Pneumatic, P	Steel, S	Scraper Blade, SB	P	**S**	SB	P	**S**	SB
1	39	21	24	42	22	24	100%	100%	100%
10				39	19	20	93%	88%	82%
50				37	18	17	89%	80%	70%
100				36	17	16	87%	76%	65%
200				35	16	14	85%	72%	59%
300				35	15	14	84%	70%	56%
500	37		13	34	15	13	82%	68%	52%
750				34	14	12	81%	66%	49%
1000	37	16	12	33	14	11	80%	64%	47%
1500				33	14	11	79%	62%	44%
2500				32	13	10	78%	59%	40%
5000	32	14	10	32	12	8	76%	56%	35%
10000	30	12	5	31	11	7	74%	52%	29%
15000				30	11	6	73%	50%	26%
20000				30	11	6	72%	49%	24%
25000	29	7		30	10	5	71%	47%	22%
30000				29	10	5	71%	46%	21%
50000	29			29	10	4	69%	44%	17%
80000				28	9	3	68%	41%	13%
100000	25			28	9	3	67%	40%	12%
150000				28	8	2	66%	38%	9%
200000				27	8	2	65%	37%	6%

Appendix A.2: Artificial weathering results (Retroreflectivity measurements) White

Exposure Time (hours)	WW Dry	WW Recovery	WW Continuous Wetting	WT Dry	WT Recovery	WT Continuous Wetting	Dry Waterborne	Recovery Waterborne	Continuous Wetting White Waterborne	Dry Thermoplastic	Recovery Thermoplastic	Continuous Wetting Thermoplastic
0	414	54	27	265	46	32	100%	100%	100%	100%	100%	100%
12	414	55	27	266	46	32	100%	103%	102%	100%	101%	100%
48	417	60	29	268	48	32	101%	111%	109%	101%	104%	100%
96	419	66	32	272	49	32	101%	121%	118%	103%	108%	100%
144	422	71	34	276	51	32	102%	132%	128%	104%	112%	100%
240	428	83	39	283	55	32	103%	153%	146%	107%	120%	101%
360	435	97	45	293	59	32	105%	180%	169%	111%	129%	101%
480	442	112	51	302	64	32	107%	207%	192%	114%	139%	101%
840	464	155	70	330	77	33	112%	287%	261%	125%	169%	102%
1320	493	213	94	368	95	33	119%	394%	352%	139%	208%	103%
1560	507	241	107	387	104	33	123%	447%	398%	146%	227%	104%
1800	522	270	119	405	113	34	126%	500%	444%	153%	247%	105%
2000	534	294	129	421	120	34	129%	545%	483%	159%	263%	105%

Artificial weathering results (Retroreflectivity measurements) Yellow

Exposure Time (hours)	WW Dry	WW Recovery	WW Continuous Wetting	WT Dry	WT Recovery	WT Continuous Wetting	Dry Waterborne	Recovery Waterborne	Continuous Wetting White Waterborne	Dry Thermoplastic	Recovery Thermoplastic	Continuous Wetting Thermoplastic
0	144	45	24	137	51	32	100%	100%	100%	100%	100%	100%
12	144	46	24	138	51	32	100%	101%	100%	101%	101%	100%
48	145	46	24	141	52	32	101%	102%	102%	103%	102%	102%
96	147	47	25	146	53	33	102%	105%	103%	106%	105%	103%
144	149	48	25	150	54	33	104%	107%	105%	109%	107%	105%
240	152	50	26	158	57	34	106%	111%	109%	116%	112%	108%
360	157	53	27	169	60	36	109%	117%	113%	123%	118%	112%
480	161	56	28	180	62	37	112%	123%	117%	131%	124%	116%
840	174	63	31	212	71	41	121%	140%	131%	154%	141%	129%
1320	192	74	35	254	83	46	134%	163%	148%	186%	165%	145%
1560	201	79	37	276	89	49	140%	174%	157%	201%	176%	153%
1800	209	84	40	297	95	51	146%	186%	166%	217%	188%	162%
2000	217	89	41	315	100	54	151%	195%	173%	230%	198%	169%

Appendix B: Field Data

Appendix B.1: Weighted NGSL data and calculation for all districts

NGSL_Class	ITD_Dist	AREA (Square Meter)	NGSL
1	1	36000000	0.25% - 1%
2	1	715020099.5	1.01% - 2%
2	1	5.75389643	1.01% - 2%
3	1	4293927703	2.01% - 3%
4	1	8077350365	3.01% - 4%
5	1	1840010040	4.01% - 5%
6	1	1534724366	5.01% - 6%
7	1	2925204689	6.01% - 7%
8	1	441000000	7.01% - 8%
9	1	72000000	8.01% - 9%
10	1	607774896.5	9.01% - 10.5%
1	2	314311340.3	0.25% - 1%
2	2	10413791043	1.01% - 2%
2	2	5.75389643	1.01% - 2%
3	2	6225100479	2.01% - 3%
4	2	8345917919	3.01% - 4%
5	2	2958322668	4.01% - 5%
6	2	3268224334	5.01% - 6%
7	2	2533392311	6.01% - 7%
8	2	648000000	7.01% - 8%
1	3	17830652301	0.25% - 1%
2	3	20123398843	1.01% - 2%
3	3	11513815989	2.01% - 3%
4	3	5511378351	3.01% - 4%
5	3	1353995957	4.01% - 5%
6	3	441000000	5.01% - 6%
1	4	13342551672	0.25% - 1%
2	4	12489416315	1.01% - 2%
3	4	3419647902	2.01% - 3%
4	4	628071531.8	3.01% - 4%
1	5	6886126309	0.25% - 1%
2	5	12937781260	1.01% - 2%
3	5	4159538037	2.01% - 3%
4	5	429394634.4	3.01% - 4%
1	6	19610383054	0.25% - 1%
2	6	20021962409	1.01% - 2%
3	6	9497952392	2.01% - 3%
4	6	924594248.6	3.01% - 4%

NGSL	ITD_Dist	AREA (Square Meter)	Average NGSL Range	%	Area ratio	Weighted NGSL
0.25% - 1%	2	314311340.3	0.625	0.00625	0.009056	5.66008E-05
1.01% - 2%	2	10413791048.3	1.5	0.015	0.300048	0.004500723
2.01% - 3%	2	6225100478.6	2.5	0.025	0.179361	0.00448403
3.01% - 4%	2	8345917918.6	3.5	0.035	0.240467	0.00841636
4.01% - 5%	2	2958322668.1	4.5	0.045	0.085237	0.003835661
5.01% - 6%	2	3268224334.0	5.5	0.055	0.094166	0.005179129
6.01% - 7%	2	2533392310.7	6.5	0.065	0.072994	0.004744582
7.01% - 8%	2	648000000.0	7.5	0.075	0.018671	0.001400291
Total		34707060098.6				0.032617378

NGSL	ITD_Dist	AREA (Square Meter)	Average NGSL Range	Area ratio	Weighted NGSL
0.25% - 1%	3	17830652300.7	0.625	0.314062361	0.00196289
1.01% - 2%	3	20123398842.9	1.5	0.354445931	0.005316689
2.01% - 3%	3	11513815989.1	2.5	0.202799997	0.00507
3.01% - 4%	3	5511378350.6	3.5	0.097075332	0.003397637
4.01% - 5%	3	1353995957.3	4.5	0.023848772	0.001073195
5.01% - 6%	3	441000000.0	5.5	0.007767607	0.000427218
Total		56774241440.6			0.017247628

NGSL	ITD_Dist	AREA (Square Meter)	Average NGSL Range	%	Area ratio	Weighted NGSL
0.25% - 1%	4	13342551671.9	0.652	0.00652	0.4465425	0.0029115
1.01% - 2%	4	12489416315.0	1.5	0.015	0.4179902	0.0062699
2.01% - 3%	4	3419647901.9	2.5	0.025	0.1144472	0.0028612
3.01% - 4%	4	628071531.8	3.5	0.035	0.02102	0.0007357
Total		29879687420.5				0.0127782

NGSL	ITD_Dist	AREA (Square Meter)	Average NGSL Range	%	Area ratio	Weighted NGSL
0.25% - 1%	5	6886126308.8	0.625	0.00625	0.2820699	0.0017629
1.01% - 2%	5	12937781259.6	1.5	0.015	0.5299581	0.0079494
2.01% - 3%	5	4159538037.1	2.5	0.025	0.1703832	0.0042596
3.01% - 4%	5	429394634.4	3.5	0.035	0.0175889	0.0006156
Total		24412840239.9				0.0145875

NGSL	ITD_Dist	AREA (Square Meter)	Average NGSL Range	%	Area ratio	Weighted NGSL
0.25% - 1%	6	19610383054.1	0.625	0.00625	0.3917776	0.0024486
1.01% - 2%	6	20021962409.1	1.5	0.015	0.4000001	0.006
2.01% - 3%	6	9497952392.1	2.5	0.025	0.1897507	0.0047438
3.01% - 4%	6	924594248.6	3.5	0.035	0.0184716	0.0006465
Total		50054892104.0				0.0138389

Appendix B.2: Test sites for the six districts

District	Route	Segment	Beg. MP	End MP	Segment Length (mile)	District	Route	Segment	Beg. MP	End MP	Segment Length (mile)
1	SH001	1580	5.58	11.175	5.595	1	SH001	1580	0	6	6
1	SH003	1800	114.103	116.894	2.791	1	SH003	1800	111	114	3
1	SH200	1610	55.66	62.975	7.315	1	SH200	1610	48	55	7
1	SH041	1630	19.38	22.8	3.42	1	SH041	1630	24	27	3
1	SH003	1800	92.517	95.331	2.814	1	SH003	1800	96	99	3
1	US095	1540	525.971	527.284	1.313	1	US095	1540	528	530	2
1	SH097	1790	74.3	81.5	7.2	1	SH097	1790	83	90	7
		Total District 1 Miles			**30.448**			**Total District 1 Miles**			**31**
2	SH009	1860	7.26	13.522	6.262	2	SH009	1860	1	7	6
2	US095	8605	263.8	269.648	5.848	2	US095	8605	271	277	6
	SH128	6780	0	2.2	2.2	2	SH128	6780			3
2	SH099	1880	0	2.8	2.8	2	SH099	1880	4	7	3
2	SH006	1850	17.157	20.286	3.129	2	SH006	1850	21	24	3
2	US012	1910	106	113.8	7.8	2	US012	1910	115	123	8
		Total District 2 Miles			**28.039**			**Total District 2 Miles**			**29**
3	US095	1540	4.9	7	2.1	3	US095	1540	8	10	2
3	US095	1540	22.71	28	5.29	3	US095	1540	29	34	5
3	US020	2070	96.05	103.837	7.787	3	US020	2070	104	110	6
3	SH051	2170	19.89	28.9	9.01	3	SH051	2170	30	36	6
3	SH021	2140	28	34	6	3	SH021	2140	35	41	6
		Total District 3 Miles			**30.187**			**Total District 3 Miles**			**25**
4	SH046	2200	135.625	137.423	1.798	4	SH046	2200	138	140	2
4	SH075	2230	87.248	92.192	4.944	4	SH075	2230	93	98	5
4	SH025	2270	37.57	42.472	4.902	4	SH025	2270	43	48	5
4	SH081	2310	23.608	26.2	2.592	4	SH081	2310	27	30	3
4	SH021	2140	111	116.5	5.5	4	SH021	2140	118	123	5
4	SH046	2200	121.139	125.674	4.535	4	SH046	2200	127	131	4
4	US030	2040	176.3	177.51	1.21	4	US030	2040	179	182	3
4	SH024	2280	66.916	67.533	0.617	4	SH024	2280	65	66	1
		Total District 4 Miles			**26.098**			**Total District 4 Miles**			**28**
5	US026	2240	272	279.5	7.5	5	US026	2240	281	287	6
5	SH036	2370	0	4.752	4.752	5	SH036	2370	6	11	5
5	I15 B BlackF	1370	0	2.18	2.18	5	I15 B BlackF	1370	2	4	2
5	SH036	2370	29.73	33.926	4.196	5	SH036	2370	24	28	4
5	SH034	2360	70.47	76	5.53	5	SH034	2360	77	82	5
5	SH034	2360	93.3	98.71	5.41	5	SH034	2360	100	105	5
		Total District 5 Miles			**29.568**			**Total District 5 Miles**			**27**
6	US093	2220	299	304.3	5.3	6	US093	2220	305	310	5
6	SH033	2460	8.5	17	8.5	6	SH033	2460	18	24	6
6	SH043	2400	0.3	3.42	3.12	6	SH043	2400	4	7	3
6	US093	2220	263	268.66	5.66	6	US093	2220	270	276	6
6	US093	2220	137	144.5	7.5	6	US093	2220	146	151	5
6	SH031	2450	4.735	5.705	0.97	6	SH031	2450	7	10	3
		Total District 6 Miles			**31.05**			**Total District 6 Miles**			**28**
Total Length					**343.39**						

Appendix C: Permissions for reusing published journal articles

RE: Permission for reuse in dissertation_Maged Mohamed

PERMISSIONS <permissions@asce.org>
Fri 4/26/2019 4:57 AM
To: Mohamed, Maged (moha9447@vandals.uidaho.edu) <moha9447@vandals.uidaho.edu>

Dear Maged Mohamed,
Thank you for your inquiry. As an original author of an ASCE journal article or proceedings paper, you are permitted to reuse your own content (including figures and tables) for another ASCE or non-ASCE publication, provided it does not account for more than 25% of the new work. This email serves as permission to reuse your work Deterioration Characteristics of Waterborne Pavement Markings Subjected to Different Operating Conditions."*Journal of Transportation Engineering, Part B: Pavements*, Vol. 145, no. 2 (2019): 04019003, https://doi.org/10.1061/JPEODX.0000101.

A full credit line must be added to the material being reprinted. For reuse in non-ASCE publications, add the words "With permission from ASCE" to your source citation. For Intranet posting, add the following additional notice: "This material may be downloaded for personal use only. Any other use requires prior permission of the American Society of Civil Engineers. This material may be found at [URL/link of abstract in the ASCE Library or Civil Engineering Database]."

Each license is unique, covering only the terms and conditions specified in it. Even if you have obtained a license for certain ASCE copyrighted content, you will need to obtain another license if you plan to reuse that content outside the terms of the existing license. For example: If you already have a license to reuse a figure in a journal, you still need a new license to use the same figure in a magazine. You need a separate license for each edition.

For more information on how an author may reuse their own material, please view:
http://ascelibrary.org/page/informationforasceauthorsreusingyourownmaterial

Sincerely,

Leslie Connelly
Senior Marketing Coordinator
American Society of Civil Engineers
1801 Alexander Bell Drive
Reston, VA 20191

PERMISSIONS@asce.org

4/25/2019 Rightslink® by Copyright Clearance Center

Copyright Clearance Center RightsLink®

Home Create Account Help

Title: Effects of longitudinal pavement edgeline condition on driver lane deviation

Author: Kevin Chang,Marvin V. Ramirez,Brian Dyre,Maged Mohamed,Ahmed Abdel-Rahim

Publication: Accident Analysis & Prevention

Publisher: Elsevier

Date: July 2019

Published by Elsevier Ltd.

LOGIN

If you're a copyright.com user, you can login to RightsLink using your copyright.com credentials.

Already **a RightsLink user** or want to learn more?

Please note that, as the author of this Elsevier article, you retain the right to include it in a thesis or dissertation, provided it is not published commercially. Permission is not required, but please ensure that you reference the journal as the original source. For more information on this and on your other retained rights, please visit: https://www.elsevier.com/about/our-business/policies/copyright#Author-rights

BACK CLOSE WINDOW

Copyright © 2019 Copyright Clearance Center, Inc. All Rights Reserved. Privacy statement. Terms and Conditions.
Comments? We would like to hear from you. E-mail us at customercare@copyright.com